

Statistical Inference for Score Decompositions

Timo Dimitriadis*

Marius Puke†

March 5, 2026

Abstract

We introduce inference methods for score decompositions, which partition scoring functions for predictive assessment into three interpretable components: miscalibration, discrimination, and uncertainty. Our estimation and inference relies on a linear recalibration of the forecasts, which is applicable to general multi-step ahead point forecasts such as means and quantiles due to its validity for both smooth and non-smooth scoring functions. This approach ensures desirable finite-sample properties, enables asymptotic inference, and establishes a direct connection to the classical Mincer-Zarnowitz regression. The resulting inference framework facilitates tests for equal forecast calibration or discrimination, which yield three key advantages. They enhance the information content of predictive ability tests by decomposing scores, deliver higher statistical power in certain scenarios, and formally connect scoring-function-based evaluation to traditional calibration tests, such as financial backtests. Applications demonstrate the method’s utility. We find that for survey inflation forecasts, discrimination abilities can differ significantly even when overall predictive ability does not. In an application to financial risk models, our tests provide deeper insights into the calibration and information content of volatility and Value-at-Risk forecasts. By disentangling forecast accuracy from backtest performance, the method exposes critical shortcomings in current banking regulation.

1 Introduction

Forecasting—whether of macroeconomic conditions, financial market movements, or other uncertain outcomes—has become an indispensable element of modern economic analysis. From monetary policy design to investment planning and risk management, economic decisions increasingly rely on the ability to anticipate what lies ahead. The value of these decisions, however, depends critically on the accuracy and credibility of the underlying forecasts. Therefore, establishing rigorous standards for evaluating predictions is essential, ensuring that economic forecasts are not only informative but also empirically grounded and verifiable.

Two main concepts have emerged for evaluating a forecast X_t of an uncertain future real-valued outcome Y_t . First, the statistical theory of forecast comparison ranks competing forecasts according to their empirical score (or loss) (Savage, 1971; Gneiting, 2011). The appropriate

*Faculty of Economics and Business, Goethe University Frankfurt, Campus Westend, Theodor-W.-Adorno-Platz 4, 60629 Frankfurt am Main, Germany, and Heidelberg Institute for Theoretical Studies (HITS), dimitriadis@econ.uni-frankfurt.de.

†Institute of Economics, University of Hohenheim, Schloss Hohenheim 1 C, 70593 Stuttgart, Germany, marius.puke@uni-hohenheim.de.

scoring function depends on the forecast target—e.g., whether the aim is to predict the full distribution of Y_t , its mean, or a particular quantile. For meaningful comparisons, these scoring functions must be *strictly consistent*: the ideal forecast should minimize the expected score, ensuring that lower score values reliably indicate superior predictive performance.

Second, forecasts are evaluated in terms of their alignment with the realized outcomes—a property referred to as *calibration* in statistics (Gneiting et al., 2007; Gneiting and Resin, 2023), *forecast optimality, rationality* or *efficiency* in economics (Diebold et al., 1998; Elliott et al., 2016), and *backtesting* in finance (Basel Committee, 2019a,b). For example, when forecasting the mean, the average forecast should coincide with the average realized outcome—both unconditionally and conditional on the forecast itself, the latter being referred to as auto-calibration. In economics, this property is most commonly assessed using the test of Mincer and Zarnowitz (1969, henceforth MZ), which examines whether the forecast X_t equals the conditional expectation of Y_t given X_t through a linear regression framework. Extensions to other targets, such as quantiles, follow naturally by replacing the mean regression with the corresponding quantile regression (Gaglianone et al., 2011; Guler et al., 2017; Bayer and Dimitriadis, 2022).

These two evaluation paradigms are known to occasionally produce counterintuitive results, a point illustrated by our following motivational example. In this paper, we develop asymptotic inference for the components of so-called score decompositions, which provide a transparent link between the two forecast evaluation regimes described above. Beyond delivering a sharper theoretical understanding of the respective strengths and limitations of these approaches, the motivational example underscores their practical relevance by demonstrating how, in applied settings, the two methods can lead to seemingly contradictory conclusions.

1.1 Motivational example

Consider the daily logarithmic returns of the S&P E-mini future as the world’s most actively traded equity index futures contract. We evaluate one-day ahead forecasts for its variance as well as its 1%-quantile, known as the Value-at-Risk (VaR), between January 1, 2008 and January 1, 2022. Both forecast types are important tools in banking regulation; see (Basel Committee, 2019a, CRE 36.153) and Basel Committee (2019b, MAR 32.5 and MAR 99.9 – MAR 99.21) for volatility and VaR backtesting, respectively. Section 5.2 provides additional details on this application.

We use the following state of the art forecasting models: First, the Heterogeneous Auto-Regressive (HAR) model of Corsi (2009) uses intraday trading information through the Realized Variance (RV) estimator to forecast the variance through a linear model. Second, we employ a baseline GARCH model of Bollerslev (1986) and for both the HAR and GARCH model, we obtain quantile forecasts through a Gaussianity assumption on the model residuals. For the case of VaR forecasts, we further employ the basic Historical Simulation (HS) approach that uses the unconditional quantile of the past 250 trading days as its quantile forecast.

Table 1 shows that, for both forecast types, the HAR model achieves the lowest average scores. These improvements are statistically significant at the 1% level according to the Diebold and Mariano (1995, henceforth DM) test, with the sole exception of the HAR–GARCH comparison for VaR forecasts. Thus, the HAR forecasts deliver the strongest predictive performance. At

Table 1: [Mincer and Zarnowitz \(1969\)](#) test p -values, average scores (QLIKE for variance, and check loss for the quantile) and its decomposition terms for variance and VaR forecasts. See Sections 1.1 and 5.2 for details.

Forecast Type	Model i	MZ p -value	Score	Score Decomposition		
			S_i	MCB $_i$	DSC $_i$	UNC
Variance	HAR	0.001	1.775	0.034	6.732	8.473
	GARCH	0.991	2.522	0.000	5.951	
1%-Quantile	HAR	0.003	4.018	0.270	1.831	5.579
	GARCH	0.006	4.089	0.148	1.638	
	HS	0.321	5.114	0.077	0.543	

the same time, the MZ test decisively rejects auto-calibration of the HAR forecasts. In contrast, the GARCH variance forecasts yield significantly higher scores, yet auto-calibration cannot be rejected. A similar pattern emerges for the HS VaR forecasts: they record the largest scores but constitute the only forecasting sequence for which calibration is not rejected.

This example illustrates that good predictive performance and proper auto-calibration do not necessarily coincide and may diverge sharply. Since both evaluation approaches are widely applied in practice, developing tools to reconcile and interpret these seemingly contradictory conclusions is of central importance.

We shed light on these results by examining the *score decomposition* reported in Table 1. Score decompositions have a long tradition in meteorology ([Murphy, 1973](#); [Dawid, 1986](#); [Murphy and Winkler, 1987](#); [Bröcker, 2009](#); [Bentzen and Friederichs, 2014](#)) and have recently attracted renewed interest in statistics ([Dimitriadis et al., 2021](#); [Gneiting and Resin, 2023](#); [Gneiting et al., 2023](#)), yet they have received comparatively little attention in economics. In essence, the average score S_i of forecaster i can be decomposed additively into three non-negative components capturing miscalibration (MCB $_i$), discrimination (DSC $_i$), and a forecast-independent uncertainty term (UNC):

$$S_i = \text{MCB}_i - \text{DSC}_i + \text{UNC}. \quad (1)$$

Intuitively, the MCB component measures the extent of miscalibration relative to the scoring function by quantifying how much the score would improve if the forecasts were perfectly calibrated—thus capturing a concept closely related to what the MZ test evaluates. Likewise, the DSC component reflects the forecaster’s ability to distinguish (or “discriminate”) between higher and lower outcome realizations, conditional on the forecasts being calibrated. The remaining UNC term does not depend on the forecast itself and therefore serves as a normalization.

The last columns of Table 1 help reconcile the discrepancies between the score-based and calibration-based assessments. For both forecast types, the HAR model attains the highest (and thus best) DSC values, which is intuitive given that it incorporates the richest information set through high-frequency returns. However, it also yields the largest (worst) MCB values, accounting for its rejection in the MZ test. By contrast, the GARCH model—and even more so the HS model—exhibits weaker discrimination but achieves substantially better calibration. Yet, despite the clear interpretive value of these decomposition terms, formal inference methods for them are not available, limiting their practical usefulness as reflected in [Elliott and Timmermann](#)

(2016, p. 355), who point out that “an important limitation of these decompositions is that there are no objective measures for how large or small the terms should be”.

This gap is particularly problematic in settings such as banking regulation under the Basel framework, where calibration-based backtesting plays a central role. Such procedures risk creating misguided incentives: the best-performing HAR forecasts may be labeled “invalid,” whereas HS forecasts—whose poor discriminatory ability makes them slow to respond to emerging crises—may be deemed acceptable. These tensions highlight the need for both a deeper understanding of the distinct properties captured by the decomposition and the development of rigorous statistical inference for its components—needs that this paper directly addresses.

1.2 Contributions

In this paper, we propose augmenting scoring-function-based forecast comparisons with the corresponding decomposition terms, as illustrated in Table 1, and we are the first to develop asymptotic inference for these components. To estimate the decomposition components in (1), we advocate the use of a simple linear regression—either mean or quantile, depending on the forecast target. This specification is motivated by several considerations: its stability and resistance to overfitting; its good empirical fit in our applications; its close conceptual connection to the [Mincer and Zarnowitz \(1969\)](#) framework; its attractive non-negativity guarantees for the resulting decomposition terms; and, crucially, its tractability for developing valid asymptotic inference procedures. Recent contributions have suggested nonparametric (isotonic) regression approaches instead ([Dimitriadis et al., 2021](#); [Gneiting and Resin, 2023](#); [Arnold et al., 2024](#)). However, their asymptotic properties remain unclear—particularly in time-series settings—and they are prone to overfitting, which can introduce biases that further complicate or even undermine asymptotic inference.

We derive the joint asymptotic distribution of the estimated MCB and DSC components for competing forecasts allowing for possibly non-smooth scoring functions, thereby enabling formal tests of equal miscalibration or equal discrimination for, e.g., mean or quantile forecasts. These tests extend the classical framework of [Diebold and Mariano \(1995\)](#) by incorporating two layers of uncertainty: the sampling variation arising from averaging over time and the additional variation introduced by the linear “recalibration regression” used in constructing the MCB and DSC components. A key complication is that the limiting distribution depends on whether the population values of MCB or DSC are zero or strictly positive. Our testing procedures account for these cases through a p -value adjustment inspired by a hybrid intersection–union/union–intersection (IU/UI) testing principles ([Berger, 1997](#)).

Our simulations demonstrate that the proposed tests are valid—though potentially conservative due to the underlying IU/UI principles—under their respective null hypotheses for both mean and quantile forecasting settings. We also show that the tests exhibit strong power properties, and in particular achieve a substantial power increase relative to the classical DM test in fair comparisons where differences in average scores stem exclusively from a single component, either MCB or DSC. This perhaps surprising power gain arises because our tests isolate a single aspect of forecast performance—either discrimination or miscalibration—whereas score-based tests must aggregate both components into a single, and consequently noisier, metric.

Our first application compares the predictive performance of two survey forecasts for U.S. inflation—the Survey of Professional Forecasters (SPF) and the Michigan Survey of Consumers. While professional forecasters unsurprisingly attain better average scores than consumers, these differences are typically insignificant (Ehm et al., 2016; Patton, 2020). In contrast, the score decomposition shows that both groups exhibit similar calibration, whereas our new tests detect a significant difference in discrimination. This finding is consistent with the power gains demonstrated in our simulations. Given that professional forecasters draw on a richer information set, their superior discrimination is a natural consequence.

The second application extends the motivating example of Section 1.1 and clarifies the relationship between scoring-function-based forecast evaluation and backtests for both, variance and VaR forecasts. Moreover, we disentangle several widely used VaR backtests by characterizing them through the conditioning sets they implicitly impose within the framework of conditional quantile calibration, thereby revealing the precise properties they actually test.

1.3 Literature

Early approaches to score decompositions resembling (1) date back to Sanders (1963), Theil (1966), and Murphy (1973), and primarily focus on the squared error in the context of probability forecasts for binary outcomes, which can be interpreted as a mean. DeGroot and Fienberg (1981) and Bröcker (2009) demonstrated that such decompositions can be derived for any strictly proper scoring rule, including those for full distributional forecasts. More recently, Gneiting and Resin (2023) developed a general framework for score decompositions for scoring functions, extending these concepts to point forecasts. This line of research has spurred a growing body of both theoretical and applied work; see, for example, Bentzien and Friederichs (2014); Siegert (2017); Pohle (2020); Fissler et al. (2022); Wüthrich et al. (2025); Brehmer et al. (2024). For a more detailed historical overview of score decompositions, see Mitchell (2019, Section 1.1).

In practice, the score decompositions rely on estimates of recalibrated forecasts, and the choice of estimation method remains an active area of research. Recently, isotonic regression—which estimates, for example, a conditional mean nonparametrically under a monotonicity constraint—has been widely used for both point and distributional forecasts (Dimitriadis et al., 2021; Gneiting et al., 2023; Dimitriadis et al., 2024b; Arnold et al., 2024; Allen et al., 2025). A key reason for its popularity is that it satisfies attractive finite-sample non-negativity conditions, which facilitate the interpretation of the decomposition terms; these conditions are generally not satisfied by alternative methods such as binning or kernel regressions (Dimitriadis et al., 2021). We show that, under mild conditions, these non-negativity properties are also preserved when recalibration is performed using linear regressions.

As we develop asymptotic inference methods for the estimated decomposition terms on the right-hand side of (1), our approach is closely related to statistical tests for predictive performance, which focus on the sampling variability of the left-hand side of (1). The seminal contribution of Diebold and Mariano (1995) laid the foundation for a large econometric literature on testing for equal forecast performance. Numerous extensions have since been proposed, including methods for model-based forecasts (West, 1996; Clark and McCracken, 2001), multiple forecast comparisons (Hansen, 2005; Hansen et al., 2011), conditional predictive ability (Giaco-

mini and White, 2006; Li et al., 2022), and anytime-valid procedures (Henzi and Ziegel, 2022; Choe and Ramdas, 2024). For comprehensive surveys of this literature, see, for example, West (2006), Clark and McCracken (2013), and Diebold (2015).

In contrast, the assessment of sampling uncertainty for the right-hand side of (1) has received relatively little attention. Existing contributions, such as Siegert (2014) and Gneiting and Resin (2023), propose ad-hoc (resampling) methods to quantify the uncertainty for a single forecaster, but they do not provide tools for comparative inference across multiple forecasters. Our work addresses this gap by developing a unified framework for inference on the decomposition components.

VaR backtests are widely used to evaluate the reliability, i.e., the calibration, of risk models via their quantile forecasts. Classic procedures include the unconditional coverage test of Kupiec (1995), which underlies the traffic-light system of Basel Committee (1996, 2019b), as well as the conditional coverage test of Christoffersen (1998), which additionally assesses the independence of exceedances. A large body of subsequent work tests slightly differing notions of conditional calibration (Berkowitz et al., 2011; Gaglianone et al., 2011; Berkowitz et al., 2011; Hoga and Demetrescu, 2023; Fosten et al., 2024; Wang et al., 2025); see He et al. (2022) for a recent overview. Our score decompositions—and in particular the application in Section 5.2—show that well-calibrated forecasts do not necessarily exhibit strong predictive performance. This underscores the importance of evaluating VaR forecasts through both calibration and discrimination, rather than relying solely on traditional backtesting metrics; also see Section 3.5.

A growing strand of the macroeconomic literature—including, among many others, Coibion and Gorodnichenko (2015), Bordalo et al. (2020), Kohlhas and Walther (2021), Angeletos et al. (2021), Broer and Kohlhas (2024), and Farmer et al. (2024)—examines how forecast errors respond to observable information. This line of work effectively tests conditional calibration, asking whether forecast errors are predictable given the information available at the time forecasts are made. Our methodology suggests a natural refinement of these approaches by additionally assessing forecast discrimination, since calibration captures only one dimension of predictive performance. This refinement is particularly relevant because forecasts that discriminate well between outcomes are often found to be miscalibrated, and thus appear to deviate from rational expectations more frequently.

1.4 Plan of the article

Section 2 introduces key concepts of forecast evaluation. The theory in Section 3 develops asymptotic inference under high-level conditions, which are subsequently verified for mean and quantile forecast. Section 4 contains simulations and we present two applications in Section 5. Section 6 concludes. Appendix A contains all proofs and we discuss the relation to further decompositions in Appendix B. Appendix C presents technical details for the simulations and Appendix D contains additional figures.

We provide replication material at https://github.com/marius-cp/SDI_replications for the simulations and applications, which draws on the SDI package for the statistical software R (R Core Team, 2026), available at <https://github.com/marius-cp/SDI>.

2 Fundamentals of forecast evaluation

After fixing notation in Section 2.1, we discuss relative and absolute forecast evaluation in Sections 2.2 and 2.3.

2.1 Setup and notation

We follow Gneiting (2011) and Hoga and Dimitriadis (2023) and consider a complete probability space $(\Omega, \mathcal{F}, \mathbb{P})$ with a series of stationary random variables $Y_t : \Omega \rightarrow \mathcal{O} \subseteq \mathbb{R}$, $t \in \mathbb{N}$, that take values in the interval-valued observation domain \mathcal{O} . The setting allows for time series (where t represents time points) as well as cross-sectional (where t represents cross-sectional units) applications. For some information set (in the form of a sigma-algebra) $\mathcal{F}_t \subset \mathcal{F}$, where Y_t is in general not \mathcal{F}_t -measurable, we denote the conditional distribution of Y_t given \mathcal{F}_t by $F_t(\bullet, \omega) = \mathbb{P}(Y_t \leq \bullet \mid \mathcal{F}_t)(\omega)$, where we assume that $F_t(\bullet, \omega) \in \mathcal{P}$ for all $\omega \in \Omega$, for some convex class of distributions \mathcal{P} taking values in \mathcal{O} , which contains the Dirac measures δ_y for all $y \in \mathcal{O}$. We write $F_t(\bullet)$ for the random variable defined by $\omega \mapsto F_t(\omega, \bullet)$. The information set \mathcal{F}_t represents the full information that could be used for forecast Y_t , but competing forecasters might have less information at hand.

For an interval-valued action domain $\mathcal{A} \subseteq \mathbb{R}$, we consider a stationary sequence of forecasts for some target functional $\Gamma : \mathcal{P} \rightarrow \mathcal{A}$ of the conditional distribution F_t . Prominent functionals are the conditional expectation $\mathbb{E}[Y_t \mid \mathcal{F}_t]$, or a conditional α -quantile $Q_\alpha(Y_t \mid \mathcal{F}_t)$ for some $\alpha \in (0, 1)$, which is assumed to be unique for simplicity. We sometimes abuse notation and write $\Gamma(Y_t \mid \mathcal{F}_t)$ instead of $\Gamma(F_t)$ for a functional of the conditional distribution.

The point forecasts are denoted by X_{it} where the index $i = 1, 2$ captures a series of competing forecasts. These forecasts are assumed to be \mathcal{F}_t -measurable throughout the article but they are in general based on different (less) information, $\mathcal{I}_{it} \subseteq \mathcal{F}_t$, or might be misspecified through other aspects such as model misspecification or estimation noise.

Throughout, (in)equalities of random variables are meant to hold almost surely (a.s.) unless stated otherwise, and for a vector $\mathbf{z} \in \mathbb{R}^k$, $k \in \mathbb{N}$, $\|\mathbf{z}\|$ denotes the Euclidean norm and \mathbf{z}^\top its transpose. We write $\nabla_{\mathbf{z}} f$ for the (column-vector) gradient of the mapping $\mathbf{z} \mapsto f(\mathbf{z}) \in \mathbb{R}$ and $\nabla_{\mathbf{z}\mathbf{z}} f$ for its second derivative, the Hessian matrix. In the univariate case, $f'(z)$ denotes the derivative of $f(z)$ with respect to $z \in \mathbb{R}$. For functions with multiple real-valued arguments, a prime indicates partial differentiation with respect to the first argument, and multiple primes denote higher-order derivatives.

2.2 Forecast comparison through scoring functions

Following Gneiting (2011), point forecasts are compared by strictly consistent scoring (or loss) functions $\mathbf{S} : \mathcal{A} \times \mathcal{O} \rightarrow \mathbb{R}$, where lower values indicate higher predictive ability. A scoring function \mathbf{S} is said to be *consistent* for $\Gamma(F)$ with respect to a (usually large) class of distributions \mathcal{P} if

$$\mathbb{E}_{Y \sim F}[\mathbf{S}(\Gamma(F), Y)] \leq \mathbb{E}_{Y \sim F}[\mathbf{S}(x, Y)] \quad (2)$$

for all $F \in \mathcal{P}$ and all (deterministic) $x \in \mathcal{A}$, where $\mathbb{E}_{Y \sim F}[\cdot]$ denotes the expectation with respect to $Y \sim F \in \mathcal{P}$. A scoring function is said to be *strictly consistent* if equality in (2) implies

$x = \Gamma(F)$ such that the optimal forecast $\Gamma(F)$ uniquely obtains the lowest expected score. A functional is said to be *elicitable* if a strictly consistent scoring function exists.

Holzmann and Eulert (2014, Theorem 1) allows to define consistency of a scoring function relative to a generic information set $\mathcal{G}_t \subseteq \mathcal{F}_t$ as

$$\mathbb{E}[\mathbf{S}(\Gamma(Y_t | \mathcal{G}_t), Y_t) | \mathcal{G}_t] \leq \mathbb{E}[\mathbf{S}(\tilde{X}_t, Y_t) | \mathcal{G}_t], \quad (3)$$

for all $Y_t | \mathcal{G}_t \in \mathcal{P}$, and for all \mathcal{G}_t -measurable random variables \tilde{X}_t . The scoring function is strictly consistent if almost sure equality in (3) implies that $\tilde{X}_t = \Gamma(Y_t | \mathcal{G}_t)$ a.s..

If the target functional Γ is the conditional mean, under mild regularity conditions, all strictly consistent scoring functions are characterized by the so-called *Bregman class*,

$$\mathbf{S}(x, y) = \phi(y) - \phi(x) - \phi'(x)(y - x) \quad (4)$$

parametrized by a strictly convex function ϕ with subgradient ϕ' (Gneiting, 2011, Theorem 7). The omnipresent squared error

$$\mathbf{S}_{\text{SE}}(x, y) = (x - y)^2. \quad (5)$$

arises for $\phi_{\text{SE}}(x) = x^2$. For $\phi_{\text{QL}}(x) = -\log(x)$ we obtain the QLIKE scoring function,

$$\mathbf{S}_{\text{QL}}(x, y) = \frac{y}{x} - \log\left(\frac{y}{x}\right) - 1, \quad (6)$$

which is regularly used for the evaluation of variance forecasts in financial econometrics with positive action and observation domain, $\mathbf{A} = \mathbf{O} = (0, \infty)$; see e.g., Patton (2011). Under the standard assumption of a zero mean, the variance coincides with the second moment, thereby rendering the Bregman class applicable.

If the target functional is the conditional α -quantile, $\alpha \in (0, 1)$, all strictly consistent scoring functions are given by the class of generalized piecewise linear (GPL) loss functions

$$\mathbf{S}(x, y) = (\mathbf{1}\{y \leq x\} - \alpha)(g(x) - g(y)), \quad (7)$$

where the function g is non-decreasing on $\mathbf{A} = \mathbf{O} \subseteq \mathbb{R}$ (Gneiting, 2011, Theorem 9). All GPL loss functions are non-differentiable at $x = y$ due to the indicator function. The check loss $\mathbf{S}_{\text{CL}}(x, y) = (\mathbf{1}\{y \leq x\} - \alpha)(x - y)$ as the most popular candidate arises for $g_{\text{CL}}(x) = x$.

In practice, scoring functions are employed to compare forecast sequences X_{it} , $i = 1, 2$, $t = 1, \dots, T$, for the target variable Y_t through their average scores $\hat{\mathbf{S}}_{iT} = \frac{1}{T} \sum_{t=1}^T \mathbf{S}(X_{it}, Y_t)$. The sample average serves as an empirical approximation to the expectation appearing in (2)–(3). Following Diebold and Mariano (1995), a rich body of asymptotic inference methods is available for constructing tests based on such average score differences.

2.3 Forecast validation and calibration assessment

A known practical limitation of purely score-based forecast evaluations lies in their inability to identify specific deficiencies of the forecasts, such as systematic biases, which we formalize

through the theory of forecast calibration. A forecast X_{it} for $\Gamma(Y_t)$ is said to be *conditionally calibrated* with respect to the information set $\mathcal{G}_{it} \subseteq \mathcal{F}_t$ if

$$X_{it} = \Gamma(Y_t | \mathcal{G}_{it}) \quad \text{a.s.} \quad (8)$$

This property asserts a certain compatibility of the forecast X_{it} with its forecasting target $\Gamma(Y_t | \mathcal{G}_{it})$. A conditionally calibrated forecast w.r.t. the full information set \mathcal{F}_t minimizes the \mathcal{F}_t -conditional expectation of the scoring function by (3), such that the econometric literature also calls it *optimal* or *efficient* (Elliott and Timmermann, 2016, Chapter 15). As the forecast might not have used—or even have access to—all information in \mathcal{F}_t , it is, however, often more appropriate to consider calibration based on some reduced information set $\mathcal{G}_{it} \subset \mathcal{F}_t$ in (8).

An important special case is that of an *auto-calibrated* forecast, obtained for $\mathcal{G}_{it} = \sigma\{X_{it}\}$, i.e.,

$$X_{it} = \Gamma(Y_t | X_{it}), \quad \text{a.s.} \quad (9)$$

Conditioning on the forecast itself guarantees that the information encoded in the forecast was indeed used, and it remains feasible even when the evaluator does not have access to the full information set of the forecaster \mathcal{I}_{it} .

A common tool to assess auto-calibration is to plot $x \in \mathbf{A}$ against an estimate of $\Gamma(Y_t | X_{it} = x)$, where deviations from the diagonal indicate miscalibration. In the meteorological literature, this is known as a *reliability diagram*, typically estimated nonparametrically (Murphy and Winkler, 1992; Pohle, 2020; Dimitriadis et al., 2021). In economic mean forecast evaluation, this idea goes back to Mincer and Zarnowitz (1969), who regress Y_t on X_{it} and test whether the intercept is zero and the slope is one—essentially a linear reliability diagram. Gaglianone et al. (2011); Guler et al. (2017); Bayer and Dimitriadis (2022) cover extensions to other functionals.

A further important tool for calibration assessment are *identification functions*. Under smoothness conditions, they correspond to derivatives of the scoring function (Nolde and Ziegel, 2017). Formally, an identification function $\mathbf{V} : \mathbf{A} \times \mathbf{O} \rightarrow \mathbb{R}$ is increasing and left-continuous in its first argument, and it is called *strict* if $\mathbb{E}_{Y \sim F}[\mathbf{V}(x, Y)] = 0$ if and only if $x = \Gamma(Y)$. For example, $\mathbf{V}(x, y) = 2(x - y)$ is the canonical identification function that arises as the derivative of the squared error loss and for the α -quantile, $\mathbf{V}(x, y) = \mathbb{1}\{y \leq x\} - \alpha$ is the almost sure derivative of the check loss. Identification functions allow for a (subject to regularity conditions) equivalent definition of conditional calibration from (8) as

$$\mathbb{E}[\mathbf{V}(X_{it}, Y_t) | \mathcal{G}_{it}] = 0, \quad \text{a.s.}, \quad (10)$$

which specializes to auto-calibration when $\mathcal{G}_{it} = \sigma\{X_{it}\}$. Taking expectations on both sides of (10) allows to define *unconditional calibration* of X_{it} as $\mathbb{E}[\mathbf{V}(X_{it}, Y_t)] = 0$.

3 Theory

We introduce linear score decompositions in Section 3.1, develop asymptotic inference in Section 3.2, discuss testable hypotheses in Section 3.3, and derive low-level inference conditions for mean and quantile forecasts in Section 3.4. Section 3.5 discusses the connection to VaR

backtests. Related decompositions are discussed in Section B.

3.1 Score decompositions based on linear recalibration

For an elicitable functional Γ and corresponding strictly consistent scoring function S , we denote the expected score of the forecasts X_{it} by $\bar{S}_i := \mathbb{E}[S(X_{it}, Y_t)]$. Throughout this paper, an overline denotes population quantities.

To illustrate the mechanics of the score decomposition, we introduce an “idealized” version of the forecast: the population *reCalibrated forecast* $X_{it}^C = \Gamma(Y_t | \mathcal{W}_{it})$, where \mathcal{W}_{it} denotes the recalibration information set satisfying $\sigma\{X_{it}\} \subseteq \mathcal{W}_{it} \subseteq \mathcal{F}_t$. By construction, X_{it}^C uses at least as much information as the original forecast, but is \mathcal{W}_{it} -conditional calibrated by definition; see (8). The canonical auto-calibration case—in line with [Mincer and Zarnowitz \(1969\)](#)—arises for $\mathcal{W}_{it} = \sigma\{X_{it}\}$. Richer information sets allow connections to stronger calibration concepts, VaR backtests, and related macroeconomic applications ([Coibion and Gorodnichenko, 2015](#)). The corresponding *reCalibrated score* is denoted by $\bar{S}_i^C = \mathbb{E}[S(X_{it}^C, Y_t)]$. We further define the *Reference forecast* $\bar{r} = \Gamma(Y_t)$, which is unconditionally calibrated but constant, and the corresponding *Reference score* $\bar{S}^R = \mathbb{E}[S(\bar{r}, Y_t)]$.

With these ingredients, we define the *population score decomposition*, consisting of non-negative components ([Gneiting and Resin, 2023](#)):

$$\bar{S}_i = \underbrace{(\bar{S}_i - \bar{S}_i^C)}_{\text{MCB}_i} - \underbrace{(\bar{S}^R - \bar{S}_i^C)}_{\text{DSC}_i} + \underbrace{\bar{S}^R}_{\text{UNC}}. \quad (11)$$

In the canonical case $\mathcal{W}_{it} = \sigma\{X_{it}\}$, the component $\overline{\text{MCB}}_i = \bar{S}_i - \bar{S}_i^C$ quantifies the increase in the score’s predictive ability that can be achieved by recalibration, hence providing a measure of miscalibration such that low $\overline{\text{MCB}}_i$ values are desirable. As the recalibrated forecast is a measurable transformation of X_{it} , it incorporates no additional information; thus, any score gains stem purely from improved calibration. If $\overline{\text{MCB}}_i = 0$, recalibration yields no score improvement, indicating that the original forecast was already calibrated.

The component $\overline{\text{DSC}}_i = \bar{S}^R - \bar{S}_i^C$ compares the scores of two recalibrated forecasts: \bar{S}_i^C based on information in X_{it} , and \bar{S}^R unconditionally without additional information. As this “controls for calibration”, the remaining score improvement in $\overline{\text{DSC}}_i$ reflects the forecast’s information content, that is, its discrimination ability. Larger values are therefore desirable. The final component $\overline{\text{UNC}} = \bar{S}^R$ is forecast-independent and serves as a normalizing constant.

In practice, the components in (11) require estimated versions of both the recalibrated and reference forecasts. While estimating the reference forecast as the unconditional functional is straightforward, the estimation of the recalibrated forecast remains debated, with proposals including binning methods ([Murphy and Winkler, 1987](#)), kernel regression ([Pohle, 2020](#)), and more recently isotonic regression ([Dimitriadis et al., 2021](#); [Gneiting and Resin, 2023](#)). We instead propose the use of linear regression, which mitigates biases from nonparametric overfitting that can hinder valid inference, particularly in settings of close to auto-calibration, aligns with [Mincer and Zarnowitz \(1969\)](#), and easily accommodates additional covariates beyond the forecasts themselves.

For this, we consider the *recalibration variables* $\mathbf{W}_{it} = (1, X_{it}, \dots)^\top \in \mathbb{R}^k$ that generate the recalibration information $\mathcal{W}_{it} = \sigma\{\mathbf{W}_{it}\}$ and impose the following:

Assumption 3.1. S is a strictly consistent scoring function for the functional Γ , the random variables Y_t , X_{it} and \mathbf{W}_{it} are strictly stationary for all $t \in \mathbb{N}$, and $\Gamma(Y_t | \mathbf{W}_{it}) = \mathbf{W}_{it}^\top \bar{\boldsymbol{\theta}}_i$ a.s. for some true parameter $\bar{\boldsymbol{\theta}}_i \in \text{int}(\boldsymbol{\Theta}) \subseteq \mathbb{R}^k$, where $\boldsymbol{\Theta}$ is convex and compact.

Besides stationarity, Assumption 3.1 imposes linearity of the recalibration function $X_{it}^C = \Gamma(Y_t | \mathbf{W}_{it}) = \mathbf{W}_{it}^\top \bar{\boldsymbol{\theta}}_i$, which is required for correct specification of the linear “recalibration regression”. For the finite-sample statements of Theorem 3.2 below, it is crucial that we use M-estimation for the regression parameters by using the *same* scoring function that is used for the decomposition¹

$$\hat{\boldsymbol{\theta}}_{iT} = \arg \min_{\boldsymbol{\theta} \in \boldsymbol{\Theta}} \frac{1}{T} \sum_{t=1}^T S(\mathbf{W}_{it}^\top \boldsymbol{\theta}, Y_t), \quad (12)$$

where we assume for simplicity that the arg min in (12) is unique. Moreover, the empirical reference forecast \hat{r}_T is the unconditional functional Γ of the sample Y_1, \dots, Y_T . Then, the empirical counterpart of the score decomposition in (11) is given by

$$\hat{S}_{iT} = \widehat{\text{MCB}}_{iT} - \widehat{\text{DSC}}_{iT} + \widehat{\text{UNC}}_T := \left(\hat{S}_{iT} - \hat{S}_{iT}^C \right) - \left(\hat{S}_T^R - \hat{S}_{iT}^C \right) + \hat{S}_T^R, \quad (13)$$

where

$$\hat{S}_{iT} = \frac{1}{T} \sum_{t=1}^T S(X_{it}, Y_t), \quad \hat{S}_{iT}^C = \frac{1}{T} \sum_{t=1}^T S(\mathbf{W}_{it}^\top \hat{\boldsymbol{\theta}}_{iT}, Y_t), \quad \hat{S}_T^R = \frac{1}{T} \sum_{t=1}^T S(\hat{r}_T, Y_t).$$

The following theorem ensures (strict) positivity of the sampling versions of the decomposition in (13). While similar results for the population decomposition (11) are established in Gneiting and Resin (2023, Theorem 2.23), it is noteworthy that these results extend to the sampling versions under linear recalibration, even without imposing correct specification in Assumption 3.1.

Theorem 3.2. *Assume that the recalibrated forecasts are obtained by (12) using the same strictly consistent score S as used in (13). Furthermore, let \mathbf{W}_{it} contain a constant and the forecast X_{it} , and let $(\hat{r}_T, 0, \dots)^\top \in \boldsymbol{\Theta}$ almost surely. Then, for the decomposition in (13), it holds that:*

- (a) $\widehat{\text{MCB}}_{iT} \geq 0$, which holds with equality if $X_{it} = \mathbf{W}_{it}^\top \hat{\boldsymbol{\theta}}_{iT}$ a.s. for all $t = 1, \dots, T$.
- (b) If the arg min in (12) is unique, then $\widehat{\text{MCB}}_{iT} = 0$ a.s. implies $X_{it} = \mathbf{W}_{it}^\top \hat{\boldsymbol{\theta}}_{iT}$ a.s. for all $t = 1, \dots, T$.
- (c) $\widehat{\text{DSC}}_{iT} \geq 0$, which holds with equality if $\mathbf{W}_{it}^\top \hat{\boldsymbol{\theta}}_{iT} = \hat{r}_T$ a.s. for all $t = 1, \dots, T$.
- (d) If the arg min in (12) and \hat{r}_T are unique, then $\widehat{\text{DSC}}_{iT} = 0$ a.s. implies $\mathbf{W}_{it}^\top \hat{\boldsymbol{\theta}}_{iT} = \hat{r}_T$ a.s. for all $t = 1, \dots, T$.

¹While Dimitriadis et al. (2024a) show that strictly consistent loss functions (and only these) produce consistent parameter estimates, the resulting estimates generally differ in value across loss functions (Elliott et al., 2016; Mühlemann, 2021), motivating the need to employ the *same* scoring function in (11) and (12).

The non-negativity guarantees of Theorem 3.2 are essential, as zero miscalibration and discrimination components are routinely interpreted as perfect calibration and no discrimination, respectively (Dimitriadis et al., 2021; Gneiting and Resin, 2023; Allen et al., 2025). The proof of Theorem 3.2 applies to any recalibration method estimated by global score minimization and which is flexible enough to nest both a constant and the identity line, such as isotonic regression (Dimitriadis et al., 2021; Gneiting and Resin, 2023). In contrast, kernel regressions (Pohle, 2020), logistic regressions and Beta-CDF models for binary events (Siegert, 2017; Ranjan and Gneiting, 2010) do not offer such guarantees. Although kernels can represent constants and the identity line, they are not fitted via global score minimization; Beta-CDFs, being strictly increasing, cannot produce constants; and logistic regressions generally cannot reproduce the identity line.

3.2 Asymptotic approximations

We now provide new distributional convergence results for the considered linear score decomposition, which are derived under the following high-level regularity conditions, for which we derive more explicit conditions for mean and quantile forecasts in Section 3.4.

Assumption 3.3. *The following conditions hold for $i = 1, 2$:*

(i) *The parametric estimators are of rate $\sqrt{T}(\widehat{\boldsymbol{\theta}}_{iT} - \bar{\boldsymbol{\theta}}_i) = \mathcal{O}_{\mathbb{P}}(1)$ and $\sqrt{T}(\widehat{r}_T - \bar{r}) = \mathcal{O}_{\mathbb{P}}(1)$.*

(ii) *The following CLT holds,*

$$T^{-1/2} \boldsymbol{\Omega}_T^{-1/2} \sum_{t=1}^T (a_{1t}, c_{1t}, a_{2t}, c_{2t}, e_t)^\top \xrightarrow{d} \mathcal{N}(0, I_5),$$

where $a_{it} := \mathbb{S}(X_{it}, Y_t) - \mathbb{E}[\mathbb{S}(X_{it}, Y_t)]$, $c_{it} := \mathbb{S}(\mathbf{W}_{it}^\top \bar{\boldsymbol{\theta}}_i, Y_t) - \mathbb{E}[\mathbb{S}(\mathbf{W}_{it}^\top \bar{\boldsymbol{\theta}}_i, Y_t)]$, $e_t := \mathbb{S}(\bar{r}, Y_t) - \mathbb{E}[\mathbb{S}(\bar{r}, Y_t)]$ and where

$$\boldsymbol{\Omega}_T = \text{Var} \left(T^{-1/2} \sum_{t=1}^T (a_{1t}, c_{1t}, a_{2t}, c_{2t}, e_t)^\top \right). \quad (14)$$

(iii) *The expected score $\mathbb{E}[\mathbb{S}(\mathbf{W}_{it}^\top \boldsymbol{\theta}, Y_t)]$ is continuously differentiable in $\boldsymbol{\theta}$ for all $\boldsymbol{\theta} \in \text{int}(\boldsymbol{\Theta})$.*

(iv) *The empirical process*

$$\nu_{iT}(\boldsymbol{\theta}) := T^{-1/2} \sum_{t=1}^T \mathbb{S}(\mathbf{W}_{it}^\top \boldsymbol{\theta}, Y_t) - \mathbb{E}[\mathbb{S}(\mathbf{W}_{it}^\top \boldsymbol{\theta}, Y_t)] \quad (15)$$

is stochastically equicontinuous, i.e., for all $\varepsilon > 0$ and $\eta > 0$, there exists $\delta > 0$ such that

$$\limsup_{T \rightarrow \infty} \mathbb{P} \left(\sup_{\{\boldsymbol{\theta}, \boldsymbol{\tau} \in \boldsymbol{\Theta} : \|\boldsymbol{\theta} - \boldsymbol{\tau}\| \leq \delta\}} |\nu_{iT}(\boldsymbol{\theta}) - \nu_{iT}(\boldsymbol{\tau})| \geq \eta \right) < \varepsilon. \quad (16)$$

Assumption 3.3 provides high-level conditions on the scoring function and the parametric estimators. These conditions can accommodate a wide range of settings, including various

estimation methods, target functionals, and forms of temporal dependence. They are verified for the mean and quantile cases in Section 3.4 below, and their generality allows for straightforward extensions to other functionals. In a nutshell, conditions (i) and (ii) can be verified based on classical dependence and moment conditions on the forecast-realization pairs. Conditions (iii) and (iv) ensure applicability to non-smooth scoring functions, such as the check loss, by imposing smoothness on the *expected* score and controlling empirical deviations via stochastic equicontinuity (Andrews, 1994; van der Vaart and Wellner, 1996).

Theorem 3.4. *Let Assumptions 3.1 and 3.3 hold and assume that $\overline{\text{MCB}}_i, \overline{\text{DSC}}_i > 0$ for $i = 1, 2$. Then, as $T \rightarrow \infty$,*

$$\sqrt{T} (\Xi \Omega_T \Xi^\top)^{-1/2} \begin{pmatrix} \widehat{\text{MCB}}_{1T} - \overline{\text{MCB}}_1 \\ \widehat{\text{DSC}}_{1T} - \overline{\text{DSC}}_1 \\ \widehat{\text{MCB}}_{2T} - \overline{\text{MCB}}_2 \\ \widehat{\text{DSC}}_{2T} - \overline{\text{DSC}}_2 \end{pmatrix} \xrightarrow{d} \mathcal{N}(0, I_4), \quad \text{with } \Xi = \begin{pmatrix} 1 & -1 & 0 & 0 & 0 \\ 0 & -1 & 0 & 0 & 1 \\ 0 & 0 & 1 & -1 & 0 \\ 0 & 0 & 0 & -1 & 1 \end{pmatrix}.$$

The joint asymptotic approximation of Theorem 3.4 is required for the construction of “comparative” confidence intervals and hypothesis tests—for instance, tests for equal miscalibration or discriminatory ability across the two forecast sequences. Notably, the resulting asymptotic distribution—with covariance matrix Ω_T from (14)—is unaffected by the estimation uncertainty of $\widehat{\boldsymbol{\theta}}_{iT}$ and \widehat{r}_T , due to an orthogonality between these estimators and the sampling error from replacing expected scores with their empirical averages.

Theorem 3.4 requires strict positivity of the population values $\overline{\text{MCB}}_i, \overline{\text{DSC}}_i > 0$, hence excluding the boundary cases $\overline{\text{MCB}}_i = 0$ and $\overline{\text{DSC}}_i = 0$, which necessitate a separate treatment for which we impose the following high-level assumptions.

Assumption 3.5. *Assume that the following conditions hold for $i = 1, 2$:*

(i) *For the estimators \widehat{r}_T and $\widehat{\boldsymbol{\theta}}_{iT}$, the following joint asymptotic behavior holds*

$$\sqrt{T} \begin{pmatrix} \widehat{r}_T - \bar{r} \\ \widehat{\boldsymbol{\theta}}_{iT} - \bar{\boldsymbol{\theta}}_i \end{pmatrix} = - \begin{pmatrix} \left(\frac{1}{T} \sum_{t=1}^T \mathbf{S}''(\bar{r}, Y_t) \right)^{-1} & 0 \\ \left(\frac{1}{T} \sum_{t=1}^T \mathbf{S}''(\mathbf{W}_{it}^\top \bar{\boldsymbol{\theta}}_i, Y_t) \mathbf{W}_{it} \mathbf{W}_{it}^\top \right)^{-1} & \end{pmatrix} T^{-1/2} \sum_{t=1}^T \mathbf{S}'(\bar{r}, Y_t) \mathbf{W}_{it} + o_{\mathbb{P}}(1), \quad (17)$$

where $T^{-1/2} \sum_{t=1}^T \mathbf{S}'(\mathbf{W}_{it}^\top \bar{\boldsymbol{\theta}}_i, Y_t) \mathbf{W}_{it}$ satisfies a central limit theorem (CLT) and the terms $\frac{1}{T} \sum_{t=1}^T \mathbf{S}''(\bar{r}, Y_t)$ and $\frac{1}{T} \sum_{t=1}^T \mathbf{S}''(\mathbf{W}_{it}^\top \bar{\boldsymbol{\theta}}_i, Y_t) \mathbf{W}_{it} \mathbf{W}_{it}^\top$ are invertible for T large enough and satisfy laws of large numbers (LLN).

(ii) *The scoring function \mathbf{S} is three times continuously differentiable in its first argument and for $h_T(\boldsymbol{\theta}) := \frac{1}{T} \sum_{t=1}^T |\mathbf{S}'''(\mathbf{W}_{it}^\top \boldsymbol{\theta}, Y_t)| \|\mathbf{W}_{it}\|^3$, we have that*

$$T^{-1/2} \sup_{\|\boldsymbol{\theta} - \bar{\boldsymbol{\theta}}_i\| \leq \delta} |h_T(\boldsymbol{\theta}) - h_T(\bar{\boldsymbol{\theta}}_i)| = o_{\mathbb{P}}(1) \quad \text{and} \quad T^{-1/2} h_T(\bar{\boldsymbol{\theta}}_i) = o_{\mathbb{P}}(1).$$

As before, the high-level conditions in Assumption 3.5 allow for case-by-case verifications for specific functionals, scoring functions, and estimators as exemplified in Section 3.4. Condition (i)

provides a standard asymptotic linear representation of the estimators, slightly strengthening Assumption 3.3 (i). Notably, the MCB result below could be derived using only the representation for $\widehat{\boldsymbol{\theta}}_{iT}$. Condition (ii) applies to smooth loss functions and imposes a uniform LLN type requirement, although this condition is substantially weakened by the $T^{-1/2}$ scaling factor.

Theorem 3.6. *Suppose that Assumptions 3.1 and 3.5 hold. Then, as $T \rightarrow \infty$,*

- *if $\overline{\text{MCB}}_i = 0$, then $T \widehat{\text{MCB}}_{iT} - \frac{1}{2} \mathbf{N}_{iT}^\top \boldsymbol{\Upsilon}_i^{-1} \mathbf{N}_{iT} \xrightarrow{\mathbb{P}} 0$; and*
- *if $\overline{\text{DSC}}_i = 0$, then $T \widehat{\text{DSC}}_{iT} - \frac{1}{2} \mathbf{N}_{iT}^\top \mathbf{H}_i^{-1} \mathbf{N}_{iT} \xrightarrow{\mathbb{P}} 0$,*

where $\boldsymbol{\Upsilon}_i := \mathbb{E} [\mathbf{S}''(\mathbf{W}_{it}^\top \bar{\boldsymbol{\theta}}_i, Y_t) \mathbf{W}_{it} \mathbf{W}_{it}^\top]$, $\mathbf{H}_i^{-1} := \left(\mathbb{E} [\mathbf{S}''(\bar{r}, Y_t) \mathbf{W}_{it} \mathbf{W}_{it}^\top]^{-1} - \begin{pmatrix} \mathbb{E} [\mathbf{S}''(\bar{r}, Y_t)]^{-1} & 0 \\ 0 & 0 \end{pmatrix} \right)$, and $\mathbf{N}_{iT} \sim \mathcal{N}(0, \boldsymbol{\Pi}_{iT})$ with $\boldsymbol{\Pi}_{iT} := \text{Var} \left(T^{-1/2} \sum_{t=1}^T \mathbf{S}'(\mathbf{W}_{it}^\top \bar{\boldsymbol{\theta}}_i, Y_t) \mathbf{W}_{it} \right)$.

Theorem 3.6 shows for smooth scoring functions that when the population quantities $\overline{\text{MCB}}_i$ or $\overline{\text{DSC}}_i$ attain their boundary value of zero, the non-negative test statistics $T \widehat{\text{MCB}}_{iT}$ and $T \widehat{\text{DSC}}_{iT}$ (see Theorem 3.2) converge to generalized χ^2 -distributions. Extending Theorem 3.6 to non-smooth scoring functions via the proof strategy of Theorem 3.4 would necessitate establishing stochastic equicontinuity of $\sqrt{T} \nu_{iT}(\boldsymbol{\theta}) = \sum_{t=1}^T \mathbf{S}(\mathbf{W}_{it}^\top \boldsymbol{\theta}, Y_t) - \mathbb{E} [\mathbf{S}(\mathbf{W}_{it}^\top \boldsymbol{\theta}, Y_t)]$. To the best of our knowledge, established techniques for such a derivation are currently unavailable in this context.

Recall that the asymptotic variance in the Gaussian case of Theorem 3.4 is unaffected by the estimation error in \widehat{r}_T and $\widehat{\boldsymbol{\theta}}_{iT}$; it depends solely on the sampling uncertainty from approximating expected scores by empirical averages, as captured by $\boldsymbol{\Omega}_T$ in (14). In contrast, the limiting distributions in Theorem 3.6 depend exclusively on the estimation effects, as summarized by $\boldsymbol{\Upsilon}_i$, \mathbf{H}_i , and $\boldsymbol{\Pi}_{iT}$, which correspond to the population counterparts of the asymptotic expansion in (17). Technically, this distinction arises because the asymptotic distribution in Theorem 3.4 is driven by *first-order* Taylor expansion terms, whereas the distributions in Theorem 3.6 are governed by *second-order* terms; see the proofs for details.

Feasible inference requires consistent estimators of the population matrices $\boldsymbol{\Omega}_T$, $\boldsymbol{\Pi}_{iT}$, $\boldsymbol{\Upsilon}_i^{-1}$, and \mathbf{H}_i^{-1} so that the asymptotic results in Theorems 3.4 and 3.6 remain valid when replacing population quantities by their estimates. While $\boldsymbol{\Upsilon}_i^{-1}$ and \mathbf{H}_i^{-1} admit consistent estimation via sample averages, we use HAC estimators for the long-run covariance matrices $\boldsymbol{\Omega}_T$ and $\boldsymbol{\Pi}_{iT}$ to accommodate serial dependence (Newey and West, 1987; Andrews, 1991). Consistency follows by standard arguments, see e.g., White (2001, Chapter 6.4) for smooth and Galvao and Yoon (2024) for non-smooth scoring functions.

3.3 Testable hypotheses

For “one-sample” hypotheses of the form $\overline{\text{MCB}}_i = c$ or $\overline{\text{DSC}}_i = c$ for some $c \geq 0$, the appropriate asymptotic distribution—Gaussian or generalized χ^2 —can be selected directly based on the value of c . Under “two-sample” hypotheses such as $\overline{\text{MCB}}_1 = \overline{\text{MCB}}_2$ or $\overline{\text{DSC}}_1 = \overline{\text{DSC}}_2$, however, the *population* values $\overline{\text{MCB}}_i$ and $\overline{\text{DSC}}_i$ may be either zero or strictly positive, so it is *a priori* unclear whether the Gaussian or the generalized χ^2 approximation applies. A valid testing procedure must therefore remain robust to both possibilities. We achieve this by employing a hybrid of intersection–union and union–intersection testing principles (Berger, 1997).

For example, consider the hypothesis $\mathcal{H}_{\text{MCB}} : \overline{\text{MCB}}_1 = \overline{\text{MCB}}_2$, which we can rewrite as

$$\begin{aligned}\mathcal{H}_{\text{MCB}} &= \{\overline{\text{MCB}}_1 = \overline{\text{MCB}}_2\} \\ &= \{\overline{\text{MCB}}_1 = \overline{\text{MCB}}_2 > 0\} \cup \{\overline{\text{MCB}}_1 = \overline{\text{MCB}}_2 = 0\} \\ &= \{\overline{\text{MCB}}_1 = \overline{\text{MCB}}_2 > 0\} \cup (\{\overline{\text{MCB}}_1 = 0\} \cap \{\overline{\text{MCB}}_2 = 0\}) \\ &=: \mathcal{H}_{\text{MCB}}^+ \cup (\mathcal{H}_{\text{MCB}_1}^0 \cap \mathcal{H}_{\text{MCB}_2}^0).\end{aligned}\tag{18}$$

For the hypothesis $\mathcal{H}_{\text{MCB}}^+$, we employ the *selection vector* $\boldsymbol{\omega} = (1, 0, -1, 0)^\top$ such that Theorem 3.4 yields

$$\left(\boldsymbol{\omega}^\top \boldsymbol{\Xi} \boldsymbol{\Omega}_T \boldsymbol{\Xi}^\top \boldsymbol{\omega}\right)^{-1/2} \sqrt{T} \left((\widehat{\text{MCB}}_{1T} - \widehat{\text{MCB}}_{2T}) - (\overline{\text{MCB}}_1 - \overline{\text{MCB}}_2) \right) \xrightarrow{d} \mathcal{N}(0, 1),\tag{19}$$

which immediately gives an asymptotically valid p -value called p_{MCB}^+ .

For smooth scoring functions, we test the hypothesis $\mathcal{H}_{\text{MCB}_i}^0$ for $i = 1, 2$ based on the test statistic $T \widehat{\text{MCB}}_{iT}$ and the asymptotic approximation from Theorem 3.6. For a realized value of $T \widehat{\text{MCB}}_{iT}$, we compute the associated p -values $p_{\text{MCB}_i}^0 = \mathbb{P}(0.5 \mathbf{N}_{iT}^\top \boldsymbol{\Upsilon}_i^{-1} \mathbf{N}_{iT} > T \widehat{\text{MCB}}_{iT})$ by using the method of Imhof (1961), which uses an inversion formula to express the probability as a definite integral of the characteristic function that is solved via numerical integration by using the R package `CompQuadForm` (Duchesne and Lafaye De Micheaux, 2010). For non-smooth scoring functions as the GPL score from (7), we test the hypothesis $\mathcal{H}_{\text{MCB}_i}^0$ by using the VQR test of Gaglianone et al. (2011) and denote its p -value by $p_{\text{MCB}_i}^0$.

Using (18), an asymptotically valid p -value for the combined null hypothesis \mathcal{H}_{MCB} is

$$p_{\text{MCB}} := \max(p_{\text{MCB}}^+, 2 \min(p_{\text{MCB}_1}^0, p_{\text{MCB}_2}^0)).\tag{20}$$

Similarly, we obtain an asymptotically valid p -value, p_{DSC} , for testing equal discrimination,

$$\mathcal{H}_{\text{DSC}} = \{\overline{\text{DSC}}_1 = \overline{\text{DSC}}_2\} = \{\overline{\text{DSC}}_1 = \overline{\text{DSC}}_2 > 0\} \cup (\{\overline{\text{DSC}}_1 = 0\} \cap \{\overline{\text{DSC}}_2 = 0\}),\tag{21}$$

by adapting (18) and (20). The Gaussian p -value follows from (19) by setting $\boldsymbol{\omega} = (0, 1, 0, -1)^\top$, while for smooth scoring functions, the corresponding generalized χ^2 -probability is computed analogously using the method of Imhof (1961). For non-smooth scoring functions, we test $\overline{\text{DSC}}_i = 0$ through the MZ-type regression of the VQR test, but by simply testing the hypothesis of a zero slope.

A classical DM test for equal expected scores, $\mathcal{H}_S = \{\bar{S}_1 = \bar{S}_2\}$, arises as a special case of Theorem 3.4 for $\boldsymbol{\omega} = (1, -1, -1, 1)^\top$. Confidence intervals for the individual decomposition terms as well as their differences can be obtained by inverting the above tests.

3.4 Low-level inference conditions for mean and quantile forecasts

We begin with mean forecasts, where Γ corresponds to the expectation. In this case, all strictly consistent scoring functions belong to the Bregman class given in (4). For this class, we verify the high-level Assumptions 3.3 and 3.5—and hence the validity of Theorems 3.4 and 3.6—in a general time-series setting.

Assumption 3.7. *The following holds for $i = 1, 2$:*

- (i) *The function $\phi(z)$ in (4) is five times continuously differentiable with $\phi''(z) > 0$ for all $z \in \mathbf{A} = \mathbf{O}$.*
- (ii) *$(Y_t, \mathbf{W}_{it}^\top)_{t \in \mathbb{N}}$ is strong mixing of size $-s/(s-2)$, $s > 2$; see [White \(2001, Definition 3.45\)](#).*
- (iii) *The matrix $\mathbb{E}[\mathbf{W}_{it} \mathbf{W}_{it}^\top]$ is positive definite.*
- (iv) *The matrix $\mathbf{V}_T := \text{Var}\left(T^{-1/2} \sum_{t=1}^T \phi''(\mathbf{W}_{it}^\top \bar{\boldsymbol{\theta}}_i) \mathbf{W}_{it} (\mathbf{W}_{it}^\top \bar{\boldsymbol{\theta}}_i - Y_t)\right)$ is uniformly positive definite for T large enough.*
- (v) *The following moments exist and are finite for all $\boldsymbol{\theta} \in \Theta$, $t \in \mathbb{N}$, and $s > 2$ from condition (ii): $\mathbb{E}\left[|\phi(Y_t)|^{2s}\right]$; $\mathbb{E}\left[|\phi(\mathbf{W}_{it}^\top \boldsymbol{\theta})|^{2s}\right]$; $\mathbb{E}\left[|\phi'(\mathbf{W}_{it}^\top \boldsymbol{\theta})(Y_t - \mathbf{W}_{it}^\top \boldsymbol{\theta})|\right]$;
 $\mathbb{E}\left[\sup_{\boldsymbol{\theta} \in \Theta} \|\phi''(\mathbf{W}_{it}^\top \boldsymbol{\theta})(Y_t - \mathbf{W}_{it}^\top \boldsymbol{\theta}) \mathbf{W}_{it}\|^s\right]$; $\mathbb{E}\left[\sup_{\boldsymbol{\theta} \in \Theta} \|\phi'''(\mathbf{W}_{it}^\top \boldsymbol{\theta})(\mathbf{W}_{it}^\top \boldsymbol{\theta} - Y_t) \mathbf{W}_{it} \mathbf{W}_{it}^\top\|\right]$;
 $\mathbb{E}\left[\sup_{\boldsymbol{\theta} \in \Theta} |\phi''''(\mathbf{W}_{it}^\top \boldsymbol{\theta})| \|\mathbf{W}_{it}^\top \boldsymbol{\theta} - Y_t\| \|\mathbf{W}_{it}\|^3\right]$; and $\mathbb{E}\left[\sup_{\boldsymbol{\theta} \in \Theta} |\phi'''''(\mathbf{W}_{it}^\top \boldsymbol{\theta})| (\mathbf{W}_{it}^\top \boldsymbol{\theta} - Y_t) \|\mathbf{W}_{it}\|^4\right]$.*

Assumption 3.7 resembles standard time series conditions for mean regression. Item (i) is a smoothness and convexity condition on the scoring function. For the SE scoring function, we often use $\mathbf{A} = \mathbf{O} = \mathbb{R}$, whereas the QLIKE score requires positive values such as $\mathbf{A} = \mathbf{O} = (0, \infty)$. Item (ii) is a classical mixing condition that ensures that suitable LLNs and CLTs apply and items (iii) and (iv) are standard in M-estimation ([Newey and McFadden, 1994](#), Chapter 3.1). Item (v) collects moment conditions, which simplify considerably for the common choices $\phi_{\text{SE}}(z) = z^2$ and $\phi_{\text{QL}}(z) = -\log(z)$ of the SE and QLIKE scores in (5) and (6).

Assumption 3.8. *The matrix $\boldsymbol{\Omega}_T$ from (14) is uniformly positive definite for T large enough.*

Positive definiteness of $\boldsymbol{\Omega}_T$ is stated in the separate Assumption 3.8 as it is required for the asymptotic normality result in Theorem 3.4, but is violated in the cases $\overline{\text{MCB}}_i = 0$ and $\overline{\text{DSC}}_i = 0$, and is as such not required for the verification of the conditions of Theorem 3.6. The positive definiteness of $\boldsymbol{\Omega}_T$ essentially imposes non-collinearity conditions for the (sum over time of the) original, recalibrated, and reference scores. Violations arise, for instance, if the recalibrated score is a constant multiple of the original score for all $t \in \mathbb{N}$, in which case $\overline{\text{MCB}}_i = 0$ follows.

Proposition 3.9. *Consider a Bregman score from (4) for the decomposition, which is also used in (12). Then:*

- *Assumptions 3.1, 3.7, and 3.8 imply Assumption 3.3 such that Theorem 3.4 holds; and*
- *Assumptions 3.1 and 3.7 imply Assumption 3.5 such that Theorem 3.6 holds.*

We continue with the case where Γ is the α -quantile for some $\alpha \in (0, 1)$, where all strictly consistent loss functions are given by the GPL class in (7). For a linear GPL score decomposition, we employ (generalized) quantile regression by combining the estimator (12) with the loss in (7) and impose the following conditions.

Assumption 3.10. *The following holds for $i = 1, 2$:*

- (i) The function g from (7) is twice continuously differentiable with $g'(z) > 0$ for all $z \in \mathbf{A} = \mathbf{O}$.
- (ii) The sequence $(Y_t, \mathbf{W}_{it}^\top)_{t \in \mathbb{N}}$ is strong mixing of size $-s/(s-2)$ for some $s > k + \delta$ with $\delta > 0$, and where k is the dimensionality of Θ from Assumption 3.1.
- (iii) For all $t \in \mathbb{N}$, F_{it} , the conditional distribution of Y_t given \mathcal{W}_{it} , belongs to a class of distributions that possess a positive Lebesgue density f_{it} with $0 < f_{it}(x) \leq K < \infty$, uniformly on the support of F_{it} .
- (iv) The matrix $\mathbb{E}[\mathbf{W}_{it}\mathbf{W}_{it}^\top]$ is positive definite.
- (v) The matrix $\mathbf{V}_T := \text{Var}\left(T^{-1/2} \sum_{t=1}^T g'(\mathbf{W}_{it}^\top \bar{\theta}_i)(\mathbb{1}\{Y_t \leq \mathbf{W}_{it}^\top \bar{\theta}_i\} - \alpha) \mathbf{W}_{it}\right)$ is uniformly positive definite for T large enough.
- (vi) $\mathbb{E}|Y_t| < \infty$, $\mathbb{E}|g(Y_t)| < \infty$, $\mathbb{E}\|\mathbf{W}_{it}\|^s < \infty$, $\mathbb{E}|g(\mathbf{W}_{it}^\top \boldsymbol{\theta}) - g(Y_t)|^s < \infty$, $\mathbb{E}\|\mathbf{W}_{it}\|^s < \infty$ and there exist integrable functions G and G' , G'_2 , G'' such that $\|\mathbf{W}_{it}g(\mathbf{W}_{it}^\top \boldsymbol{\theta})\| \leq G(\mathbf{W}_{it})$, $\|\mathbf{W}_{it}g'(\mathbf{W}_{it}^\top \boldsymbol{\theta})\| \leq G'(\mathbf{W}_{it})$, $\|\mathbf{W}_{it}\mathbf{W}_{it}^\top g'(\mathbf{W}_{it}^\top \boldsymbol{\theta})\| \leq G'_2(\mathbf{W}_{it})$, and $\|\mathbf{W}_{it}\mathbf{W}_{it}^\top g''(\mathbf{W}_{it}^\top \boldsymbol{\theta})\| \leq G''(\mathbf{W}_{it})$, where s is from condition (ii).
- (vii) The matrix $\boldsymbol{\Omega}_T$ from (14) is uniformly positive definite for T large enough.

The conditions of Assumption 3.10 are standard regularity conditions for quantile regression, but also cover the case of estimation through the more general GPL loss functions. The required moments of order $s > k$ are required for the derivation of stochastic equicontinuity for strong mixing processes through Hansen (1996). As we consider low dimensionalities of $\Theta \subset \mathbb{R}^k$ such as $k = 2$ in our applications, this is not overly restrictive.

Compared to Assumption 3.7, the conditions in Assumption 3.10 require the conditional distribution to be absolutely continuous, as specified in item (iii); this is a standard requirement for quantile regression frameworks. Furthermore, item (vii) is included here because the subsequent proposition specifically verifies the conditions for the asymptotic normality result established in Theorem 3.4, but does not treat the case of Theorem 3.6.

Proposition 3.11. *Consider a GPL score from (7) for the decomposition, that is also used in (12). Then, Assumptions 3.1 and 3.10 imply Assumption 3.3 such that Theorem 3.4 holds.*

Proposition 3.11 verifies the high-level conditions of Theorem 3.4 through standard conditions from (time series) quantile regression. Notice that Theorem 3.6 only applies to smooth loss functions, and hence, the cases $\overline{\text{MCB}}_i = 0$ and $\overline{\text{DSC}}_i = 0$ require a different treatment for the case of quantile forecasts. For the case $\overline{\text{MCB}}_i = 0$, we employ the quantile-specific MZ-test of Gaglianone et al. (2011), which we adapt for the case of $\overline{\text{DSC}}_i = 0$ by simply testing for a zero slope in the MZ-regression. The resulting p -values are accordingly used in the combination method in (20).

3.5 Relation to Value-at-Risk backtests

VaR backtesting is a fundamental pillar of financial risk management, used to assess whether a model accurately predicts the frequency and magnitude of potential losses. Traditional backtests

Table 2: Summary of prominent VaR backtests, including the underlying hypothesis, methodology and relation to conditional calibration in (10) through $\mathcal{G}_{it} = \sigma(\mathbf{G}_{it})$. We use the shorthand $\mathbf{V}_{it-l} := \mathbf{V}(X_{it-l}, Y_{t-l})$ for $l \geq 0$.

Reference	Label	Covariates/Instruments \mathbf{G}_{it}	Method	Hypothesis \mathcal{H}_0
<u>Two-sided backtests</u>				
Kupiec (1995)	UC	$\mathbf{G}_{it} = 1$	$\mathbb{E}[\mathbf{V}(X_{it}, Y_t) \mathbf{G}_{it}] = \mathbf{G}_{it}^\top \bar{\boldsymbol{\beta}}_i$	$\bar{\boldsymbol{\beta}}_i = \mathbf{0}$
Christoffersen (1998)	CC	$\mathbf{G}_{it} = (1, \mathbf{V}_{it-1})^\top$	$\mathbb{E}[\mathbf{V}(X_{it}, Y_t) \mathbf{G}_{it}] = \mathbf{G}_{it}^\top \bar{\boldsymbol{\beta}}_i$	$\bar{\boldsymbol{\beta}}_i = \mathbf{0}$
Engle and Manganelli (2004)	DQ	$\mathbf{G}_{it} = (1, \mathbf{V}_{it-1}, \dots, \mathbf{V}_{it-4})^\top$	$\mathbb{E}[\mathbf{V}(X_{it}, Y_t) \mathbf{G}_{it}] = \mathbf{G}_{it}^\top \bar{\boldsymbol{\beta}}_i$	$\bar{\boldsymbol{\beta}}_i = \mathbf{0}$
Kuester et al. (2005)	DQX	$\mathbf{G}_{it} = (1, X_{it}, \mathbf{V}_{it-1}, \dots, \mathbf{V}_{it-4})^\top$	$\mathbb{E}[\mathbf{V}(X_{it}, Y_t) \mathbf{G}_{it}] = \mathbf{G}_{it}^\top \bar{\boldsymbol{\beta}}_i$	$\bar{\boldsymbol{\beta}}_i = \mathbf{0}$
Gaglianone et al. (2011)	VQR	$\mathbf{G}_{it} = (1, X_{it})^\top$	$Q_\alpha(Y_t \mathbf{G}_{it}) = \mathbf{G}_{it}^\top \bar{\boldsymbol{\beta}}_i$	$\bar{\boldsymbol{\beta}}_i = (0, 1)^\top$
<u>One-sided backtests</u>				
Basel Committee (1996)	Basel	$\mathbf{G}_{it} = 1$	Binomial CDF	$\mathbb{E}[\mathbf{V}_{it}] \leq 0$
Nolde and Ziegel (2017)	NZ	$\mathbf{G}_{it} = (1, X_{it})^\top$	Moment Condition	$\mathbb{E}[\mathbf{G}_{it}^\top \mathbf{V}_{it}] \leq 0$

such as by Kupiec (1995) and the traffic light system of Basel Committee (1996, 2019b) typically focus on unconditional counts for the “violations” or “hits”, where realized losses exceed the VaR predictions as captured through the quantile identification functions, $\mathbf{V}_{it} = \mathbf{V}(X_{it}, Y_t) = \mathbb{1}\{Y_t \leq X_{it}\} - \alpha$, from (10). These unconditional tests, however, remain insensitive to the clustering of violations—a phenomenon particularly critical during financial crises, when consecutive days of unpredicted losses can lead to rapid capital depletion.

Following the seminal work of Christoffersen (1998), a plethora of *conditional* backtests has been proposed over the past decades. See e.g., Campbell (2007) and Nieto and Ruiz (2016) for comprehensive reviews on VaR backtesting. Most of these methods test hypotheses closely related to the conditional calibration property in (10) by utilizing varying information sets $\mathcal{G}_{it} = \sigma(\mathbf{G}_{it})$. Table 2 provides a non-exhaustive list of prominent VaR backtests, illustrating the intrinsic connection between their choice of covariates (or instruments) \mathbf{G}_{it} and our recalibration variables \mathbf{W}_{it} . Notably, the equivalence between (8) and (10) permits specifications based on either quantile regressions for Y_t , or mean regressions for the respective identification function.

As a canonical case of assessing auto-calibration, the quantile-specific adaptation of the MZ backtest by Gaglianone et al. (2011) utilizes the same recalibration technique as our linear score decomposition when $\mathbf{W}_{it}^\top = (1, X_{it})$. By matching the recalibration variables \mathbf{W}_{it} with the covariates \mathbf{G}_{it} , both the score decompositions and the underlying inference can be tailored to the specific notion of conditional calibration underlying the other backtests presented in Table 2.

4 Simulations

We now assess the finite-sample performance of the proposed tests from Section 3.3. Section 4.1 describes the simulation setup and Section 4.2 reports the results.

4.1 Simulation setup

To empirically validate our tests for equal miscalibration, with null hypothesis $\mathcal{H}_{\text{MCB}} : \overline{\text{MCB}}_1 = \overline{\text{MCB}}_2$, or for equal discrimination, with $\mathcal{H}_{\text{DSC}} : \overline{\text{DSC}}_1 = \overline{\text{DSC}}_2$, between competing mean or quantile forecasts, we use the following data-generating process (DGP) for the realizations,

$$Y_t = \mathbf{V}_t^\top \boldsymbol{\gamma} + \varepsilon_{Y,t}, \quad \text{with} \quad \mathbf{V}_t = (K_t, L_t, M_t, N_t)^\top \quad \text{and} \quad \boldsymbol{\gamma} = (\gamma_K, \gamma_L, \gamma_M, \gamma_N)^\top, \quad (22)$$

with $\varepsilon_{Y,t} \stackrel{\text{iid}}{\sim} \mathcal{N}(0, 1)$. The predictor variables in \mathbf{V}_t follow independent autoregressive AR(1) processes $K_t = \beta K_{t-1} + \varepsilon_{K,t}$, $L_t = \beta L_{t-1} + \varepsilon_{L,t}$, $M_t = \beta M_{t-1} + \varepsilon_{M,t}$, $N_t = \beta N_{t-1} + \varepsilon_{N,t}$, with fixed $\beta = 0.25$ and $\varepsilon_{K,t}, \varepsilon_{L,t}, \varepsilon_{M,t}, \varepsilon_{N,t} \stackrel{\text{iid}}{\sim} \mathcal{N}(0, 1)$, which are all mutually independent.

Forecaster X_{1t} has exclusive access to K_t and forecaster X_{2t} to L_t , while both forecasters share information on M_t and N_t as formalized by $\mathcal{I}_{1t} = \sigma\{K_t, M_t, N_t\}$ and $\mathcal{I}_{2t} = \sigma\{L_t, M_t, N_t\}$. Notice that our setup requires both “joint” predictors M_t and N_t in order to construct non-collinear forecasts with equal $\overline{\text{MCB}}$ and/or $\overline{\text{DSC}}$ values.

Based on the distinct information sets \mathcal{I}_{1t} and \mathcal{I}_{2t} , the forecasters issue *mean* forecasts

$$X_{1t} = \delta_0 + \mathbf{V}_t^\top \boldsymbol{\delta}, \quad \text{with} \quad \boldsymbol{\delta} = (\delta_K, 0, \delta_M, \delta_N)^\top \in \mathbb{R}^4, \quad (23)$$

$$X_{2t} = \xi_0 + \mathbf{V}_t^\top \boldsymbol{\xi}, \quad \text{with} \quad \boldsymbol{\xi} = (0, \xi_L, \xi_M, \xi_N)^\top \in \mathbb{R}^4, \quad (24)$$

and $\delta_0, \xi_0 \in \mathbb{R}$. The imposed zeros in $\boldsymbol{\delta}$ and $\boldsymbol{\xi}$ reflect the absence of the corresponding predictor variables in the information sets of the respective forecaster. The coefficients $(\delta_0, \boldsymbol{\delta}^\top)$ and $(\xi_0, \boldsymbol{\xi}^\top)$ and their relation to $\boldsymbol{\gamma}$ allows to generate forecasts with different calibration and discrimination properties, as formalized in the following proposition for the squared error score from (5).

Proposition 4.1. *For realizations Y_t and forecasts X_{1t} and X_{2t} following (22)–(24) with $\boldsymbol{\delta} \neq 0$ and $\boldsymbol{\xi} \neq 0$, and given the recalibration information $\mathcal{W}_{it} = \sigma\{\mathbf{W}_{it}\}$, with $\mathbf{W}_{it} = (1, X_{it})^\top$, $i = 1, 2$, the population squared error score decomposition of the forecasts X_{1t} is*

$$\overline{\text{MCB}}_1 = \delta_0^2 + \varsigma \cdot \frac{(\boldsymbol{\delta}^\top \boldsymbol{\delta} - \boldsymbol{\delta}^\top \boldsymbol{\gamma})^2}{\boldsymbol{\delta}^\top \boldsymbol{\delta}}, \quad \overline{\text{DSC}}_1 = \varsigma \cdot \frac{(\boldsymbol{\delta}^\top \boldsymbol{\gamma})^2}{\boldsymbol{\delta}^\top \boldsymbol{\delta}}, \quad \overline{\text{UNC}} = \varsigma \cdot \boldsymbol{\gamma}^\top \boldsymbol{\gamma} + 1, \quad (25)$$

where $\varsigma = \frac{1}{1-\beta^2}$ is the variance of the zero-mean AR(1) processes K_t, L_t, M_t, N_t . For $\overline{\text{MCB}}_2$ and $\overline{\text{DSC}}_2$ interchange δ_0^2 and $\boldsymbol{\delta}$ with ξ_0^2 and $\boldsymbol{\xi}$, respectively.

The expressions in Proposition 4.1 illustrate that for non-constant forecasts, $\overline{\text{MCB}}_1 = 0$ holds if and only if $\boldsymbol{\delta}^\top \boldsymbol{\delta} = \boldsymbol{\delta}^\top \boldsymbol{\gamma}$ and $\delta_0 = 0$. Hence, perfect calibration, $\overline{\text{MCB}}_1 = 0$, can be achieved even if the forecaster omits relevant variables. In fact, $\overline{\text{MCB}}_1 = 0$ implies that if a predictor (say M_t) is used, it must be used with exactly the right parameter value ($\delta_M = \gamma_M$). This also implies that the use (e.g., $\delta_M \neq 0$) of irrelevant predictor variables (e.g., $\gamma_M = 0$) causes miscalibrated forecasts.

The $\overline{\text{DSC}}_1$ component is unaffected by the intercept δ_0 that does not carry any information. $\overline{\text{DSC}}_1$ is positive whenever $\boldsymbol{\delta}^\top \boldsymbol{\gamma} \neq 0$, that is, whenever X_{1t} reacts to the signal in Y_t , even incorrectly such as in the wrong direction. Moreover, by Cauchy-Schwarz, $\frac{(\boldsymbol{\delta}^\top \boldsymbol{\gamma})^2}{\boldsymbol{\delta}^\top \boldsymbol{\delta}} \leq \boldsymbol{\gamma}^\top \boldsymbol{\gamma}$, such that the maximal value of $\overline{\text{DSC}}_1$ is $\varsigma \boldsymbol{\gamma}^\top \boldsymbol{\gamma}$, which is attained if and only if the parameters $\boldsymbol{\delta}$ are chosen proportionally to $\boldsymbol{\gamma}$, i.e., $\boldsymbol{\delta} = c\boldsymbol{\gamma}$ for some $c \in \mathbb{R}$ as then, $\frac{(\boldsymbol{\delta}^\top \boldsymbol{\gamma})^2}{\boldsymbol{\delta}^\top \boldsymbol{\delta}} = \frac{c^2(\boldsymbol{\gamma}^\top \boldsymbol{\gamma})^2}{c^2 \boldsymbol{\gamma}^\top \boldsymbol{\gamma}} = \boldsymbol{\gamma}^\top \boldsymbol{\gamma}$. Hence, maximal discrimination can arise even for miscalibrated forecasts. If only some relevant variables are observed, the best achievable discrimination is obtained when the available predictors are used correctly. Analogous conclusions hold for the second forecaster X_{2t} by replacing $\boldsymbol{\delta}$ with $\boldsymbol{\xi}$.

The closed-form expressions in Proposition 4.1 enable diverse specifications of $\overline{\text{MCB}}_i$ and $\overline{\text{DSC}}_i$, allowing us to study the size and power of our proposed tests across different settings by appropriately choosing the parameters $\boldsymbol{\gamma}$, $(\delta_0, \boldsymbol{\delta}^\top)$, and $(\xi_0, \boldsymbol{\xi}^\top)$. In detail, Table 3 specifies twelve different parameterizations that result in illustrative settings for $\overline{\text{MCB}}_i$ and $\overline{\text{DSC}}_i$ as given in the

Table 3: Twelve *mean forecasting* specifications of the parameters $\gamma, \delta_0, \delta, \xi_0, \xi$ in (22)–(24) based on a flexible $k \in \{0, 0.05, \dots, 0.45, 0.5\}$. All setups guarantee non-collinear forecasts and generate different relations of the $\overline{\text{MCB}}$ and $\overline{\text{DSC}}$ values as given in the numbered rows and the last column termed “Implications”.

Realization				Forecaster X_{1t}					Forecaster X_{2t}					Implications
γ_K	γ_L	γ_M	γ_N	δ_0	δ_K	δ_L	δ_M	δ_N	ξ_0	ξ_K	ξ_L	ξ_M	ξ_N	
(A) Parameterization of $\overline{\text{MCB}}$ difference														
1) $\overline{\text{MCB}}_1(k) = \overline{\text{MCB}}_2(k) = \frac{8k^2}{15}$														
0	$\frac{1}{4}$	$\frac{1}{4}$	0	0	0	0	$\frac{k}{\sqrt{2}} + \frac{1}{4}$	0	0	0	$\frac{k}{2} + \frac{1}{4}$	$\frac{k}{2} + \frac{1}{4}$	0	$0 < \overline{\text{DSC}}_1 < \overline{\text{DSC}}_2$
$\frac{1}{4}$	$\frac{1}{4}$	$\frac{1}{4}$	0	0	$\frac{k}{2} + \frac{1}{4}$	0	$\frac{k}{2} + \frac{1}{4}$	0	0	0	$\frac{k}{2} + \frac{1}{4}$	$\frac{k}{2} + \frac{1}{4}$	0	$0 < \overline{\text{DSC}}_1 = \overline{\text{DSC}}_2$
2) $\overline{\text{MCB}}_1 = 0$ and $\overline{\text{MCB}}_2(k) = \frac{8k^2}{15}$														
0	$\frac{1}{4}$	$\frac{1}{4}$	0	0	0	0	$\frac{1}{4}$	0	0	0	$\frac{k}{2} + \frac{1}{4}$	$\frac{k}{2} + \frac{1}{4}$	0	$0 < \overline{\text{DSC}}_1 < \overline{\text{DSC}}_2$
$\frac{1}{4}$	$\frac{1}{4}$	$\frac{1}{4}$	0	0	$\frac{1}{4}$	0	$\frac{1}{4}$	0	0	0	$\frac{k}{2} + \frac{1}{4}$	$\frac{k}{2} + \frac{1}{4}$	0	$0 < \overline{\text{DSC}}_1 = \overline{\text{DSC}}_2$
3) $\overline{\text{MCB}}_1(k) = 2\overline{\text{MCB}}_2(k) = \frac{16k^2}{15}$														
0	$\frac{1}{4}$	$\frac{1}{4}$	0	0	0	0	$k + \frac{1}{4}$	0	0	0	$\frac{k}{2} + \frac{1}{4}$	$\frac{k}{2} + \frac{1}{4}$	0	$0 < \overline{\text{DSC}}_1 < \overline{\text{DSC}}_2$
$\frac{1}{4}$	$\frac{1}{4}$	$\frac{1}{4}$	0	0	$\frac{k}{\sqrt{2}} + \frac{1}{4}$	0	$\frac{k}{\sqrt{2}} + \frac{1}{4}$	0	0	0	$\frac{k}{2} + \frac{1}{4}$	$\frac{k}{2} + \frac{1}{4}$	0	$0 < \overline{\text{DSC}}_1 = \overline{\text{DSC}}_2$
(B) Parameterization of $\overline{\text{DSC}}$ difference														
4) $\overline{\text{DSC}}_1(k) = \overline{\text{DSC}}_2(k) = \frac{8k^2}{15}$														
0	0	0	k	0	$\frac{k}{2} + \frac{1}{4\sqrt{2}}$	0	0	$\frac{k}{2} + \frac{1}{4\sqrt{2}}$	0	0	$\frac{k}{2} + \frac{1}{4}$	0	$\frac{k}{2} + \frac{1}{4}$	$0 < \overline{\text{MCB}}_1 < \overline{\text{MCB}}_2$
0	0	0	k	0	$\frac{k}{2} + \frac{1}{4}$	0	0	$\frac{k}{2} + \frac{1}{4}$	0	0	$\frac{k}{2} + \frac{1}{4}$	0	$\frac{k}{2} + \frac{1}{4}$	$0 < \overline{\text{MCB}}_1 = \overline{\text{MCB}}_2$
5) $\overline{\text{DSC}}_1 = 0$ and $\overline{\text{DSC}}_2(k) = \frac{8k^2}{15}$														
0	0	0	k	0	0	0	$\frac{1}{4}$	0	0	0	$\frac{k}{2} + \frac{1}{4}$	0	$\frac{k}{2} + \frac{1}{4}$	$0 < \overline{\text{MCB}}_1 < \overline{\text{MCB}}_2$
0	0	0	k	0	$\frac{1}{4}$	0	$\frac{1}{4}$	0	0	0	$\frac{k}{2} + \frac{1}{4}$	0	$\frac{k}{2} + \frac{1}{4}$	$0 < \overline{\text{MCB}}_1 = \overline{\text{MCB}}_2$
6) $\overline{\text{DSC}}_1(k) = 2\overline{\text{DSC}}_2(k) = \frac{16k^2}{15}$														
0	0	0	k	0	0	0	0	$k + \frac{1}{4}$	0	0	$\frac{k}{2} + \frac{1}{4}$	0	$\frac{k}{2} + \frac{1}{4}$	$0 < \overline{\text{MCB}}_1 < \overline{\text{MCB}}_2$
0	0	0	k	$\frac{1}{\sqrt{15}}$	0	0	0	$k + \frac{1}{4}$	0	0	$\frac{k}{2} + \frac{1}{4}$	0	$\frac{k}{2} + \frac{1}{4}$	$0 < \overline{\text{MCB}}_1 = \overline{\text{MCB}}_2$

Table 4: Four *quantile forecasting* specifications of the parameters $\gamma, \delta_0, \delta, \xi_0, \xi$ in (22) and (26) based on a flexible $k \in \{0, 0.05, \dots, 0.95, 1\}$. All setups guarantee non-collinear forecasts and generate different relations of the $\overline{\text{MCB}}$ and $\overline{\text{DSC}}$ values as given in the numbered rows and the last column termed “Implications”. The values of $\xi_0(k, \alpha)$ are chosen numerically such that $\overline{\text{MCB}}_1(k) = \overline{\text{MCB}}_2(k)$ holds; see Appendix C and Figure C.1 for details.

Realization				Forecaster X_{1t}^α					Forecaster X_{2t}^α					Implications
γ_K	γ_L	γ_M	γ_N	δ_0	δ_K	δ_L	δ_M	δ_N	ξ_0	ξ_K	ξ_L	ξ_M	ξ_N	
(A) Parameterization of $\overline{\text{MCB}}$ difference														
1) $\overline{\text{MCB}}_1(k) = \overline{\text{MCB}}_2(k)$ increasing with $k \geq 0$, starting from 0														
$\frac{1}{4}$	$\frac{1}{4}$	$\frac{1}{4}$	0	0	$\frac{k}{2} + \frac{1}{4}$	0	$\frac{k}{2} + \frac{1}{4}$	0	0	0	$\frac{k}{2} + \frac{1}{4}$	$\frac{k}{2} + \frac{1}{4}$	0	$0 < \overline{\text{DSC}}_1 = \overline{\text{DSC}}_2$
2) $\overline{\text{MCB}}_1 = 0$ and $\overline{\text{MCB}}_2(k)$ increasing with $k \geq 0$, starting from 0														
$\frac{1}{4}$	$\frac{1}{4}$	$\frac{1}{4}$	0	0	$\frac{1}{4}$	0	$\frac{1}{4}$	0	0	0	$\frac{k}{2} + \frac{1}{4}$	$\frac{k}{2} + \frac{1}{4}$	0	$0 < \overline{\text{DSC}}_1 = \overline{\text{DSC}}_2$
(B) Parameterization of $\overline{\text{DSC}}$ difference														
4) $\overline{\text{DSC}}_1(k) = \overline{\text{DSC}}_2(k)$ increasing with $k \geq 0$, starting from 0														
0	0	0	k	0	$\frac{k}{2} + \frac{1}{4}$	0	0	$\frac{k}{2} + \frac{1}{4}$	0	0	$\frac{k}{2} + \frac{1}{4}$	0	$\frac{k}{2} + \frac{1}{4}$	$0 < \overline{\text{MCB}}_1(k) = \overline{\text{MCB}}_2(k)$
5) $\overline{\text{DSC}}_1 = 0$ and $\overline{\text{DSC}}_2(k)$ increasing with $k \geq 0$, starting from 0														
0	0	0	k	$\frac{1}{2}$	$\frac{1}{4}$	0	$\frac{1}{4}$	0	$\xi_0(k, \alpha)$	0	$\frac{k}{2} + \frac{1}{4}$	0	$\frac{k}{2} + \frac{1}{4}$	$0 < \overline{\text{MCB}}_1(k) = \overline{\text{MCB}}_2(k)$

facet labels of Figure 1. To analyze test power, we continuously misspecify the respective null hypotheses through a parameter $k > 0$ that affects $\gamma, (\delta_0, \delta^\top)$, and (ξ_0, ξ^\top) . The specifications of Table 3 are chosen to guarantee that either $\overline{\text{MCB}}_2(k)$ or $\overline{\text{DSC}}_2(k)$ depend on k and equal $\frac{8k^2}{15}$ for all $k \geq 0$. Figure D.1 in Appendix D plots the population values $\overline{\text{MCB}}_i$ and $\overline{\text{DSC}}_i, i = 1, 2$ as functions of k for all twelve setups.

For example, we generate the scenario $\overline{\text{MCB}}_1 = 0$ and $\overline{\text{MCB}}_2(k) = \frac{8k^2}{15}$ while maintaining $0 < \overline{\text{DSC}}_1 < \overline{\text{DSC}}_2$ independent of k by setting $\gamma^\top = (0, \frac{1}{4}, \frac{1}{4}, 0)$ as well as $(\delta_0, \delta^\top) = (0, 0, 0, \frac{1}{4}, 0)$ and $(\xi_0, \xi^\top) = (0, 0, \frac{1}{4} + \frac{k}{2}, \frac{1}{4} + \frac{k}{2}, 0)$. Here, the realizations are only driven by L_t and M_t with equal magnitudes, $\gamma_L = \gamma_M$. The first forecaster X_{1t} does not have access to L_t , but she correctly uses M_t through $\delta_M = \gamma_M$ such that her forecasts are perfectly calibrated, $\overline{\text{MCB}}_1 = 0$. The sole access to M_t however limits her discrimination to $\overline{\text{DSC}}_1 = \frac{1}{15}$. By contrast, the second forecaster X_{2t} uses both relevant variables L_t and M_t , and hence achieves a higher discrimination $\overline{\text{DSC}}_2 = \frac{2}{15} > \overline{\text{DSC}}_1$ for any $k \geq 0$. However, for values $k > 0$, she uses the information incorrectly with $\xi \neq \gamma$ such that $\overline{\text{MCB}}_2(k) = \frac{8k^2}{15}$ increases with k .

For the evaluation of our tests for *quantile forecasts*, we use the same DGP in (22). As the information in \mathbf{V}_t only affects the conditional mean of Y_t in (22), we generate the quantile forecasts at level $\alpha \in (0, 1)$ as

$$X_{1t}^\alpha = \mathbf{V}_t^\top \boldsymbol{\delta} + \delta_0 + \Phi^{-1}(\alpha), \quad \text{and} \quad X_{2t}^\alpha = \mathbf{V}_t^\top \boldsymbol{\xi} + \xi_0 + \Phi^{-1}(\alpha), \quad (26)$$

using the inverse of the standard normal CDF, denoted by $\Phi^{-1}(\cdot)$.

We deliberately use the pure location process (22) for quantile forecasts, allowing us to explicitly control the population miscalibration and discrimination values for the check loss in Proposition C.1, albeit these closed-form expressions become much more complicated as for the squared error. Due to this additional complication, we only consider four informative param-

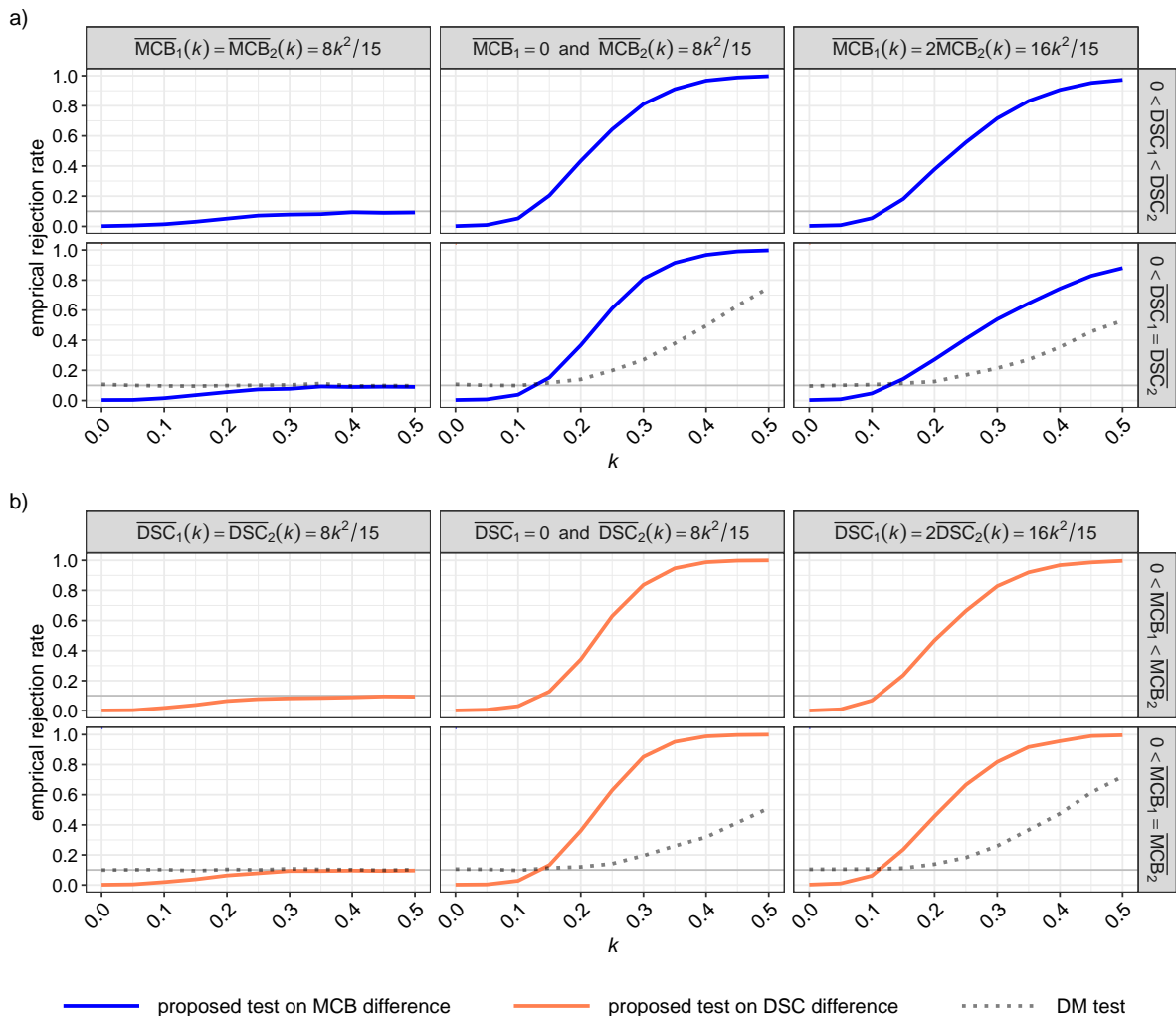


Figure 1: Empirical rejection rates for mean forecasts and the squared error score for the proposed tests of equal miscalibration (in blue) in the upper panel a), equal discrimination (in orange) in the lower panel b), and of the DM test of equal predictive performance (in gray) in the lower plots of both panels. We generate the data according to (22)–(24) with the twelve parameterizations of Table 3, which depend on the parameter $k \geq 0$ that is displayed on the x -axes. We use $T = 500$ and a nominal level of 10%.

eterizations as given in Table 4. For these, Appendix C provides the closed-form expressions for \overline{MCB}_i and \overline{DSC}_i as explicit functions of k, α and the parameters of the DGP. Notably, for the last parametrization, (approximate) equality of the miscalibration values is achieved by a numerical choice for the values of $\xi_0 = \xi_0(k, \alpha)$; see Figure C.1 and the text of Appendix C.

4.2 Simulation results

All results are based on 5000 Monte Carlo replications, a nominal significance level of 10% and $T = 500$. We estimate all long-run covariance matrices by the HAC estimator of Andrews (1991), adapted to quantile regressions by Galvao and Yoon (2024). For the implementation, we follow the default `vcovHAC` procedure from the R package `sandwich` of Zeileis (2004).

For *mean forecasts* and the associated squared error score, Figure 1 shows the rejection rates of the test for equal miscalibration $\mathcal{H}_{\text{MCB}} : \overline{MCB}_1 = \overline{MCB}_2$ in the upper panel in blue color, and

of the test for equal discrimination $\mathcal{H}_{\text{DSC}} : \overline{\text{DSC}}_1 = \overline{\text{DSC}}_2$ in orange color in the lower panel. For comparison, we also show rejection rates of the DM test of equal predictive power $\mathcal{H}_{\text{S}} : \bar{S}_1 = \bar{S}_2$ with gray and dotted lines. We only show these rejection rates when the underlying population score difference coincides with the respective difference in $\overline{\text{MCB}}$ or $\overline{\text{DSC}}$ values. E.g., in the lower row of panel a), we ensure $\overline{\text{DSC}}_1 = \overline{\text{DSC}}_2$ such that $\bar{S}_1 - \bar{S}_2 = \overline{\text{MCB}}_1 - \overline{\text{MCB}}_2$ and the tests of the hypotheses \mathcal{H}_{S} and \mathcal{H}_{MCB} are comparable.

Throughout the four plots in the left column, as well as for $k = 0$ in all twelve plots, the data is generated under the respective null hypotheses of equal miscalibration in panel a), and equal discrimination in panel b). Here, we find correct or conservative rejection rates below the nominal level of 10% for our tests, which is to be expected given the Bonferroni-type corrections from Section 3.3. In the left panel, our tests approach the correct size for larger values of k as e.g., for the MCB-test, miscalibration of both forecasts increases with k such that $2 \min\{p_{\text{MCB}_1}^0, p_{\text{MCB}_2}^0\}$ becomes much smaller than p_{MCB}^+ , which operates under its null hypothesis and hence generates asymptotically exact size control.

The middle and right plot columns show that for increasing k , power increases naturally in all subplots. This illustrates the robustness of our testing procedure to zero or positive values of the respective population $\overline{\text{MCB}}_i$ and $\overline{\text{DSC}}_i$ values. Importantly, in the cases where score differences coincide with $\overline{\text{MCB}}$ ($\overline{\text{DSC}}$) differences in the upper (lower) panel, the component tests' power increases substantially with respect to the DM test. This can be explained as in these cases, the DM test's (estimated) variance is affected by fluctuations of both, (estimated) MCB and DSC values whereas the MCB test is unaffected by noise in the DSC component, and vice versa. Hence, we can expect power gains by testing on the respective components, as will become evident in our applications in Section 5.

Figure 2 displays rejection rates for quantile forecasts at levels $\alpha \in \{0.01, 0.05, 0.1, 0.25, 0.5\}$ and within the four most informative parameterizations that allow for comparison with the DM test. These four scenarios correspond to the lower left and middle plots in panels a) and b) from Figure 1. The results for median forecasts with $\alpha = 0.5$ are comparable to the mean forecasting results from Figure 1: The tests are conservative under the null, develop power with $k > 0$ and despite their conservative size², our tests dominate the DM-test in terms of power. For more extreme quantile levels, power naturally declines. Importantly, and especially for the DSC test, the dominance of the DM test is even more pronounced for extreme quantile levels.

²In unreported simulations, we find that the elevated type I error of the DSC test in the third column for $\alpha = 0.01$ does not increase with k and declines as the sample size grows. This pattern suggests that the distortion is attributable to finite-sample effects.

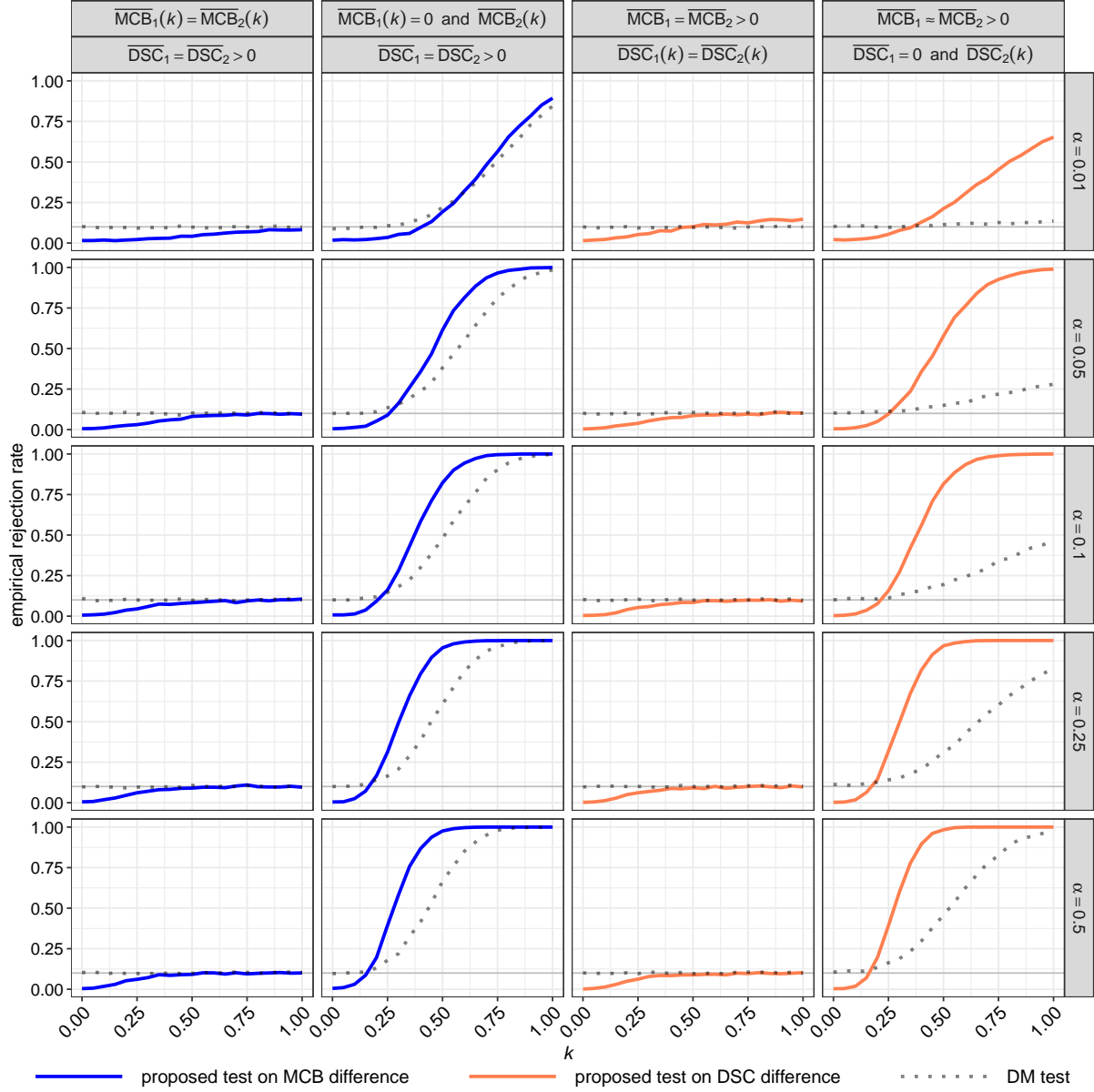


Figure 2: Empirical rejection rates for α -quantile forecasts and the check loss for the proposed tests of equal miscalibration (in blue) in the left two columns, equal discrimination (in orange) in the right two columns, and of the DM test of equal predictive performance (in gray) in all subplots. We generate the data according to (22) and (26) with the four parameterizations of Table 4, which depend on the parameter $k \geq 0$ that is displayed on the x -axes. We use $T = 500$ and a nominal level of 10%.

5 Applications

Here, we apply the proposed tests for equal miscalibration and discrimination in two central forecasting domains: inflation rates in Section 5.1 and financial risks in Section 5.2. Replication code and details on the data are available at https://github.com/marius-cp/SDI_replications.

5.1 Survey forecasts of U.S. annual CPI inflation

Inflation is renowned for being difficult to forecast, and survey forecasts often outperform sophisticated econometric models (Faust and Wright, 2013). We compare two popular one-year-ahead survey forecasts for quarterly U.S. CPI inflation: the Survey of Professional Forecasters (SPF) of the Federal Reserve Bank of Philadelphia, and the Michigan Survey of Consumers.³ The SPF is considered an expert forecast, as its panelists are professionals with extensive macroeconomic forecasting experience. In contrast, the Michigan survey randomly samples U.S. cell phone numbers, without targeting professionals. One might therefore expect the experts to outperform consumers, yet overall forecast comparisons are often inconclusive as e.g., in the empirical applications of Ehm et al. (2016) and Patton (2020).

The aim of this application is to demonstrate that, even when inference on the overall scores is inconclusive, the improved test power of the individual MCB and DSC decomposition terms illustrated in Section 4 can produce significant results with clear and interpretable insights while being applicable in general multi-step ahead forecast environments.

We replicate the analyses of Ehm et al. (2016) and Patton (2020), comparing the predictive performance of the SPF and Michigan survey forecasts, and extend their approach by applying our novel tests for equal forecast calibration and discrimination. Our evaluation sample covers $T = 154$ quarters, from 1982:Q3 to 2020:Q2, thereby excluding the high-inflation period following the COVID-19 pandemic. Figure 3 displays the forecasts alongside the corresponding realizations.

Michigan survey respondents report their expectations of the percentage change in prices over the next 12 months. To ensure comparability, we follow Ehm et al. (2016) and Patton

³Data sources: SPF forecasts (`Individual_CPI.xlsx`) from Philadelphia Fed; Michigan forecasts (Table 32) from their `data site`; and CPI data (`cpiQvMd.xlsx`) from Philadelphia Fed.

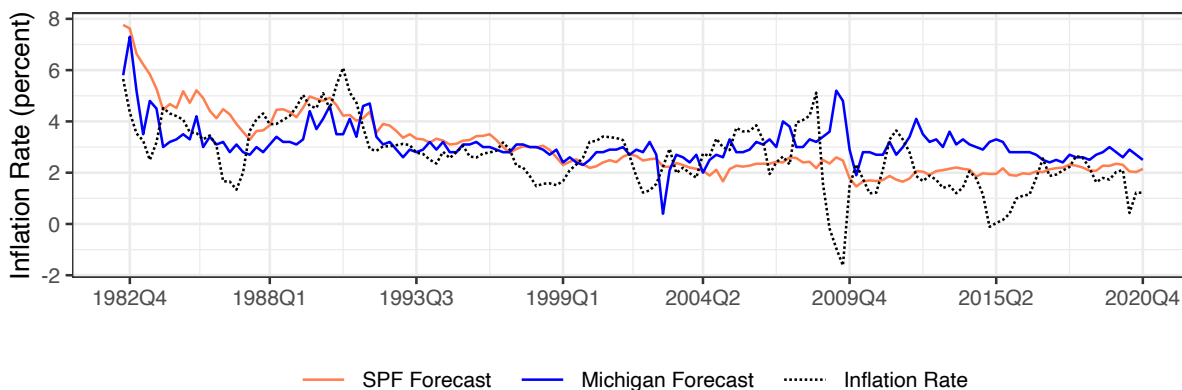


Figure 3: Quarterly year-over-year CPI inflation rate together with the SPF and Michigan forecasts. For details, see the text in Section 5.1.

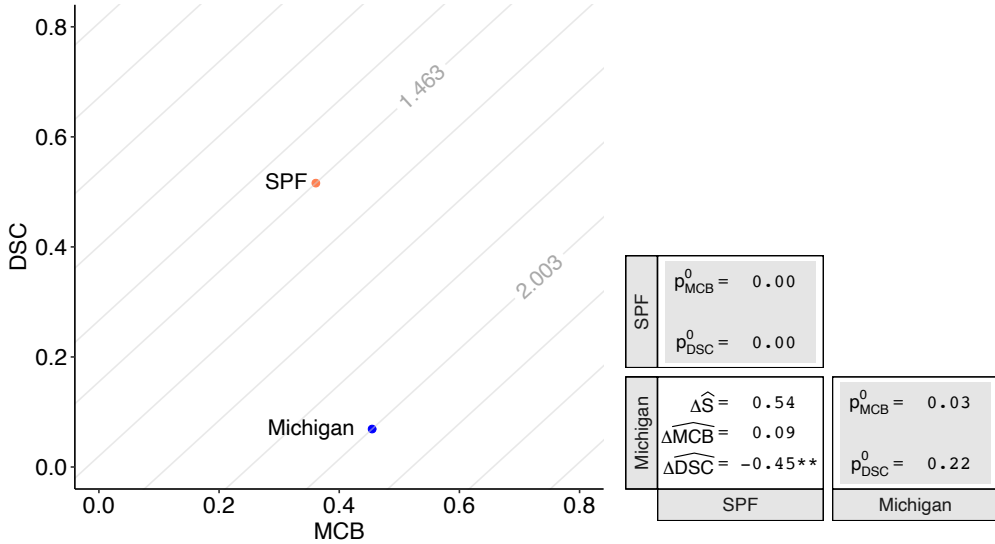


Figure 4: Inflation forecast evaluation results for the SPF and Michigan forecasts using the squared error scoring function. The left “MCB–DSC” plots show the average score as iso-lines together with its decomposition into miscalibration and discrimination components for the four competing forecasts. The gray boxes in the right panels display the p -values of tests for zero miscalibration and discrimination, respectively. The white box displays the average score, miscalibration and discrimination differences, together with 0 to 3 stars indicating significance at the 10%, 5%, and 1% levels.

(2020) and construct a corresponding SPF measure by averaging the one- to four-quarter-ahead consensus forecasts (where the consensus is defined as the median across respondents). Averaging is appropriate because SPF forecasts are stated in terms of annualized quarter-over-quarter inflation rates. As the evaluation target Y_t , we use the four-quarter logarithmic growth rate of the consumer price index (CPI), based on the 2023:Q3 vintage, over the year following the forecast date.

The left panel of Figure 4 reports the average squared error score together with its decomposition into miscalibration and discrimination components for the two competing forecasts. Calibration appears broadly similar across the two surveys. In contrast, the SPF forecasts display a markedly higher degree of discrimination—a difference that is not visible in the purely scoring-function-based analyses of Ehm et al. (2016) and Patton (2020). The right panel corroborates their main finding: the overall difference in predictive performance is statistically insignificant, with a p -value of 0.284.

Consistent with the visual impression from the left panel, the difference in miscalibration is not statistically significant. However, the SPF forecasts exhibit significantly stronger discrimination, with a p -value of 0.037. For the Michigan survey forecasts, we cannot even reject the null hypothesis of no discrimination. These findings suggest that professional forecasters’ predictions contain more information about future inflation outcomes, which is plausible given their field-specific expertise and experience.

Figure D.3 in Appendix D reports diagnostic checks for the linear recalibration regression and reveals no evidence of misspecification, supporting the use of linear recalibration for inference on score decompositions.

The macroeconomic literature following Coibion and Gorodnichenko (2015), as discussed

in the introduction, examines the sensitivity of forecast errors to additional covariates. These covariates can be integrated into our framework through the recalibration vector \mathbf{W}_{it} . Consequently, their tests for rational expectations focus on a specific dimension of forecast calibration. However, such evaluations fail to account for the underlying forecast discrimination—a component that our application to survey forecasts reveals to be fundamentally distinct from calibration performance.

From a methodological perspective, this application underscores the utility of our proposed inference framework. Beyond partitioning forecast performance into interpretable economic components, our tests can exhibit superior statistical power compared to the DM test in these settings. Furthermore, the framework is applicable in general time-series environments, including multi-step-ahead forecasting horizons.

5.2 Financial volatility and Value-at-Risk forecast performance

Here, we extend the motivational example from Section 1.1 and consider one-day-ahead forecasts of the variance and the α -quantiles (α -VaR), with $\alpha \in \{1\%, 5\%\}$, of financial log returns R_t . This application demonstrates the value of inference based on score decompositions, as it helps reconcile the partly contradictory findings that often arise between traditional backtests reviewed in Section 3.5 and scoring-function-based forecast evaluations in applied work such as in Section 1.1.

Given the standard assumption $\mathbb{E}[R_t] = 0$ such that $\text{Var}(R_t) = \mathbb{E}[R_t^2]$, the variance forecasts can be treated as forecasts for the expectation of R_t^2 , or as introduced below, the expectation of an unbiased RV estimator. Hence, we follow Patton (2011) and evaluate the forecasts with the squared error and QLIKE loss functions that are special cases of the Bregman class (4), considered in Proposition 3.9. For the VaR forecasts, we use the check loss from (7), as covered by Proposition 3.11.

For R_t , we use logarithmic returns of the S&P 500 E-mini futures, a highly liquid instrument central to practical portfolio management, which is widely used in the financial variance forecasting literature (Corsi, 2009; Liu et al., 2015; Bollerslev et al., 2018). E-mini contracts trade almost continuously from Sunday evening to Friday afternoon, with brief daily interruptions from 3:15–3:30 p.m. and 4:00–5:00 p.m. CT. A trading day is defined as the interval spanning from 5:00 p.m. CT of the preceding calendar day to 4:59 p.m. CT. We use intraday price observations from the data provider Refinitiv (ticker: ES_c1), spanning the period from January 1, 2000, to January 1, 2022. From this, we compute the daily open-to-close return R_t and the 5-minute realized variance, $\text{RV}_t := \sum_{m=1}^M r_{tm}^2$, where r_{tm} is the m -th intraday return on day t and M denotes the number of equally spaced observations per trading day.

We employ several standard models to generate one-step-ahead variance forecasts. Specifically, we consider the Gaussian GARCH model of Bollerslev (1986) and its asymmetric extension, the GJR-GARCH model of Glosten et al. (1993), estimated with Student’s t residuals, given by

$$\begin{aligned} R_t &= \sqrt{\sigma_t^2} \varepsilon_t, & \text{with } \varepsilon_t &\stackrel{\text{iid}}{\sim} t_\nu, \\ \sigma_t^2 &= \alpha_0 + \alpha_1 \sigma_{t-1}^2 + \alpha_2 R_{t-1}^2 + \alpha_3 R_{t-1}^2 \mathbb{1}\{R_{t-1} < 0\}. \end{aligned} \tag{27}$$

We further use two models that use high-frequency information through the RV estimator. The third model is the Heterogeneous Autoregressive (HAR) model proposed by [Corsi \(2009\)](#),

$$RV_t^{1/2} = \beta_0 + \beta_1 RV_{t-1}^{1/2} + \beta_2 \overline{RV}_{w,t-1}^{1/2} + \beta_3 \overline{RV}_{m,t-1}^{1/2} + \varepsilon_t, \quad \text{with} \quad \varepsilon_t \stackrel{\text{iid}}{\sim} \mathcal{N}(0, \sigma^2),$$

where $\overline{RV}_{w,t}^{1/2} := \frac{1}{5} \sum_{j=0}^4 RV_{t-j}^{1/2}$ and $\overline{RV}_{m,t}^{1/2} := \frac{1}{22} \sum_{j=0}^{21} RV_{t-j}^{1/2}$ are weekly and monthly averages, respectively. Fourth, we employ the MIDAS model of [Ghysels et al. \(2006, 2016\)](#), where $RV_t^{1/2}$ is predicted based on a weighted average of its lagged values,

$$RV_t^{1/2} = \phi_0 + \sum_{l=1}^{20} w_l RV_{t-l}^{1/2} + \varepsilon_t, \quad \text{with} \quad \varepsilon_t \stackrel{\text{iid}}{\sim} \mathcal{N}(0, \sigma^2),$$

where the MIDAS weights w_l are parameterized through the exponential Almon polynomial.

We construct VaR forecasts for these four models by using the α -quantile of the imposed residual distribution multiplied by the square root of the respective variance forecast. For quantile forecasts, we additionally use the classical Historical Simulation (HS) method, that uses the empirical α -quantile of the preceding 250 trading days as a quantile forecast.

For the first four models, we estimate the parameters by maximum likelihood using the imposed residual distributions, based on a fixed estimation window from January 1, 2000, to December 31, 2007, corresponding to approximately the first third of the sample. The subsequent period from January 1, 2008 to January 1, 2022 serves as evaluation period, yielding $T = 3617$ one-step ahead forecasts and corresponding realizations. [Figure D.2](#) in [Appendix D](#) shows the variance and VaR forecasts together with their evaluation targets.

[Figure 5](#) presents the evaluation of variance forecasts under the QLIKE and SE scoring functions. The left panels, following [Dimitriadis et al. \(2024b\)](#), plot the estimated miscalibration and discrimination of the four forecasting methods along the axes. Gray iso-lines represent average score levels, with observations closer to the upper-left corner indicating superior performance. We find that the RV-based forecasting methods exhibit markedly stronger discrimination, which translates into better overall predictive accuracy as reflected in the average scores.

The right panel of [Figure 5](#) reports the corresponding test results: Gray-shaded boxes display p -values for tests of zero miscalibration and zero discrimination. While all models show significantly positive discrimination, the null of correct calibration is rejected more frequently for the RV-based models than for the two GARCH-type specifications.

The remaining off-diagonal panels present pairwise differences in average scores ($\Delta \widehat{S}$), miscalibration ($\Delta \widehat{MCB}$), and discrimination ($\Delta \widehat{DSC}$), with significance indicated by 0 to 3 stars corresponding to the 10%, 5%, and 1% levels. Focusing on the lower column, which compares the GARCH model to the three alternatives, most differences are highly significant. In particular, the inferior performance of the GARCH model is primarily driven by its significantly weaker discrimination, consistent with the informational advantage of RV-based models that exploit high-frequency data.

Turning to the VaR evaluation results, [Table 5](#) reports the p -values of seven standard VaR backtests—described in [Section 3.5](#) and [Table 2](#)—along with the unconditional hit frequency in the final column. Strikingly, particularly at the 1% level, the simple HS model appears

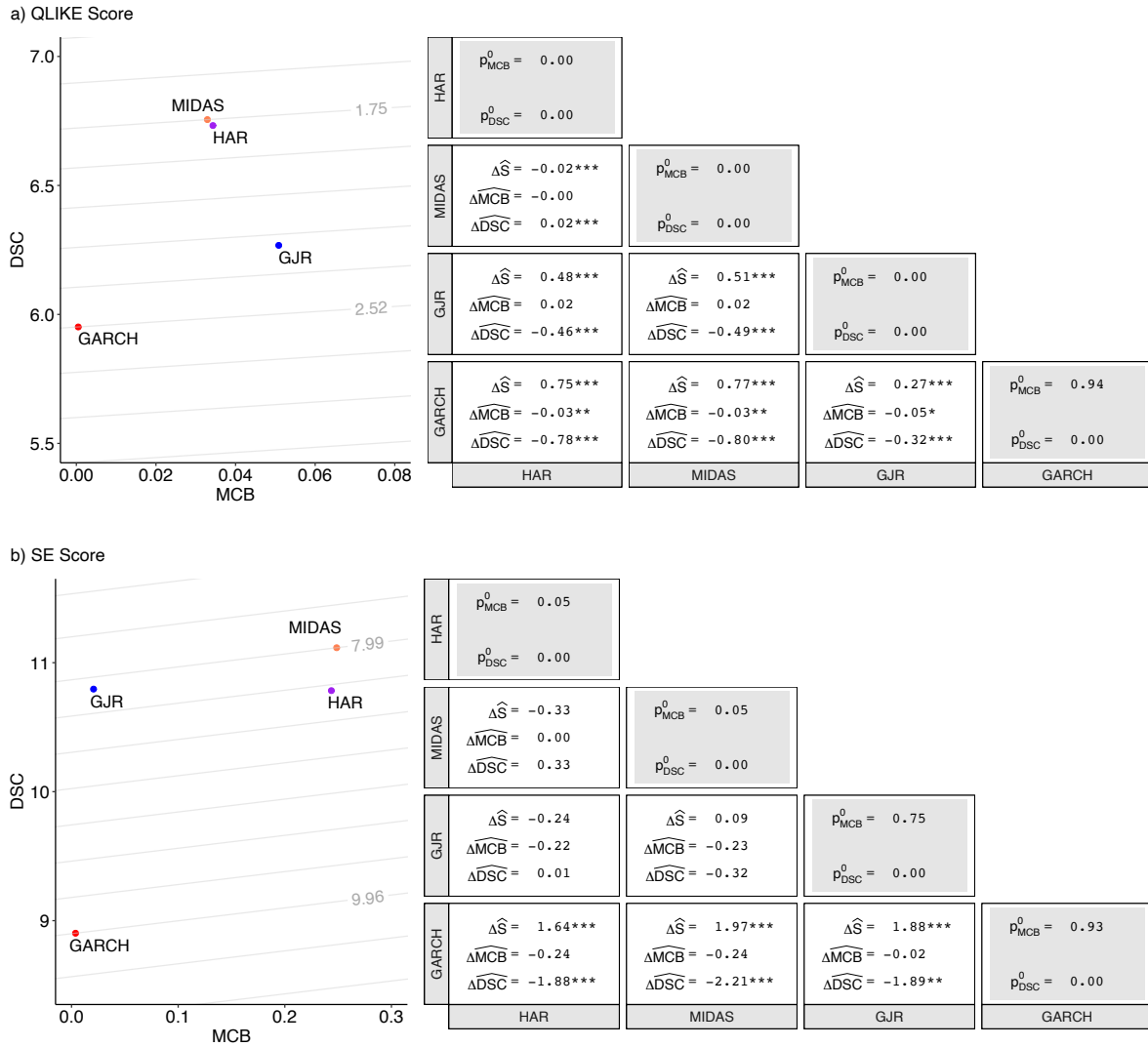


Figure 5: Variance forecast evaluation results for the E-mini futures using a) the QLIKE and b) the squared error scoring functions. The left “MCB–DSC” plots show the average score as iso-lines together with its decomposition into miscalibration and discrimination components for the four competing forecasts. The gray boxes in the right panels display the p -values of tests for zero miscalibration and discrimination, respectively. The white boxes display the average score, miscalibration and discrimination differences, together with 0 to 3 stars indicating significance at the 10%, 5%, and 1% levels.

Table 5: Backtesting results for 1% and 5% VaR forecasts. The first panel displays the p -values of the backtests summarized in Table 2. The column “Basel” also displays the colors of their traffic light system. The last column reports the relative frequencies of hits, i.e., how often the realizations exceed the VaR forecasts.

		p-values backtests							
	Model	UC	Basel	CC	NZ	VQR	DQ	DQX	hit freq.
1%-VaR	HS	0.137	0.024	0.149	0.124	0.321	0.002	0.004	1.3%
	GARCH	0.001	0.000	0.002	0.000	0.006	0.023	0.016	1.8%
	GJR	0.000	0.000	0.000	0.000	0.000	0.002	0.001	2.0%
	HAR	0.000	0.000	0.000	0.000	0.003	0.000	0.000	2.3%
	MIDAS	0.000	0.000	0.000	0.000	0.000	0.000	0.000	2.3%
5%-VaR	HS	0.700	0.303	0.006	0.416	0.013	0.000	0.000	5.2%
	GARCH	0.266	0.117	0.543	0.140	0.452	0.066	0.052	5.4%
	GJR	0.161	0.069	0.313	0.073	0.360	0.207	0.534	5.5%
	HAR	0.298	0.132	0.588	0.159	0.518	0.190	0.132	5.4%
	MIDAS	0.266	0.117	0.544	0.145	0.568	0.183	0.134	5.4%

to be the best calibrated, whereas all competing models are consistently rejected across the backtests. Although evidence at the 5% level and for conditional calibration backtests is weak or inconclusive, the 1% level remains the most relevant for risk management (Basel Committee, 2019b, p. 81).

Score decompositions with their associated inference help explain the seemingly superior performance of the HS model. Figure 6 presents these decompositions, analogous to Figure 5, using the check loss function for 1% and 5% VaR forecasts.

At the 1% level, the MCB–DSC plot in Figure 6 shows that, although the HS model exhibits the best calibration, it has by far the weakest discrimination. This results in clearly inferior predictive performance according to the check loss, as further confirmed by the strongly significant results in the right panel. These findings resolve the seemingly contradictory results highlighted in the motivational example from Section 1.1 and underscore the risk of evaluating forecasts solely on calibration. As such, they point to a potentially serious shortcoming in current banking regulation.

At the 5% level, the HS model shows markedly poorer *conditional* calibration, as reflected both in the backtest results in Table 5 and in the score decomposition in Figure 6. The relative ordering of the other four models, however, is similar to that observed at the 1% level, with generally stronger significance, which can be attributed to lower noise at less extreme probability levels.

A general pattern evident in the MCB–DSC plot at the 1% level—and, to a lesser extent, at the 5% level and for the variance forecasts in Figure 5—is that models incorporating more information can convert it into higher discrimination. However, this often comes at the cost of increased miscalibration. Notably, achieving auto-calibration conditional on $\mathbf{W}_{it} = (1, X_{it})$ is relatively easy when forecasts X_{it} are nearly constant, but much more difficult for highly discriminating forecasts that vary substantially over time. This observation calls into question the common practice of evaluating risk measure forecasts primarily through MZ-type backtests (Gaglianone et al., 2011; Guler et al., 2017; Bayer and Dimitriadis, 2022), which focus on auto-

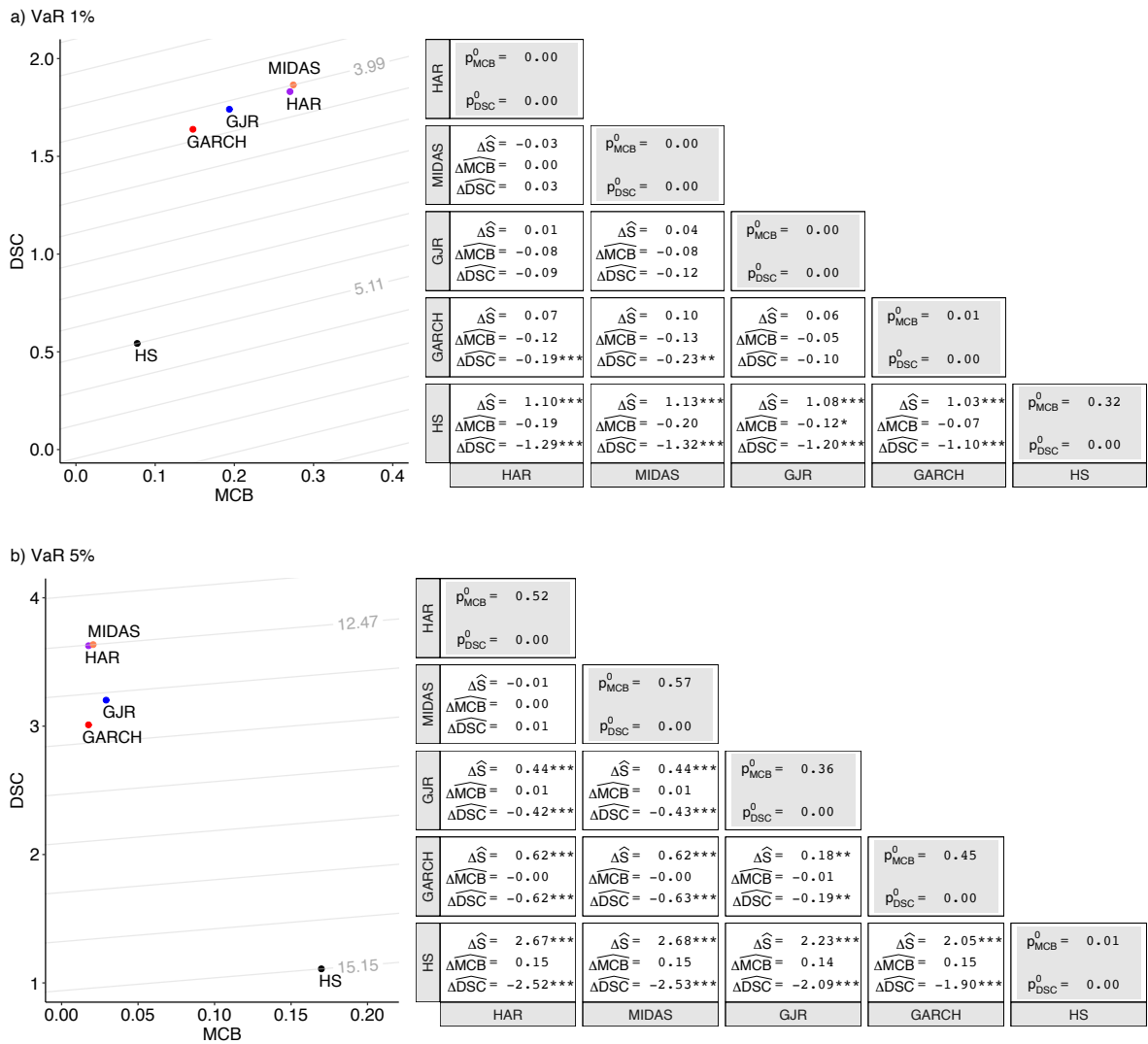


Figure 6: VaR forecast evaluation results for the E-mini futures at quantile levels a) 1% and b) 5% for the check loss function and its decomposition terms. For details, see the caption of Figure 5.

calibration.

Figures D.4–D.5 in Appendix D present diagnostic checks for the linear recalibration regressions underlying the score decompositions of the variance and VaR forecasts. The pointwise confidence bands largely cover the null specification, providing no evidence against correct model specification. This supports the use of linear recalibration for score decompositions in these applications, combining robustness and adequate fit with the ability to conduct inference, which is essential in the settings considered.

6 Conclusion

This paper has established a comprehensive inferential framework for score decompositions, enabling a more granular assessment of predictive performance through the lenses of miscalibration, discrimination, and uncertainty. By utilizing a linear recalibration technique, we have shown that it is possible to derive robust inference for a wide range of point forecasts—including those governed by non-smooth loss functions—while maintaining attractive finite sample non-negativity conditions and a formal bridge to the classical Mincer and Zarnowitz (1969) regression. Our results demonstrate that this decomposition approach not only enriches the informational content of traditional predictive ability tests but also offers tangible gains in statistical power. Through our empirical applications, we have highlighted how these methods can reveal significant latent differences in forecast discrimination and, crucially, identify systemic deficiencies in financial risk backtesting that current banking regulations fail to capture.

The assumption of linear recalibration is guaranteed to hold under the null hypotheses of zero discrimination or perfect calibration, though it may be violated in more general settings. Nevertheless, this linear specification provides essential stability and allows for the inclusion of further recalibration variables, allowing for direct generalizations to e.g., cross-calibration (Strähl and Ziegel, 2017), and enabling direct links to VaR backtests and the literature on macroeconomic survey forecasts following Coibion and Gorodnichenko (2015). The linearity assumption further guards against the overfitting that often plagues nonparametric techniques in this context. Such overfitting typically manifests as a positive bias in the non-negative MCB and DSC components—a risk that is particularly acute in the small-to-medium sample sizes characteristic of our applications. Notably, we find no empirical evidence against the linearity assumption in our data, which supports the robustness of our approach.

Nonetheless, particularly in data-rich environments, semiparametric extensions that estimate the recalibration curve nonparametrically—using kernel, spline, or isotonic regression—represent promising avenues for future research. Such developments could build on the seminal work of Newey (1994) regarding two-step semiparametric inference and more recent advances in isotonic plug-in estimation, such as Xu (2022).

We treat the possibly model-based forecasts as the finalized output of a specific sequence of modeling choices, including parameter estimation. Consequently, we formulate our hypotheses based on the realized quality of these forecasts rather than on the properties of the underlying models themselves. In contrast, the framework of West (1996) assesses whether two forecasting *models* based on their pseudo-true parameters would exhibit equal predictive accuracy, hence requiring that the test statistic’s standardization explicitly accounts for the asymptotic noise

introduced by parameter estimation. This extension can be integrated into our framework by redefining the population $\overline{\text{MCB}}$ and $\overline{\text{DSC}}$ components in a model-based environment and replacing the central limit theorem in Assumption 3.3 (ii) with the asymptotic approximations of West (1996), or with the numerous refinements and generalizations proposed in subsequent work.

Generalizations of our framework to other elicitable functionals, such as expectiles, are straightforward. However, functionals that are merely jointly or multi-objective elicitable following Fissler and Ziegel (2016) and Fissler and Hoga (2024)—such as the variance (when the mean is unknown), the Expected Shortfall, or the systemic risk measures Co-Value-at-Risk and Marginal Expected Shortfall—require additional care. In these cases, the underlying recalibration regressions necessitate the estimation of conditional models for the associated nuisance components, such as the mean or the VaR (Patton et al., 2019; Bayer and Dimitriadis, 2022; Dimitriadis and Hoga, 2026). The propagation of estimation risk from these nuisance quantities into the final score decomposition represents a non-trivial extension of the current inferential framework.

In conclusion, the contributions of this paper extend beyond their immediate applications in econometrics and finance. The principles of score decomposition and linear recalibration constitute a versatile toolkit for any domain where predictive accuracy is paramount, from meteorology to machine learning. The framework proposed herein represents a fundamental shift in perspective: from merely asking *which* forecast is better to diagnosing *why* it is better. As the complexity of our models and the richness of our data continue to grow, this diagnostic approach will be essential for robust and reliable decision-making.

Acknowledgments

Timo Dimitriadis acknowledges funding by the German Research Foundation (DFG) through the projects 502572912 and 568876076. We gratefully acknowledge the Hohenheim Datalab (DALAHO) for providing access to Refinitiv TickHistory. We thank all seminar and conference participants who provided feedback on earlier versions of this paper. In particular, we are grateful to Sam Allen, Tillman Gneiting, Alexander Jordan, Robert Jung, Fabian Krüger, Andrew Patton, Winfried Pohlmeier, Johannes Resin, Karsten Schweikert, and Johanna Ziegel for their valuable comments and suggestions.

Appendix

The appendix contains all proofs in Appendix A, a discussion of related score decompositions in Appendix B, details on the quantile simulation DGP in Appendix C, and additional figures for the simulations and applications in Appendix D.

A Proofs

Proof of Theorem 3.2. For item (a), notice that by the definition of the M-estimator in (12), we have that

$$\begin{aligned}\widehat{\text{MCB}}_{iT} &= \widehat{S}_{iT} - \widehat{S}_{iT}^{\text{C}} = \frac{1}{T} \sum_{t=1}^T \text{S}(X_{it}, Y_t) - \frac{1}{T} \sum_{t=1}^T \text{S}(\mathbf{W}_{it}^\top \widehat{\boldsymbol{\theta}}_{iT}, Y_t) \\ &= \frac{1}{T} \sum_{t=1}^T \text{S}(X_{it}, Y_t) - \min_{\boldsymbol{\theta} \in \Theta} \frac{1}{T} \sum_{t=1}^T \text{S}(\mathbf{W}_{it}^\top \boldsymbol{\theta}, Y_t) \geq 0,\end{aligned}$$

since \mathbf{W}_{it} is assumed to contain an intercept and the forecast X_{it} . If $X_{it} = \mathbf{W}_{it}^\top \widehat{\boldsymbol{\theta}}_{iT}$ almost surely, $\widehat{\text{MCB}}_{iT} = 0$ is immediate.

For item (b), let $X_{it} \neq \mathbf{W}_{it}^\top \widehat{\boldsymbol{\theta}}_{iT}$ for some $t \in \{1, \dots, T\}$ with positive probability. Then, we get that

$$\frac{1}{T} \sum_{t=1}^T \text{S}(X_{it}, Y_t) > \frac{1}{T} \sum_{t=1}^T \text{S}(\mathbf{W}_{it}^\top \widehat{\boldsymbol{\theta}}_{iT}, Y_t) = \min_{\boldsymbol{\theta} \in \Theta} \frac{1}{T} \sum_{t=1}^T \text{S}(\mathbf{W}_{it}^\top \boldsymbol{\theta}, Y_t),$$

with positive probability, where the inequality holds as the latter minimum is assumed to be unique and $(0, 1, 0, \dots)^\top \in \Theta$, for which $\mathbf{W}_{it}^\top (0, 1, 0, \dots)^\top = X_{it}$. Thus, $\widehat{\text{MCB}}_{iT} > 0$ with positive probability follows.

For item (c), first notice that the empirical distribution of the sample Y_1, \dots, Y_T is contained in \mathcal{P} as the convex combination of Dirac measures at Y_1, \dots, Y_T , such that the strict consistency of S implies that the unconditional functional \widehat{r}_T coincides with the M-estimator $\arg \min_{r \in \mathbf{A}} \frac{1}{T} \sum_{t=1}^T \text{S}(r, Y_t)$. Hence, we have that

$$\begin{aligned}\widehat{\text{DSC}}_{iT} &= \widehat{S}_{iT}^{\text{R}} - \widehat{S}_{iT}^{\text{C}} = \frac{1}{T} \sum_{t=1}^T \text{S}(\widehat{r}_T, Y_t) - \frac{1}{T} \sum_{t=1}^T \text{S}(\mathbf{W}_{it}^\top \widehat{\boldsymbol{\theta}}_{iT}, Y_t) \\ &= \min_{r \in \mathbf{A}} \frac{1}{T} \sum_{t=1}^T \text{S}(r, Y_t) - \min_{\boldsymbol{\theta} \in \Theta} \frac{1}{T} \sum_{t=1}^T \text{S}(\mathbf{W}_{it}^\top \boldsymbol{\theta}, Y_t) \geq 0,\end{aligned}$$

as \mathbf{W}_{it} is assumed to contain an intercept, which nests the first minimization over all $r \in \mathbf{A}$. If $\widehat{r}_T = \mathbf{W}_{it}^\top \widehat{\boldsymbol{\theta}}_{iT}$ almost surely, $\widehat{\text{DSC}}_{iT} = 0$ is immediate.

For item (d), assume that $\widehat{r}_T \neq \mathbf{W}_{it}^\top \widehat{\boldsymbol{\theta}}_{iT}$ for some $t \in \{1, \dots, T\}$ with positive probability.

Then,

$$\min_{r \in \mathbf{A}} \frac{1}{T} \sum_{t=1}^T \mathsf{S}(r, Y_t) = \frac{1}{T} \sum_{t=1}^T \mathsf{S}(\widehat{r}_T, Y_t) > \frac{1}{T} \sum_{t=1}^T \mathsf{S}(\mathbf{W}_{it}^\top \widehat{\boldsymbol{\theta}}_{iT}, Y_t) = \min_{\boldsymbol{\theta} \in \boldsymbol{\Theta}} \frac{1}{T} \sum_{t=1}^T \mathsf{S}(\mathbf{W}_{it}^\top \boldsymbol{\theta}, Y_t),$$

with positive probability, where the strict inequality holds as the latter minimum is assumed to be unique and $(\widehat{r}_T, 0, \dots)^\top \in \boldsymbol{\Theta}$, for which $\mathbf{W}_{it}^\top (\widehat{r}_T, 0, \dots)^\top = \widehat{r}_T$. Thus, $\widehat{\text{DSC}}_{iT} > 0$ with positive probability follows, which concludes the proof. \square

Proof Theorem 3.4. We start by decomposing

$$\widehat{\text{MCB}}_{iT} - \overline{\text{MCB}}_i = A_{iT} - B_{iT} - C_{iT} \quad \text{and} \quad \widehat{\text{DSC}}_{iT} - \overline{\text{DSC}}_i = -B_{iT} - C_{iT} + D_T + E_T$$

where

$$\begin{aligned} A_{iT} &:= \frac{1}{T} \sum_{t=1}^T a_{it} := \frac{1}{T} \sum_{t=1}^T \mathsf{S}(X_{it}, Y_t) - \mathbb{E}[\mathsf{S}(X_{it}, Y_t)] \\ B_{iT} &:= \frac{1}{T} \sum_{t=1}^T b_{it} := \frac{1}{T} \sum_{t=1}^T \mathsf{S}(\mathbf{W}_{it}^\top \widehat{\boldsymbol{\theta}}_{iT}, Y_t) - \mathsf{S}(\mathbf{W}_{it}^\top \bar{\boldsymbol{\theta}}_i, Y_t) \\ C_{iT} &:= \frac{1}{T} \sum_{t=1}^T c_{it} := \frac{1}{T} \sum_{t=1}^T \mathsf{S}(\mathbf{W}_{it}^\top \bar{\boldsymbol{\theta}}_i, Y_t) - \mathbb{E}[\mathsf{S}(\mathbf{W}_{it}^\top \bar{\boldsymbol{\theta}}_i, Y_t)] \\ D_T &:= \frac{1}{T} \sum_{t=1}^T d_{tT} := \frac{1}{T} \sum_{t=1}^T \mathsf{S}(\widehat{r}_T, Y_t) - \mathsf{S}(\bar{r}, Y_t) \\ E_T &:= \frac{1}{T} \sum_{t=1}^T e_t := \frac{1}{T} \sum_{t=1}^T \mathsf{S}(\bar{r}, Y_t) - \mathbb{E}[\mathsf{S}(\bar{r}, Y_t)]. \end{aligned}$$

Here, A_{iT} , C_{iT} and E_T capture the difference between sample and population versions of the scores of the original forecasts, the (population) recalibrated and the (population) reference forecasts, respectively. The terms B_{iT} and D_T capture the estimation effect of the recalibrated and reference forecast, respectively.

We start to show that the estimation effects captured in $\sqrt{T}B_{iT}$ (and similarly, in $\sqrt{T}D_T$) vanish in probability. For this, we define for all $\boldsymbol{\theta} \in \boldsymbol{\Theta}$,

$$\widehat{Q}_{iT}(\boldsymbol{\theta}) := \frac{1}{T} \sum_{t=1}^T \mathsf{S}(\mathbf{W}_{it}^\top \boldsymbol{\theta}, Y_t) \quad \text{and} \quad \overline{Q}_{iT}(\boldsymbol{\theta}) := \frac{1}{T} \sum_{t=1}^T \mathbb{E}[\mathsf{S}(\mathbf{W}_{it}^\top \boldsymbol{\theta}, Y_t)], \quad (28)$$

such that $\nu_{iT}(\boldsymbol{\theta}) = \sqrt{T}(\widehat{Q}_{iT}(\boldsymbol{\theta}) - \overline{Q}_{iT}(\boldsymbol{\theta}))$ for $\nu_{iT}(\boldsymbol{\theta})$ defined in (15).

Then, we employ a mean-value theorem in the third equality below to get for some (possibly

random) $\tilde{\boldsymbol{\theta}}_{iT}$ that is on the line between $\hat{\boldsymbol{\theta}}_{iT}$ and $\bar{\boldsymbol{\theta}}_i$ that

$$\begin{aligned}
\sqrt{T}B_{iT} &= \sqrt{T}\hat{Q}_{iT}(\hat{\boldsymbol{\theta}}_{iT}) - \sqrt{T}\hat{Q}_{iT}(\bar{\boldsymbol{\theta}}_i) \\
&= \sqrt{T}\left(\bar{Q}_{iT}(\hat{\boldsymbol{\theta}}_{iT}) - \bar{Q}_{iT}(\bar{\boldsymbol{\theta}}_i)\right) + \left(\nu_{iT}(\hat{\boldsymbol{\theta}}_{iT}) - \nu_{iT}(\bar{\boldsymbol{\theta}}_i)\right) \\
&= \nabla_{\boldsymbol{\theta}}\bar{Q}_{iT}(\tilde{\boldsymbol{\theta}}_{iT}) \cdot \sqrt{T}(\hat{\boldsymbol{\theta}}_{iT} - \bar{\boldsymbol{\theta}}_i) + \left(\nu_{iT}(\hat{\boldsymbol{\theta}}_{iT}) - \nu_{iT}(\bar{\boldsymbol{\theta}}_i)\right) \\
&= o_{\mathbb{P}}(1) \cdot \mathcal{O}_{\mathbb{P}}(1) + o_{\mathbb{P}}(1) = o_{\mathbb{P}}(1).
\end{aligned} \tag{29}$$

We now provide more details on the derivation of the order terms in the last line of (29). For the last summand, we use the stochastic equicontinuity imposed in Assumption 3.3 (iv): For any $\eta > 0$ and $\varepsilon > 0$, there exists a $\delta > 0$ such that

$$\begin{aligned}
&\limsup_{T \rightarrow \infty} \mathbb{P}\left(\left|\nu_{iT}(\hat{\boldsymbol{\theta}}_{iT}) - \nu_{iT}(\bar{\boldsymbol{\theta}}_i)\right| > \eta\right) \\
&\leq \limsup_{T \rightarrow \infty} \mathbb{P}\left(\left|\nu_{iT}(\hat{\boldsymbol{\theta}}_{iT}) - \nu_{iT}(\bar{\boldsymbol{\theta}}_i)\right| > \eta, \|\hat{\boldsymbol{\theta}}_{iT} - \bar{\boldsymbol{\theta}}_i\| \leq \delta\right) + \limsup_{T \rightarrow \infty} \mathbb{P}\left(\|\hat{\boldsymbol{\theta}}_{iT} - \bar{\boldsymbol{\theta}}_i\| > \delta\right) \\
&\leq \limsup_{T \rightarrow \infty} \mathbb{P}\left(\sup_{\{\boldsymbol{\theta} \in \Theta: \|\boldsymbol{\theta} - \bar{\boldsymbol{\theta}}_i\| \leq \delta\}} \left|\nu_{iT}(\boldsymbol{\theta}) - \nu_{iT}(\bar{\boldsymbol{\theta}}_i)\right| > \eta\right) + o(1) \\
&< \varepsilon,
\end{aligned}$$

where we have used that $\hat{\boldsymbol{\theta}}_{iT}$ is a consistent estimator for $\bar{\boldsymbol{\theta}}_i$.

For the first order term in the last line of (29), notice that $\tilde{\boldsymbol{\theta}}_{iT} \xrightarrow{\mathbb{P}} \bar{\boldsymbol{\theta}}_i$ as $\tilde{\boldsymbol{\theta}}_{iT}$ is between $\bar{\boldsymbol{\theta}}_i$ and the consistent estimator $\hat{\boldsymbol{\theta}}_{iT}$. As by Assumption 3.3 (iii), the map $\boldsymbol{\theta} \mapsto g(\boldsymbol{\theta}) = \nabla_{\boldsymbol{\theta}}\mathbb{E}[\mathbf{S}(\mathbf{W}_{it}^{\top}\boldsymbol{\theta}, Y_t)]$ is locally Lipschitz-continuous, i.e., $|g(\boldsymbol{\theta}) - g(\boldsymbol{\tau})| \leq C\|\boldsymbol{\theta} - \boldsymbol{\tau}\|$ for all $\boldsymbol{\theta}, \boldsymbol{\tau}$ in a neighborhood of $\bar{\boldsymbol{\theta}}_i$, for some constant $C < \infty$, we can employ similar arguments as in Dimitriadis and Hoga (2025, Lemma V.3) to get that

$$\begin{aligned}
&\mathbb{P}\left(\left\|g(\tilde{\boldsymbol{\theta}}_{iT}) - g(\bar{\boldsymbol{\theta}}_i)\right\| > \varepsilon\right) \\
&\leq \mathbb{P}\left(\left\|g(\tilde{\boldsymbol{\theta}}_{iT}) - g(\bar{\boldsymbol{\theta}}_i)\right\| > \varepsilon, \|\tilde{\boldsymbol{\theta}}_{iT} - \bar{\boldsymbol{\theta}}_i\| \leq \delta\right) + \mathbb{P}\left(\|\tilde{\boldsymbol{\theta}}_{iT} - \bar{\boldsymbol{\theta}}_i\| > \delta\right) \\
&\leq \mathbb{P}\left(\sup_{\|\boldsymbol{\theta} - \bar{\boldsymbol{\theta}}_i\| \leq \delta} \left\|g(\boldsymbol{\theta}) - g(\bar{\boldsymbol{\theta}}_i)\right\| > \varepsilon\right) + o(1) \\
&\leq \mathbb{P}\left(\sup_{\|\boldsymbol{\theta} - \bar{\boldsymbol{\theta}}_i\| \leq \delta} C\|\boldsymbol{\theta} - \bar{\boldsymbol{\theta}}_i\| > \varepsilon\right) + o(1) \\
&= o(1),
\end{aligned} \tag{30}$$

where the final equality requires that we choose $\delta < \varepsilon/C$. Hence, we get that

$$\nabla_{\boldsymbol{\theta}}\bar{Q}_{iT}(\tilde{\boldsymbol{\theta}}_{iT}) = g(\tilde{\boldsymbol{\theta}}_{iT}) = \nabla_{\boldsymbol{\theta}}\mathbb{E}[\mathbf{S}(\mathbf{W}_{it}^{\top}\tilde{\boldsymbol{\theta}}_i, Y_t)] + o_{\mathbb{P}}(1) = o_{\mathbb{P}}(1),$$

as $\nabla_{\boldsymbol{\theta}}\mathbb{E}[\mathbf{S}(\mathbf{W}_{it}^{\top}\bar{\boldsymbol{\theta}}_i, Y_t)] = 0$ since the (continuously differentiable) expected score is minimized by the conditional functional $\Gamma(Y_t | \mathbf{W}_{it}) = \mathbf{W}_{it}^{\top}\bar{\boldsymbol{\theta}}_i$ by Assumption 3.1 together with (3) and the tower property. An equivalent reasoning shows that $\sqrt{T}D_T = o_{\mathbb{P}}(1)$ (by simply setting $\mathbf{W}_{it} = 1$ in (28) and the following.)

Hence, using $\sqrt{T}B_{iT} = o_{\mathbb{P}}(1)$ and $\sqrt{T}D_T = o_{\mathbb{P}}(1)$, we can write

$$\sqrt{T} \begin{pmatrix} \widehat{\text{MCB}}_{1T} - \overline{\text{MCB}}_1 \\ \widehat{\text{DSC}}_{1T} - \overline{\text{DSC}}_1 \\ \widehat{\text{MCB}}_{2T} - \overline{\text{MCB}}_2 \\ \widehat{\text{DSC}}_{2T} - \overline{\text{DSC}}_2 \end{pmatrix} = \begin{pmatrix} 1 & -1 & 0 & 0 & 0 \\ 0 & -1 & 0 & 0 & 1 \\ 0 & 0 & 1 & -1 & 0 \\ 0 & 0 & 0 & -1 & 1 \end{pmatrix} T^{-1/2} \sum_{t=1}^T (a_{1t}, c_{1t}, a_{2t}, c_{2t}, e_t)^\top + o_{\mathbb{P}}(1),$$

and as

$$T^{-1/2} \boldsymbol{\Omega}_T^{-1/2} \sum_{t=1}^T (a_{1t}, c_{1t}, a_{2t}, c_{2t}, e_t)^\top \xrightarrow{d} \mathcal{N}(0, I_5)$$

satisfies a CLT by assumption, the result of the theorem follows. \square

Proof of Theorem 3.6. We start to show the distribution of $T \widehat{\text{MCB}}_{iT}$ under $\overline{\text{MCB}}_i = 0$. For this, we have that

$$\mathbb{E}[\mathbb{S}(X_{it}, Y_t)] = \mathbb{E}[\mathbb{S}(\mathbf{W}_{it}^\top \bar{\boldsymbol{\theta}}_i, Y_t)] \quad \forall t \in \mathbb{N}. \quad (31)$$

Hence, as $\mathbf{W}_{it}^\top \bar{\boldsymbol{\theta}}_i = \Gamma(Y_t | \mathbf{W}_{it})$ a.s. by assumption, and the sigma-fields $\sigma\{X_{it}\} \subseteq \sigma\{\mathbf{W}_{it}\}$ are nested, invoking [Holzmann and Eulert \(2014, Corollary 2\)](#) shows that the equality in (31) implies that $X_{it} = \mathbf{W}_{it}^\top \bar{\boldsymbol{\theta}}_i$ a.s..

Then, by using the definitions from (28) and arguments as in (29), we get that

$$\begin{aligned} T \left(\widehat{\text{MCB}}_{iT} - \overline{\text{MCB}}_i \right) &= \sum_{t=1}^T \mathbb{S}(X_{it}, Y_t) - \mathbb{S}(\mathbf{W}_{it}^\top \hat{\boldsymbol{\theta}}_{iT}, Y_t) \\ &= - \sum_{t=1}^T \mathbb{S}(\mathbf{W}_{it}^\top \hat{\boldsymbol{\theta}}_{iT}, Y_t) - \mathbb{S}(\mathbf{W}_{it}^\top \bar{\boldsymbol{\theta}}_i, Y_t) \\ &= - \sum_{t=1}^T \mathbb{S}'(\mathbf{W}_{it}^\top \bar{\boldsymbol{\theta}}_i, Y_t) (\mathbf{W}_{it}^\top \hat{\boldsymbol{\theta}}_{iT} - \mathbf{W}_{it}^\top \bar{\boldsymbol{\theta}}_i) \\ &\quad - \frac{1}{2} \sum_{t=1}^T \mathbb{S}''(\mathbf{W}_{it}^\top \bar{\boldsymbol{\theta}}_i, Y_t) (\mathbf{W}_{it}^\top \hat{\boldsymbol{\theta}}_{iT} - \mathbf{W}_{it}^\top \bar{\boldsymbol{\theta}}_i)^2 \\ &\quad - \frac{1}{6} \sum_{t=1}^T \mathbb{S}'''(\mathbf{W}_{it}^\top \tilde{\boldsymbol{\theta}}_{iT}, Y_t) (\mathbf{W}_{it}^\top \hat{\boldsymbol{\theta}}_{iT} - \mathbf{W}_{it}^\top \bar{\boldsymbol{\theta}}_i)^3 \\ &=: -TB_{iT}^{(1)} - TB_{iT}^{(2)} - TB_{iT}^{(3)}, \end{aligned} \quad (32)$$

for some random variable $\tilde{\boldsymbol{\theta}}_{iT}$ between $\hat{\boldsymbol{\theta}}_{iT}$ and $\bar{\boldsymbol{\theta}}_i$ by a second-order Taylor expansion and a mean-value theorem.

In the following, we show that $TB_{iT}^{(3)} = o_{\mathbb{P}}(1)$, whereas $TB_{iT}^{(1)} = \mathcal{O}_{\mathbb{P}}(1)$ and $TB_{iT}^{(2)} = \mathcal{O}_{\mathbb{P}}(1)$ contribute to the asymptotic distribution of $T(\widehat{\text{MCB}}_{iT} - \overline{\text{MCB}}_i)$.

By Assumption 3.5 (i), it holds that

$$\sqrt{T}(\widehat{\boldsymbol{\theta}}_{iT} - \bar{\boldsymbol{\theta}}_i) = - \left(\frac{1}{T} \sum_{t=1}^T S''(\mathbf{W}_{it}^\top \bar{\boldsymbol{\theta}}_i, Y_t) \mathbf{W}_{it} \mathbf{W}_{it}^\top \right)^{-1} \left(T^{-1/2} \sum_{t=1}^T S'(\mathbf{W}_{it}^\top \bar{\boldsymbol{\theta}}_i, Y_t) \mathbf{W}_{it} \right) + o_{\mathbb{P}}(1). \quad (33)$$

Hence, for $B_{iT}^{(1)}$, by using (33), we get that

$$\begin{aligned} -TB_{iT}^{(1)} &= -T^{-1/2} \sum_{t=1}^T S'(\mathbf{W}_{it}^\top \bar{\boldsymbol{\theta}}_i, Y_t) \mathbf{W}_{it}^\top \times \sqrt{T}(\widehat{\boldsymbol{\theta}}_{iT} - \bar{\boldsymbol{\theta}}_i) \\ &= \left(T^{-1/2} \sum_{t=1}^T S'(\mathbf{W}_{it}^\top \bar{\boldsymbol{\theta}}_i, Y_t) \mathbf{W}_{it} \right)^\top \times \left(\frac{1}{T} \sum_{t=1}^T S''(\mathbf{W}_{it}^\top \bar{\boldsymbol{\theta}}_i, Y_t) \mathbf{W}_{it} \mathbf{W}_{it}^\top \right)^{-1} \\ &\quad \times \left(T^{-1/2} \sum_{t=1}^T S'(\mathbf{W}_{it}^\top \bar{\boldsymbol{\theta}}_i, Y_t) \mathbf{W}_{it} \right) + o_{\mathbb{P}}(1). \end{aligned}$$

Similarly, for $B_{iT}^{(2)}$, using (33) twice, we get that

$$\begin{aligned} -TB_{iT}^{(2)} &= -\frac{1}{2} \sum_{t=1}^T S''(\mathbf{W}_{it}^\top \bar{\boldsymbol{\theta}}_i, Y_t) (\mathbf{W}_{it}^\top \widehat{\boldsymbol{\theta}}_{iT} - \mathbf{W}_{it}^\top \bar{\boldsymbol{\theta}}_i)^2 \\ &= -\frac{1}{2} (\sqrt{T}(\widehat{\boldsymbol{\theta}}_{iT} - \bar{\boldsymbol{\theta}}_i))^\top \times \left(\sum_{t=1}^T S''(\mathbf{W}_{it}^\top \bar{\boldsymbol{\theta}}_i, Y_t) \mathbf{W}_{it} \mathbf{W}_{it}^\top \right) \times (\sqrt{T}(\widehat{\boldsymbol{\theta}}_{iT} - \bar{\boldsymbol{\theta}}_i)) \\ &= -\frac{1}{2} \left(T^{-1/2} \sum_{t=1}^T S'(\mathbf{W}_{it}^\top \bar{\boldsymbol{\theta}}_i, Y_t) \mathbf{W}_{it} \right)^\top \times \left(\frac{1}{T} \sum_{t=1}^T S''(\mathbf{W}_{it}^\top \bar{\boldsymbol{\theta}}_i, Y_t) \mathbf{W}_{it} \mathbf{W}_{it}^\top \right)^{-1} \\ &\quad \times \left(T^{-1/2} \sum_{t=1}^T S'(\mathbf{W}_{it}^\top \bar{\boldsymbol{\theta}}_i, Y_t) \mathbf{W}_{it} \right) + o_{\mathbb{P}}(1). \end{aligned}$$

Finally, for the absolute value of $TB_{iT}^{(3)}$, we get that

$$\begin{aligned} |TB_{iT}^{(3)}| &= \left| \frac{1}{6} \sum_{t=1}^T S'''(\mathbf{W}_{it}^\top \tilde{\boldsymbol{\theta}}_{iT}, Y_t) (\mathbf{W}_{it}^\top \widehat{\boldsymbol{\theta}}_{iT} - \mathbf{W}_{it}^\top \bar{\boldsymbol{\theta}}_i)^3 \right| \\ &\leq \frac{1}{6} \sum_{t=1}^T |S'''(\mathbf{W}_{it}^\top \tilde{\boldsymbol{\theta}}_{iT}, Y_t)| \times |\mathbf{W}_{it}^\top \widehat{\boldsymbol{\theta}}_{iT} - \mathbf{W}_{it}^\top \bar{\boldsymbol{\theta}}_i|^3 \\ &\leq \frac{1}{6} T^{-1/2} \frac{1}{T} \sum_{t=1}^T |S'''(\mathbf{W}_{it}^\top \tilde{\boldsymbol{\theta}}_{iT}, Y_t)| \|\mathbf{W}_{it}\|^3 \times \|\sqrt{T}(\widehat{\boldsymbol{\theta}}_{iT} - \bar{\boldsymbol{\theta}}_i)\|^3 \\ &= o_{\mathbb{P}}(1) \times \mathcal{O}_{\mathbb{P}}(1) = o_{\mathbb{P}}(1), \end{aligned}$$

where we now provide details for the first $o_{\mathbb{P}}(1)$ term. For $h_T(\boldsymbol{\theta}) :=$

$\frac{1}{T} \sum_{t=1}^T |S'''(\mathbf{W}_{it}^\top \boldsymbol{\theta}, Y_t)| \|\mathbf{W}_{it}\|^3$, we have that for any $\varepsilon > 0$ small enough

$$\begin{aligned}
& \mathbb{P}\left(T^{-1/2} h_T(\tilde{\boldsymbol{\theta}}_{iT}) > \varepsilon\right) \\
& \leq \mathbb{P}\left(T^{-1/2} |h_T(\tilde{\boldsymbol{\theta}}_{iT}) - h_T(\bar{\boldsymbol{\theta}}_i)| > \varepsilon/2\right) + \mathbb{P}\left(T^{-1/2} h_T(\bar{\boldsymbol{\theta}}_i) > \varepsilon/2\right) \\
& \leq \mathbb{P}\left(T^{-1/2} \sup_{\|\boldsymbol{\theta} - \bar{\boldsymbol{\theta}}_i\| \leq \delta} |h_T(\boldsymbol{\theta}) - h_T(\bar{\boldsymbol{\theta}}_i)| > \varepsilon/2\right) + \mathbb{P}\left(T^{-1/2} h_T(\bar{\boldsymbol{\theta}}_i) > \varepsilon/2\right) + \mathbb{P}\left(\|\tilde{\boldsymbol{\theta}}_{iT} - \bar{\boldsymbol{\theta}}_i\| > \delta\right) \\
& = o(1),
\end{aligned} \tag{34}$$

where the first two terms above are $o(1)$ by Assumption 3.5 (ii) and the third is $o(1)$ by the consistency of $\tilde{\boldsymbol{\theta}}_{iT}$.

Combining the previous three terms, we get that

$$\begin{aligned}
T(\widehat{\text{MCB}}_{iT} - \overline{\text{MCB}}_i) &= \frac{1}{2} \left(T^{-1/2} \sum_{t=1}^T S'(\mathbf{W}_{it}^\top \bar{\boldsymbol{\theta}}_i, Y_t) \mathbf{W}_{it} \right)^\top \times \left(\frac{1}{T} \sum_{t=1}^T S''(\mathbf{W}_{it}^\top \bar{\boldsymbol{\theta}}_i, Y_t) \mathbf{W}_{it} \mathbf{W}_{it}^\top \right)^{-1} \\
&\quad \times \left(T^{-1/2} \sum_{t=1}^T S'(\mathbf{W}_{it}^\top \bar{\boldsymbol{\theta}}_i, Y_t) \mathbf{W}_{it} \right) + o_{\mathbb{P}}(1).
\end{aligned}$$

Then, given a Gaussian random variable $\mathbf{N}_{iT} \sim \mathcal{N}(0, \boldsymbol{\Sigma}_{iT})$, the quantity of interest $T(\widehat{\text{MCB}}_{iT} - \overline{\text{MCB}}_i)$ is approximated in distribution by

$$T\left(\widehat{\text{MCB}}_{iT} - \overline{\text{MCB}}_i\right) - \frac{1}{2} \mathbf{N}_{iT}^\top \boldsymbol{\Upsilon}_i^{-1} \mathbf{N}_{iT} = o_{\mathbb{P}}(1),$$

which concludes the first part of proof.

We continue with the second part, the asymptotic distribution of $T \widehat{\text{DSC}}_{iT}$ if $\overline{\text{DSC}}_i = 0$. We then have that

$$\mathbb{E}[S(\hat{r}_T, Y_t)] = \mathbb{E}[S(\mathbf{W}_{it}^\top \bar{\boldsymbol{\theta}}_i, Y_t)] \quad \forall t \in \mathbb{N}.$$

Hence, as $\mathbf{W}_{it}^\top \bar{\boldsymbol{\theta}}_i = \Gamma(Y_t \mid \mathbf{W}_{it})$ a.s. by assumption and $\bar{r} = \Gamma(Y_t)$, and as the sigma-fields $\sigma\{\emptyset\} \subseteq \sigma\{\mathbf{W}_{it}\}$ are nested, we obtain from [Holzmann and Eulert \(2014, Corollary 2\)](#) that $\bar{r} = \mathbf{W}_{it}^\top \bar{\boldsymbol{\theta}}_i$ a.s. for all $t \in \mathbb{N}$. Hence, we have that

$$\begin{aligned}
T(\widehat{\text{DSC}}_{iT} - \overline{\text{DSC}}_i) &= \sum_{t=1}^T (S(\hat{r}_T, Y_t) - S(\bar{r}, Y_t)) + \sum_{t=1}^T (S(\mathbf{W}_{it}^\top \bar{\boldsymbol{\theta}}_i, Y_t) - S(\mathbf{W}_{it}^\top \hat{\boldsymbol{\theta}}_{iT}, Y_t)) \\
&= TD_T - TB_{iT}.
\end{aligned}$$

A third order Taylor expansion of TD_T gives that for some \tilde{r}_T on the line between \hat{r}_T and \bar{r} ,

$$TD_T = \sum_{t=1}^T S(\tilde{r}_T, Y_t) - S(\bar{r}, Y_t)$$

$$\begin{aligned}
&= \sum_{t=1}^T S'(\bar{r}, Y_t)(\hat{r}_T - \bar{r}) + \frac{1}{2} \sum_{t=1}^T S''(\bar{r}, Y_t)(\hat{r}_T - \bar{r})^2 + \frac{1}{6} \sum_{t=1}^T S'''(\tilde{r}_T, Y_t)(\hat{r}_T - \bar{r})^3 \\
&=: TD_T^{(1)} + TD_T^{(2)} + TD_T^{(3)}.
\end{aligned}$$

Together with the expansion of B_{iT} in (32), this implies

$$T(\widehat{\text{DSC}}_{iT} - \overline{\text{DSC}}_i) = T(D_T^{(1)} - B_{iT}^{(1)}) + T(D_T^{(2)} - B_{iT}^{(2)}) + T(D_T^{(3)} - B_{iT}^{(3)}). \quad (35)$$

For the vector consisting of the first terms in (35), we get

$$\begin{aligned}
T(D_T^{(1)} - B_{iT}^{(1)}) &= \begin{pmatrix} 1 & -1 \end{pmatrix} \times \begin{pmatrix} TD_T^{(1)} \\ TB_{iT}^{(1)} \end{pmatrix} \\
&= \begin{pmatrix} 1 & -1 \end{pmatrix} \times \sum_{t=1}^T \begin{pmatrix} S'(\bar{r}, Y_t)(\hat{r}_T - \bar{r}) \\ S'(\bar{r}, Y_t) \mathbf{W}_{it}^\top (\hat{\boldsymbol{\theta}}_{iT} - \bar{\boldsymbol{\theta}}_i) \end{pmatrix} \\
&= \begin{pmatrix} 1 & -1 \end{pmatrix} \times T^{-1/2} \sum_{t=1}^T \begin{pmatrix} S'(\bar{r}, Y_t) & \mathbf{0} \\ 0 & S'(\bar{r}, Y_t) \mathbf{W}_{it}^\top \end{pmatrix} \times \sqrt{T} \begin{pmatrix} \hat{r}_T - \bar{r} \\ \hat{\boldsymbol{\theta}}_{iT} - \bar{\boldsymbol{\theta}}_i \end{pmatrix} \\
&= \begin{pmatrix} 1 & -1 \end{pmatrix} \times T^{-1/2} \sum_{t=1}^T \begin{pmatrix} S'(\bar{r}, Y_t) & \mathbf{0} \\ 0 & S'(\bar{r}, Y_t) \mathbf{W}_{it}^\top \end{pmatrix} \\
&\quad \times \begin{pmatrix} \left(\frac{1}{T} \sum_{t=1}^T S''(\bar{r}, Y_t) \right)^{-1} + o_{\mathbb{P}}(1) & \mathbf{0} \\ \left(\frac{1}{T} \sum_{t=1}^T S''(\mathbf{W}_{it}^\top \bar{\boldsymbol{\theta}}_i, Y_t) \mathbf{W}_{it} \mathbf{W}_{it}^\top \right)^{-1} + o_{\mathbb{P}}(1) \end{pmatrix} \times T^{-1/2} \sum_{t=1}^T S'(\bar{r}, Y_t) \mathbf{W}_{it} \\
&= T^{-1/2} \sum_{t=1}^T \begin{pmatrix} S'(\bar{r}, Y_t) & -S'(\bar{r}, Y_t) \mathbf{W}_{it}^\top \end{pmatrix} \\
&\quad \times \begin{pmatrix} \left(\frac{1}{T} \sum_{t=1}^T S''(\bar{r}, Y_t) \right)^{-1} & \mathbf{0} \\ \left(\frac{1}{T} \sum_{t=1}^T S''(\bar{r}, Y_t) \mathbf{W}_{it} \mathbf{W}_{it}^\top \right)^{-1} \end{pmatrix} \times T^{-1/2} \sum_{t=1}^T S'(\bar{r}, Y_t) \mathbf{W}_{it} + o_{\mathbb{P}}(1) \\
&= \begin{pmatrix} T^{-1/2} \sum_{t=1}^T S'(\bar{r}, Y_t) \mathbf{W}_{it}^\top \end{pmatrix} \\
&\quad \times \begin{pmatrix} \left(\frac{1}{T} \sum_{t=1}^T S''(\bar{r}, Y_t) \mathbf{W}_{it} \mathbf{W}_{it}^\top \right)^{-1} & - \begin{pmatrix} \left(\frac{1}{T} \sum_{t=1}^T S''(\bar{r}, Y_t) \right)^{-1} & \mathbf{0} \\ \mathbf{0} & \mathbf{0} \end{pmatrix} \end{pmatrix} \\
&\quad \times \begin{pmatrix} T^{-1/2} \sum_{t=1}^T S'(\bar{r}, Y_t) \mathbf{W}_{it}^\top \end{pmatrix} + o_{\mathbb{P}}(1). \tag{36}
\end{aligned}$$

In the last step, we have used the fact that for any (column vector) $\mathbf{a} \in \mathbb{R}^k$ and matrix $\mathbf{B} \in \mathbb{R}^{k \times k}$ with first/upper-left entries $a_1, B_{11} \in \mathbb{R}$, respectively, it holds that

$$\begin{pmatrix} a_1 & -\mathbf{a}^\top \end{pmatrix} \times \begin{pmatrix} B_{11} & \mathbf{0} \\ \mathbf{B} \end{pmatrix} \times \mathbf{a} = -\mathbf{a}^\top \times \left(\mathbf{B} - \begin{pmatrix} B_{11} & \mathbf{0} \\ \mathbf{0} & \mathbf{0} \end{pmatrix} \right) \times \mathbf{a}, \quad (37)$$

where the $\mathbf{0}$ entries have the appropriate dimensions. This reformulation allows to express the term above as a quadratic form.

For the second terms in (35), similar derivations yield that

$$\begin{aligned}
& T(D_T^{(2)} - B_{iT}^{(2)}) \\
&= \begin{pmatrix} 1 & -1 \end{pmatrix} \times \begin{pmatrix} TD_T^{(2)} \\ TB_{iT}^{(2)} \end{pmatrix} \\
&= \frac{1}{2} \begin{pmatrix} 1 & -1 \end{pmatrix} \times \sum_{t=1}^T \begin{pmatrix} S''(\bar{r}, Y_t) (\hat{r}_T - \bar{r})^2 \\ S''(\bar{r}, Y_t) (\mathbf{W}_{it}^\top \hat{\boldsymbol{\theta}}_{iT} - \mathbf{W}_{it}^\top \bar{\boldsymbol{\theta}}_i)^2 \end{pmatrix} \\
&= \frac{1}{2} \begin{pmatrix} 1 & -1 \end{pmatrix} \times \begin{pmatrix} (\sqrt{T}(\hat{r}_T - \bar{r})) \times \left(\frac{1}{T} \sum_{t=1}^T S''(\bar{r}, Y_t)\right) \times (\sqrt{T}(\hat{r}_T - \bar{r})) \\ (\sqrt{T}(\hat{\boldsymbol{\theta}}_{iT} - \bar{\boldsymbol{\theta}}_i))^\top \times \left(\frac{1}{T} \sum_{t=1}^T S''(\bar{r}, Y_t) \mathbf{W}_{it} \mathbf{W}_{it}^\top\right) \times (\sqrt{T}(\hat{\boldsymbol{\theta}}_{iT} - \bar{\boldsymbol{\theta}}_i)) \end{pmatrix} \\
&= \frac{1}{2} \begin{pmatrix} 1 & -1 \end{pmatrix} \times \begin{pmatrix} \sqrt{T}(\hat{r}_T - \bar{r}) & \mathbf{0} \\ 0 & \sqrt{T}(\hat{\boldsymbol{\theta}}_{iT} - \bar{\boldsymbol{\theta}}_i)^\top \end{pmatrix} \\
&\quad \times \begin{pmatrix} \frac{1}{T} \sum_{t=1}^T S''(\bar{r}, Y_t) & \mathbf{0} \\ \mathbf{0} & \frac{1}{T} \sum_{t=1}^T S''(\bar{r}, Y_t) \mathbf{W}_{it} \mathbf{W}_{it}^\top \end{pmatrix} \times \begin{pmatrix} \sqrt{T}(\hat{r}_T - \bar{r}) \\ \sqrt{T}(\hat{\boldsymbol{\theta}}_{iT} - \bar{\boldsymbol{\theta}}_i) \end{pmatrix} \\
&= \frac{1}{2} \times \begin{pmatrix} \sqrt{T}(\hat{r}_T - \bar{r}) \\ \sqrt{T}(\hat{\boldsymbol{\theta}}_{iT} - \bar{\boldsymbol{\theta}}_i) \end{pmatrix}^\top \times \begin{pmatrix} \frac{1}{T} \sum_{t=1}^T S''(\bar{r}, Y_t) & \mathbf{0} \\ \mathbf{0} & -\frac{1}{T} \sum_{t=1}^T S''(\bar{r}, Y_t) \mathbf{W}_{it} \mathbf{W}_{it}^\top \end{pmatrix} \times \begin{pmatrix} \sqrt{T}(\hat{r}_T - \bar{r}) \\ \sqrt{T}(\hat{\boldsymbol{\theta}}_{iT} - \bar{\boldsymbol{\theta}}_i) \end{pmatrix} \\
&= \frac{1}{2} T^{-1/2} \sum_{t=1}^T S'(\bar{r}, Y_t) \mathbf{W}_{it}^\top \times \begin{pmatrix} \left(\frac{1}{T} \sum_{t=1}^T S''(\bar{r}, Y_t)\right)^{-1} & \mathbf{0} \\ \left(\frac{1}{T} \sum_{t=1}^T S''(\bar{r}, Y_t) \mathbf{W}_{it} \mathbf{W}_{it}^\top\right)^{-1} \end{pmatrix}^\top \\
&\quad \times \begin{pmatrix} \frac{1}{T} \sum_{t=1}^T S''(\bar{r}, Y_t) & \mathbf{0} \\ \mathbf{0} & -\frac{1}{T} \sum_{t=1}^T S''(\bar{r}, Y_t) \mathbf{W}_{it} \mathbf{W}_{it}^\top \end{pmatrix} \\
&\quad \times \begin{pmatrix} \left(\frac{1}{T} \sum_{t=1}^T S''(\bar{r}, Y_t)\right)^{-1} & \mathbf{0} \\ \left(\frac{1}{T} \sum_{t=1}^T S''(\bar{r}, Y_t) \mathbf{W}_{it} \mathbf{W}_{it}^\top\right)^{-1} \end{pmatrix} \times T^{-1/2} \sum_{t=1}^T S'(\bar{r}, Y_t) \mathbf{W}_{it} + o_{\mathbb{P}}(1) \\
&= - \left(T^{-1/2} \sum_{t=1}^T S'(\bar{r}, Y_t) \mathbf{W}_{it}^\top \right) \\
&\quad \times \left(\left(\frac{1}{T} \sum_{t=1}^T S''(\bar{r}, Y_t) \mathbf{W}_{it} \mathbf{W}_{it}^\top \right)^{-1} - \begin{pmatrix} \left(\frac{1}{T} \sum_{t=1}^T S''(\bar{r}, Y_t)\right)^{-1} & \mathbf{0} \\ \mathbf{0} & \mathbf{0} \end{pmatrix} \right) \\
&\quad \times \left(T^{-1/2} \sum_{t=1}^T S'(\bar{r}, Y_t) \mathbf{W}_{it}^\top \right) + o_{\mathbb{P}}(1).
\end{aligned}$$

In the penultimate equality, we have plugged in the (joint) asymptotic expansion of the estimators from (17). In the last equality above, we have used the fact that for a (column) vector $\mathbf{b} = (b_1 \mathbf{0})^\top \in \mathbb{R}^{k+1}$ with first entry $b_1 \in \mathbb{R}$, $b_1 \neq 0$ and an invertible matrix $\mathbf{B} \in \mathbb{R}^{k \times k}$, we have that

$$\begin{pmatrix} \mathbf{b} & \mathbf{B} \end{pmatrix} \times \begin{pmatrix} b_1^{-1} & \mathbf{0} \\ \mathbf{0} & -\mathbf{B}^{-1} \end{pmatrix} \times \begin{pmatrix} \mathbf{b} \\ \mathbf{B} \end{pmatrix} = \begin{pmatrix} b_1^{-1} \mathbf{b} & -\mathbf{I}_k \end{pmatrix} \times \begin{pmatrix} \mathbf{b}^\top \\ \mathbf{B} \end{pmatrix} = b_1^{-1} \mathbf{b} \mathbf{b}^\top - \mathbf{B} = \begin{pmatrix} b_1 & \mathbf{0} \\ \mathbf{0} & \mathbf{0} \end{pmatrix} - \mathbf{B}.$$

For the third term in (35), we get that

$$\begin{aligned}
\left| \begin{pmatrix} D_T^{(3)} \\ B_{iT}^{(3)} \end{pmatrix} \right| &= \frac{1}{6} \left(\begin{array}{c} \left| \sum_{t=1}^T S'''(\tilde{r}_T, Y_t) (\hat{r}_T - \bar{r})^3 \right| \\ \left| \sum_{t=1}^T S'''(\mathbf{W}_{it}^\top \tilde{\boldsymbol{\theta}}_{iT}, Y_t) (\mathbf{W}_{it}^\top \hat{\boldsymbol{\theta}}_{iT} - \mathbf{W}_{it}^\top \bar{\boldsymbol{\theta}}_i)^3 \right| \end{array} \right) \\
&\leq \frac{1}{6} \left(\begin{array}{c} \sum_{t=1}^T |S'''(\tilde{r}_T, Y_t)| \cdot |\hat{r}_T - \bar{r}|^3 \\ \sum_{t=1}^T |S'''(\mathbf{W}_{it}^\top \tilde{\boldsymbol{\theta}}_{iT}, Y_t)| \cdot \|\mathbf{W}_{it}^\top \hat{\boldsymbol{\theta}}_{iT} - \mathbf{W}_{it}^\top \bar{\boldsymbol{\theta}}_i\|^3 \end{array} \right) \\
&\leq \frac{1}{6} T^{-1/2} \left\{ \frac{1}{T} \sum_{t=1}^T \begin{pmatrix} |S'''(\tilde{r}_T, Y_t)| & 0 \\ 0 & |S'''(\tilde{\boldsymbol{\theta}}_{iT}, Y_t)| \cdot \|\mathbf{W}_{it}^\top\|^3 \end{pmatrix} \right\} \begin{pmatrix} (\sqrt{T} \|\hat{r}_T - \bar{r}\|)^3 \\ (\sqrt{T} \|\hat{\boldsymbol{\theta}}_{iT} - \bar{\boldsymbol{\theta}}_i\|)^3 \end{pmatrix} \\
&= o_{\mathbb{P}}(1) \times \begin{pmatrix} \mathcal{O}_{\mathbb{P}}(1) \\ \mathcal{O}_{\mathbb{P}}(1) \end{pmatrix} \\
&= o_{\mathbb{P}}(1), \tag{38}
\end{aligned}$$

where the proof of the $o_{\mathbb{P}}(1)$ -term follows analogously to (34). Notice for this that as \mathbf{W}_{it} contains a constant by assumption, the procedure in (34) together with Assumption 3.5 (ii) also implies that $T^{-1/2} \frac{1}{T} \sum_{t=1}^T |S'''(\tilde{r}_T, Y_t)| = o_{\mathbb{P}}(1)$.

Hence, from the above three derivations together with (35), we obtain

$$\begin{aligned}
T \left(\widehat{\text{DSC}}_{iT} - \overline{\text{DSC}}_i \right) &= \frac{1}{2} \left(T^{-1/2} \sum_{t=1}^T S'(\bar{r}, Y_t) \mathbf{W}_{it}^\top \right) \\
&\quad \times \left(\begin{pmatrix} \frac{1}{T} \sum_{t=1}^T S''(\bar{r}, Y_t) \mathbf{W}_{it} \mathbf{W}_{it}^\top \\ \mathbf{0} \end{pmatrix}^{-1} - \begin{pmatrix} \left(\frac{1}{T} \sum_{t=1}^T S''(\bar{r}, Y_t) \right)^{-1} & \mathbf{0} \\ \mathbf{0} & \mathbf{0} \end{pmatrix} \right) \\
&\quad \times \left(T^{-1/2} \sum_{t=1}^T S'(\bar{r}, Y_t) \mathbf{W}_{it} \right) + o_{\mathbb{P}}(1),
\end{aligned}$$

such that the claim of the theorem follows by applying a CLT to the outer terms and a law of large numbers to the inner one. \square

Proof of Proposition 3.9. Notice that $\phi(Y_t)$ and $\phi(\mathbf{W}_{it}^\top \boldsymbol{\theta})$ are measurable functions of α -mixing processes of size $-s/(s-2)$, $s > 2$, and thus itself mixing of the same size by White (2001, Theorem 3.49) together with Assumption 3.7(ii). Next, consider the objective functions

$$\begin{aligned}
\widehat{Q}_{iT}(\boldsymbol{\theta}) &:= \frac{1}{T} \sum_{t=1}^T S(\mathbf{W}_{it}^\top \boldsymbol{\theta}, Y_t) \quad \text{and} \\
\overline{Q}_{iT}(\boldsymbol{\theta}) &:= \mathbb{E} \left[\widehat{Q}_{iT}(\boldsymbol{\theta}) \right] = \mathbb{E} \left[\frac{1}{T} \sum_{t=1}^T S(\mathbf{W}_{it}^\top \boldsymbol{\theta}, Y_t) \right] = \mathbb{E} \left[S(\mathbf{W}_{it}^\top \boldsymbol{\theta}, Y_t) \right].
\end{aligned}$$

The first and second derivatives of the objective functions with respect to $\boldsymbol{\theta}$ are

$$\begin{aligned}\nabla_{\boldsymbol{\theta}}\widehat{Q}_{iT}(\boldsymbol{\theta}) &:= \frac{1}{T} \sum_{t=1}^T \phi''(\mathbf{W}_{it}^{\top}\boldsymbol{\theta})\mathbf{W}_{it}(\mathbf{W}_{it}^{\top}\boldsymbol{\theta} - Y_t), \\ \nabla_{\boldsymbol{\theta}}\overline{Q}_{iT}(\boldsymbol{\theta}) &:= \mathbb{E} \left[\nabla_{\boldsymbol{\theta}}\widehat{Q}_{iT}(\boldsymbol{\theta}) \right] = \mathbb{E} \left[\phi''(\mathbf{W}_{it}^{\top}\boldsymbol{\theta})\mathbf{W}_{it}(\mathbf{W}_{it}^{\top}\boldsymbol{\theta} - Y_t) \right] \\ \nabla_{\boldsymbol{\theta}\boldsymbol{\theta}}\widehat{Q}_{iT}(\boldsymbol{\theta}) &:= \frac{1}{T} \sum_{t=1}^T \phi'''(\mathbf{W}_{it}^{\top}\boldsymbol{\theta})\mathbf{W}_{it}\mathbf{W}_{it}^{\top}(\mathbf{W}_{it}^{\top}\boldsymbol{\theta} - Y_t) + \phi''(\mathbf{W}_{it}^{\top}\boldsymbol{\theta})\mathbf{W}_{it}\mathbf{W}_{it}^{\top}, \\ \nabla_{\boldsymbol{\theta}\boldsymbol{\theta}}\overline{Q}_{iT}(\boldsymbol{\theta}) &:= \mathbb{E} \left[\nabla_{\boldsymbol{\theta}\boldsymbol{\theta}}\widehat{Q}_{iT}(\boldsymbol{\theta}) \right] = \mathbb{E} \left[\phi'''(\mathbf{W}_{it}^{\top}\boldsymbol{\theta})\mathbf{W}_{it}\mathbf{W}_{it}^{\top}(\mathbf{W}_{it}^{\top}\boldsymbol{\theta} - Y_t) + \phi''(\mathbf{W}_{it}^{\top}\boldsymbol{\theta})\mathbf{W}_{it}\mathbf{W}_{it}^{\top} \right].\end{aligned}$$

Notice, when working with the derivatives of the objective function at the population level, we interchange differentiation and expectation, i.e., $\mathbb{E} \left[\nabla_{\boldsymbol{\theta}}\widehat{Q}_{iT}(\boldsymbol{\theta}) \right] = \nabla_{\boldsymbol{\theta}}\mathbb{E} \left[\widehat{Q}_{iT}(\boldsymbol{\theta}) \right]$, using a measure-theoretic version of the Leibniz rule, which requires the derivative to exist and to be absolutely bounded by an integrable function independent of $\boldsymbol{\theta}$. For $\nabla_{\boldsymbol{\theta}}\overline{Q}_{iT}(\boldsymbol{\theta})$ and $\nabla_{\boldsymbol{\theta}\boldsymbol{\theta}}\overline{Q}_{iT}(\boldsymbol{\theta})$, this is ensured by

$$\begin{aligned}d_1(\mathbf{W}_{it}, Y_t) &= \sup_{\boldsymbol{\theta} \in \Theta} \left\| \phi''(\mathbf{W}_{it}^{\top}\boldsymbol{\theta})\mathbf{W}_{it}(\mathbf{W}_{it}^{\top}\boldsymbol{\theta} - Y_t) \right\| \quad \text{and} \\ d_2(\mathbf{W}_{it}, Y_t) &= \sup_{\boldsymbol{\theta} \in \Theta} \left\| \phi'''(\mathbf{W}_{it}^{\top}\boldsymbol{\theta})\mathbf{W}_{it}\mathbf{W}_{it}^{\top}(\mathbf{W}_{it}^{\top}\boldsymbol{\theta} - Y_t) + \phi''(\mathbf{W}_{it}^{\top}\boldsymbol{\theta})\mathbf{W}_{it}\mathbf{W}_{it}^{\top} \right\|,\end{aligned}$$

together with the moment conditions in Assumption 3.7(v).

Note, throughout the proof, the L_s vector norm is denoted by $\|\cdot\|_s$ for $s > 0$. In particular, for $s = 2$, we denote the Euclidean norm by $\|\cdot\| := \|\cdot\|_2$. We proceed to verify the high-level assumptions from Section 3.2, following the order in which they are presented.

For Assumption 3.3(i), we start to show consistency and convergence of the M-estimators using Theorems 2.1 and 3.1 of Newey and McFadden (1994). This directly implies the statement in high level Assumption 3.3(i).

We start by confirming conditions (i)–(iv) of Newey and McFadden (1994, Theorem 2.1) for the parameter $\boldsymbol{\theta}$. Since the score is strictly consistent for the mean, we can apply Holzmann and Eulert (2014, Theorem 1) to state that for all $\boldsymbol{\theta} \in \Theta$,

$$\mathbb{E} \left[\mathbf{S}(\mathbf{W}_{it}^{\top}\bar{\boldsymbol{\theta}}_i, Y_t) \right] \leq \mathbb{E} \left[\mathbf{S}(\mathbf{W}_{it}^{\top}\boldsymbol{\theta}, Y_t) \right], \quad (39)$$

with equality if and only if $\mathbf{W}_{it}^{\top}\bar{\boldsymbol{\theta}}_i \stackrel{\text{a.s.}}{=} \mathbf{W}_{it}^{\top}\boldsymbol{\theta}$. From this we get the equivalences

$$\begin{aligned}\mathbf{W}_{it}^{\top}\bar{\boldsymbol{\theta}}_i \stackrel{\text{a.s.}}{=} \mathbf{W}_{it}^{\top}\boldsymbol{\theta} &\iff \mathbf{W}_{it}^{\top}(\bar{\boldsymbol{\theta}}_i - \boldsymbol{\theta}) \stackrel{\text{a.s.}}{=} \mathbf{0} \\ \iff \left(\mathbf{W}_{it}^{\top}(\bar{\boldsymbol{\theta}}_i - \boldsymbol{\theta}) \right)^2 &= (\bar{\boldsymbol{\theta}}_i - \boldsymbol{\theta})^{\top} \mathbf{W}_{it}\mathbf{W}_{it}^{\top}(\bar{\boldsymbol{\theta}}_i - \boldsymbol{\theta}) \stackrel{\text{a.s.}}{=} \mathbf{0},\end{aligned}$$

which implies

$$(\bar{\boldsymbol{\theta}}_i - \boldsymbol{\theta})^{\top} \mathbb{E} \left[\mathbf{W}_{it}\mathbf{W}_{it}^{\top} \right] (\bar{\boldsymbol{\theta}}_i - \boldsymbol{\theta}) = \mathbf{0}. \quad (40)$$

As per Assumption 3.7(iii), the matrix $\mathbb{E} \left[\mathbf{W}_{it}\mathbf{W}_{it}^{\top} \right]$ is positive definite, the equality in (40) can hold only if $\bar{\boldsymbol{\theta}}_i - \boldsymbol{\theta} = \mathbf{0}$. Hence, $\boldsymbol{\theta} = \bar{\boldsymbol{\theta}}_i$ is the unique minimizer of $\overline{Q}_{iT}(\boldsymbol{\theta})$, which verifies condition

(i) of [Newey and McFadden \(1994, Theorem 2.1\)](#).

Condition (ii) of [Newey and McFadden \(1994, Theorem 2.1\)](#), i.e., compactness of Θ , holds by imposing Assumption 3.1 and condition (iii) requires continuity of the objective function $\bar{Q}_{iT}(\boldsymbol{\theta})$ which is fulfilled as per Assumption 3.7(i).

Condition (iv) of [Newey and McFadden \(1994, Theorem 2.1\)](#) requires $\sup_{\boldsymbol{\theta} \in \Theta} \left| \widehat{Q}_{iT}(\boldsymbol{\theta}) - \bar{Q}_{iT}(\boldsymbol{\theta}) \right| = o_{\mathbb{P}}(1)$ which follows from [Davidson \(1994, Theorem 21.9\)](#) given that

(a) $\widehat{Q}_{iT}(\boldsymbol{\theta}) - \bar{Q}_{iT}(\boldsymbol{\theta}) = o_{\mathbb{P}}(1)$ for all $\boldsymbol{\theta} \in \Theta$, and

(b) $\{\widehat{Q}_{iT}(\cdot) - \bar{Q}_{iT}(\cdot)\}$ is stochastically equicontinuous.

We first prove the point-wise law of large numbers for the objective function in (a). From [White \(2001, Theorem 3.49\)](#), it follows that $\mathbf{S}(\mathbf{W}_{it}^{\top} \boldsymbol{\theta}, Y_t)$ is stationary and α -mixing of size $-s/(s-2)$, $s > 2$, by Assumptions 3.1 and 3.7(ii). Further, as of [White \(2001, Proposition 3.44\)](#), $\mathbf{S}(\mathbf{W}_{it}^{\top} \boldsymbol{\theta}, Y_t)$ is ergodic because it is a measurable function of $(Y_t, \mathbf{W}_{it}^{\top})$. Since

$$\begin{aligned} \mathbb{E} \left| \mathbf{S}(\mathbf{W}_{it}^{\top} \boldsymbol{\theta}, Y_t) \right| &= \mathbb{E} \left| \phi(Y_t) - \phi(\mathbf{W}_{it}^{\top} \boldsymbol{\theta}) - \phi'(\mathbf{W}_{it}^{\top} \boldsymbol{\theta})(Y_t - \mathbf{W}_{it}^{\top} \boldsymbol{\theta}) \right| \\ &\leq \mathbb{E} |\phi(Y_t)| + \mathbb{E} \left| \phi(\mathbf{W}_{it}^{\top} \boldsymbol{\theta}) \right| + \mathbb{E} \left| \phi'(\mathbf{W}_{it}^{\top} \boldsymbol{\theta})(Y_t - \mathbf{W}_{it}^{\top} \boldsymbol{\theta}) \right| < \infty, \end{aligned} \quad (41)$$

the ergodicity Theorem 3.34 in [White \(2001\)](#) is verified and the pointwise law of large numbers in (a) follows.

Concerning condition (b) of [Davidson \(1994, Theorem 21.9\)](#), we show that

$$\left| \frac{1}{T} \sum_{t=1}^T \mathbf{S}(\mathbf{W}_{it}^{\top} \boldsymbol{\theta}, Y_t) - \mathbf{S}(\mathbf{W}_{it}^{\top} \tilde{\boldsymbol{\theta}}, Y_t) \right| \leq B_T \|\boldsymbol{\theta} - \tilde{\boldsymbol{\theta}}\| \quad \text{for all } \boldsymbol{\theta}, \tilde{\boldsymbol{\theta}} \in \Theta,$$

where $B_T > 0$ is a stochastic sequence independent of $\boldsymbol{\theta}$ and $\tilde{\boldsymbol{\theta}}$, for which we have $B_T = \mathcal{O}_{\mathbb{P}}(1)$. To establish the result, we use that, by compactness of Θ , there exists some constant $\Delta_{\boldsymbol{\theta}} > 0$ such that

$$\sup_{\boldsymbol{\theta} \in \Theta} \|\boldsymbol{\theta}\| = \Delta_{\boldsymbol{\theta}} < \infty. \quad (42)$$

By the mean value theorem, which can be applied due to convexity of Θ as per Assumption 3.1, together with triangle inequality, we get for some mean value $\boldsymbol{\theta}^*$ on the line joining $\tilde{\boldsymbol{\theta}}$ and $\boldsymbol{\theta}$, that

$$\begin{aligned} &\left| \frac{1}{T} \sum_{t=1}^T \mathbf{S}(\mathbf{W}_{it}^{\top} \boldsymbol{\theta}, Y_t) - \frac{1}{T} \sum_{t=1}^T \mathbf{S}(\mathbf{W}_{it}^{\top} \tilde{\boldsymbol{\theta}}, Y_t) \right| = \left| \frac{1}{T} \sum_{t=1}^T \phi''(\mathbf{W}_{it}^{\top} \boldsymbol{\theta}^*) \mathbf{W}_{it}^{\top} (Y_t - \mathbf{W}_{it}^{\top} \boldsymbol{\theta}^*) (\boldsymbol{\theta} - \tilde{\boldsymbol{\theta}}) \right| \\ &\leq \frac{1}{T} \sum_{t=1}^T \left| \phi''(\mathbf{W}_{it}^{\top} \boldsymbol{\theta}^*) \right| \cdot \|\mathbf{W}_{it}\| \cdot \left| \mathbf{W}_{it}^{\top} \boldsymbol{\theta}^* - Y_t \right| \cdot \|\boldsymbol{\theta} - \tilde{\boldsymbol{\theta}}\| \\ &\leq \frac{1}{T} \sum_{t=1}^T \left| \phi''(\mathbf{W}_{it}^{\top} \boldsymbol{\theta}^*) \right| \cdot \|\mathbf{W}_{it}\| \cdot (\|\mathbf{W}_{it}\| \Delta_{\boldsymbol{\theta}} + |Y_t|) \cdot \|\boldsymbol{\theta} - \tilde{\boldsymbol{\theta}}\| \\ &\leq B_T \|\boldsymbol{\theta} - \tilde{\boldsymbol{\theta}}\|, \end{aligned} \quad (43)$$

where

$$B_T := \frac{1}{T} \sum_{t=1}^T \sup_{\boldsymbol{\theta} \in \Theta} \left| \phi''(\mathbf{W}_{it}^\top \boldsymbol{\theta}) \right| \|\mathbf{W}_{it}\| \cdot (\|\mathbf{W}_{it}\| \Delta_{\boldsymbol{\theta}} + |Y_t|). \quad (44)$$

Then, $B_T = \mathcal{O}_{\mathbb{P}}(1)$ follows from Davidson (1994, Theorem 12.11) as

$$\sup_{T \in \mathbb{N}} \mathbb{E}[B_T] \leq \mathbb{E} \left[\sup_{\boldsymbol{\theta} \in \Theta} \left| \phi''(\mathbf{W}_{it}^\top \boldsymbol{\theta}) \right| \|\mathbf{W}_{it}\|^2 \Delta_{\boldsymbol{\theta}} \right] + \mathbb{E} \left[\sup_{\boldsymbol{\theta} \in \Theta} \left| \phi''(\mathbf{W}_{it}^\top \boldsymbol{\theta}) \right| \|\mathbf{W}_{it}\| |Y_t| \right] < \infty, \quad (45)$$

where the existence of the involved expectations is implied by Assumption 3.7(v). It follows that $\{\widehat{Q}_{iT}(\cdot) - \overline{Q}_{iT}(\cdot)\}$ is stochastically equicontinuous. Hence, we can apply Theorem 2.1 of Newey and McFadden (1994) to conclude that the M-estimator is consistent, i.e. $\widehat{\boldsymbol{\theta}}_{iT} \xrightarrow{\mathbb{P}} \bar{\boldsymbol{\theta}}_i$.

Secondly, we check conditions (i)–(v) of Newey and McFadden (1994, Theorem 3.1). Since $\bar{\boldsymbol{\theta}}_i \in \text{int}(\Theta)$ by Assumption 3.1, condition (i) holds. By Assumption 3.7(i), the objective function $\widehat{Q}_{iT}(\boldsymbol{\theta})$ is twice continuously differentiable, ensuring that condition (ii) is fulfilled. To verify condition (iii), we have to show that a central limit theorem holds for $\sqrt{T} \nabla_{\boldsymbol{\theta}} \widehat{Q}_{iT}(\bar{\boldsymbol{\theta}}_i)$. By the Cramér–Wold device, this reduces to show univariate convergence, i.e.,

$$T^{-1/2} \boldsymbol{\lambda}^\top \mathbf{V}_T^{-1/2} \sum_{t=1}^T \phi''(\mathbf{W}_{it}^\top \bar{\boldsymbol{\theta}}_i) \mathbf{W}_{it} (Y_t - \mathbf{W}_{it}^\top \bar{\boldsymbol{\theta}}_i) \xrightarrow{d} \mathcal{N}(0, 1), \quad T \rightarrow \infty, \quad (46)$$

for any $\boldsymbol{\lambda} \in \mathbb{R}^k$ satisfying $\boldsymbol{\lambda}^\top \boldsymbol{\lambda} = 1$. We show this by verifying the required conditions of the CLT in White (2001, Theorem 5.20). Note that by White (2001, Theorem 3.49) and Assumption 3.7(ii), the sequences $\{\phi''(\mathbf{W}_{it}^\top \bar{\boldsymbol{\theta}}_i) \mathbf{W}_{it} (Y_t - \mathbf{W}_{it}^\top \bar{\boldsymbol{\theta}}_i)\}$ and $\{\boldsymbol{\lambda}^\top \mathbf{V}_T^{-1/2} \phi''(\mathbf{W}_{it}^\top \bar{\boldsymbol{\theta}}_i) \mathbf{W}_{it} (Y_t - \mathbf{W}_{it}^\top \bar{\boldsymbol{\theta}}_i)\}$ are α -mixing of size $-s/(s-2)$, $s > 2$. Since $\boldsymbol{\theta} = \bar{\boldsymbol{\theta}}_i$ uniquely minimizes the population objective (see the discussion around (40)) the first-order condition,

$$\begin{aligned} \nabla_{\boldsymbol{\theta}} \overline{Q}_{iT}(\bar{\boldsymbol{\theta}}_i) &= \mathbb{E} \left[\frac{1}{T} \sum_{t=1}^T \phi''(\mathbf{W}_{it}^\top \bar{\boldsymbol{\theta}}_i) \mathbf{W}_{it} (\mathbf{W}_{it}^\top \bar{\boldsymbol{\theta}}_i - Y_t) \right] \\ &= \frac{1}{T} \sum_{t=1}^T \left(\mathbb{E} \left[\phi''(\mathbf{W}_{it}^\top \bar{\boldsymbol{\theta}}_i) \mathbf{W}_{it} \mathbf{W}_{it}^\top \bar{\boldsymbol{\theta}}_i \right] - \mathbb{E} \left[\phi''(\mathbf{W}_{it}^\top \bar{\boldsymbol{\theta}}_i) \mathbf{W}_{it} Y_t \right] \right) = \mathbf{0}, \end{aligned} \quad (47)$$

holds by the law of iterated expectations, $\mathbb{E} [\phi''(\mathbf{W}_{it}^\top \bar{\boldsymbol{\theta}}_i) \mathbf{W}_{it} Y_t] = \mathbb{E} [\phi''(\mathbf{W}_{it}^\top \bar{\boldsymbol{\theta}}_i) \mathbf{W}_{it} \mathbb{E}[Y_t | \mathbf{W}_{it}]] = \mathbb{E} [\phi''(\mathbf{W}_{it}^\top \bar{\boldsymbol{\theta}}_i) \mathbf{W}_{it} \mathbf{W}_{it}^\top \bar{\boldsymbol{\theta}}_i]$, together with Assumption 3.1. This first-order condition further implies that $\mathbb{E} [\boldsymbol{\lambda}^\top \mathbf{V}_T^{-1/2} \phi''(\mathbf{W}_{it}^\top \bar{\boldsymbol{\theta}}_i) \mathbf{W}_{it} (Y_t - \mathbf{W}_{it}^\top \bar{\boldsymbol{\theta}}_i)] = \mathbf{0}$. By sub-multiplicativity of norms and Assumption 3.7(v), we get that

$$\mathbb{E} \left[\left| \boldsymbol{\lambda}^\top \mathbf{V}_T^{-1/2} \phi''(\mathbf{W}_{it}^\top \bar{\boldsymbol{\theta}}_i) \mathbf{W}_{it} (Y_t - \mathbf{W}_{it}^\top \bar{\boldsymbol{\theta}}_i) \right|^s \right] \leq \|\boldsymbol{\lambda}^\top \mathbf{V}_T^{-1/2}\|^s \mathbb{E} \left[\left| \phi''(\mathbf{W}_{it}^\top \bar{\boldsymbol{\theta}}_i) \mathbf{W}_{it} (Y_t - \mathbf{W}_{it}^\top \bar{\boldsymbol{\theta}}_i) \right|^s \right]$$

is finite for $s > 2$, $\forall t$. Therefore, given Assumption 3.7(iv), the univariate convergence result in (46) follows. Further, by the Cramér–Wold device, the conditions of the univariate central limit

theorem for mixing series hold for all linear combinations, leading to the desired result

$$T^{-1/2} \mathbf{V}_T^{-1/2} \sum_{t=1}^T \phi'' \left(\mathbf{W}_{it}^\top \bar{\boldsymbol{\theta}}_i \right) \mathbf{W}_{it} \left(Y_t - \mathbf{W}_{it}^\top \bar{\boldsymbol{\theta}}_i \right) = \mathbf{V}_T^{-1/2} \sqrt{T} \nabla_{\boldsymbol{\theta}} \widehat{Q}_{iT}(\bar{\boldsymbol{\theta}}_i) \xrightarrow{d} \mathcal{N}(0, I_k). \quad (48)$$

For the fourth condition of [Newey and McFadden \(1994, Theorem 3.1\)](#), we use [Newey and McFadden \(1994, Lemma 2.4\)](#) to show uniform convergence in probability for the Hessian, i.e.

$$\sup_{\boldsymbol{\theta} \in \Theta} \left\| \nabla_{\boldsymbol{\theta}\boldsymbol{\theta}} \widehat{Q}_{iT}(\boldsymbol{\theta}) - \nabla_{\boldsymbol{\theta}\boldsymbol{\theta}} \bar{Q}_{iT}(\boldsymbol{\theta}) \right\| \xrightarrow{\mathbb{P}} 0. \quad (49)$$

Since we consider stationary random variables, a compact Θ by Assumption 3.1, and the objective function is continuous for all $\boldsymbol{\theta} \in \Theta$ by Assumption 3.7(i), we are left to show that there exists a dominating function $d_3(\mathbf{W}_{it}, Y_t) \geq \left\| \nabla_{\boldsymbol{\theta}\boldsymbol{\theta}} \widehat{Q}_{iT}(\boldsymbol{\theta}) \right\|$ for all $\boldsymbol{\theta} \in \Theta$, with $\mathbb{E}[d_3(\mathbf{W}_{it}, Y_t)] < \infty$, which holds for

$$d_3(\mathbf{W}_{it}, Y_t) := \sup_{\boldsymbol{\theta} \in \Theta} \left(\left| \phi''' \left(\mathbf{W}_{it}^\top \boldsymbol{\theta} \right) \right| \cdot \|\mathbf{W}_{it}\|^2 \cdot \left| \mathbf{W}_{it}^\top \boldsymbol{\theta} - Y_t \right| \right) + \sup_{\boldsymbol{\theta} \in \Theta} \left| \phi'' \left(\mathbf{W}_{it}^\top \boldsymbol{\theta} \right) \right| \cdot \|\mathbf{W}_{it}\|^2, \quad (50)$$

whose expectation is finite by Assumption 3.7(v). Hence, the desired convergence result in (49) follows.

Lastly, condition (v) of [Newey and McFadden \(1994, Theorem 3.1\)](#) requires a non-singular expected Hessian, $\nabla_{\boldsymbol{\theta}\boldsymbol{\theta}} \bar{Q}_{iT}(\bar{\boldsymbol{\theta}}_i) = \mathbb{E} \left[\phi'''(\mathbf{W}_{it}^\top \bar{\boldsymbol{\theta}}_i) \mathbf{W}_{it} \mathbf{W}_{it}^\top (\mathbf{W}_{it}^\top \bar{\boldsymbol{\theta}}_i - Y_t) + \phi''(\mathbf{W}_{it}^\top \bar{\boldsymbol{\theta}}_i) \mathbf{W}_{it} \mathbf{W}_{it}^\top \right]$. Notice that by Assumption 3.1 and the law of iterated expectations, we have that $\mathbb{E} \left[\phi'''(\mathbf{W}_{it}^\top \bar{\boldsymbol{\theta}}_i) \mathbf{W}_{it} \mathbf{W}_{it}^\top (\mathbf{W}_{it}^\top \bar{\boldsymbol{\theta}}_i - Y_t) \right] = \mathbb{E} \left[\phi'''(\mathbf{W}_{it}^\top \bar{\boldsymbol{\theta}}_i) \mathbf{W}_{it} \mathbf{W}_{it}^\top (\mathbf{W}_{it}^\top \bar{\boldsymbol{\theta}}_i - \mathbb{E}[Y_t | \mathbf{W}_{it}]) \right] = \mathbf{0}$, and thus the expected Hessian simplifies to

$$\nabla_{\boldsymbol{\theta}\boldsymbol{\theta}} \bar{Q}_{iT}(\bar{\boldsymbol{\theta}}_i) = \mathbb{E} \left[\phi''(\mathbf{W}_{it}^\top \bar{\boldsymbol{\theta}}_i) \mathbf{W}_{it} \mathbf{W}_{it}^\top \right]. \quad (51)$$

Assumption 3.7(i) assures $\phi''(\mathbf{W}_{it}^\top \bar{\boldsymbol{\theta}}_i) > 0$. This, together with the positive definiteness of $\mathbb{E}[\mathbf{W}_{it} \mathbf{W}_{it}^\top]$, allows us to apply [Dimitriadis and Bayer \(2019, Lemma B.2\)](#), which establishes that the matrix $\mathbb{E} \left[\phi''(\mathbf{W}_{it}^\top \bar{\boldsymbol{\theta}}_i) \mathbf{W}_{it} \mathbf{W}_{it}^\top \right]$ is positive definite as well. Thus, $\nabla_{\boldsymbol{\theta}\boldsymbol{\theta}} \bar{Q}_{iT}(\bar{\boldsymbol{\theta}}_i)$ is non-singular.

We conclude the verification of Assumption 3.3(i) by noting that the above results generalize to the case where the reference forecast is considered, which corresponds to the setting $\mathbf{W}_{it} = 1$.

We continue to verify the high-level Assumption 3.3(ii), which invokes a CLT for the vector of scores $T^{-1/2} \sum_{t=1}^T (a_{1t}, c_{1t}, a_{2t}, c_{2t}, e_t)$. For this, we use the Cramér-Wold Device under which the problem reduces to showing that

$$T^{-1/2} \boldsymbol{\lambda}^\top \boldsymbol{\Omega}_T^{-1/2} \sum_{t=1}^T (a_{1t}, c_{1t}, a_{2t}, c_{2t}, e_t)^\top \xrightarrow{d} \mathcal{N}(0, 1), \quad (52)$$

for all $\boldsymbol{\lambda} \in \mathbb{R}^5$ with $\boldsymbol{\lambda}^\top \boldsymbol{\lambda} = 1$.

Since the scores are measurable functions of the α -mixing variables by Assumption 3.7(ii), it follows from [White \(2001, Theorem 3.49\)](#) that the components of the vector $(a_{1t}, c_{1t}, a_{2t}, c_{2t}, e_t)$ are also α -mixing of size $-s/(s-2)$ for $s > 2$. Thus, we can apply the standard central limit

theorem for mixing variables in [White \(2001, Theorem 5.20\)](#). To do so, note that a_{it}, c_{it}, e_t , $i = 1, 2$, are defined as difference in scores between the sample and population values. Hence these terms are centered around zero by construction and thus $\mathbb{E} \left[\boldsymbol{\lambda}^\top (a_{1t}, c_{1t}, a_{2t}, c_{2t}, e_t)^\top \right] = 0$. It further holds that

$$\mathbb{E} \left\| \boldsymbol{\lambda}^\top \boldsymbol{\Omega}_T^{-1/2} (a_{1t}, c_{1t}, a_{2t}, c_{2t}, e_t)^\top \right\|^s \leq \left\| \boldsymbol{\lambda}^\top \boldsymbol{\Omega}_T^{-1/2} \right\|^s \mathbb{E} \left\| (a_{1t}, c_{1t}, a_{2t}, c_{2t}, e_t) \right\|^s < \infty, \quad (53)$$

which validates the required moment conditions for [White \(2001, Theorem 5.20\)](#).

Since $\left\| \boldsymbol{\lambda}^\top \boldsymbol{\Omega}_T^{-1/2} \right\|^s$ is finite by [Assumption 3.8](#), we particularly analyze the vector $(a_{1t}, c_{1t}, a_{2t}, c_{2t}, e_t)$ and note that by linearity of expectations

$$\mathbb{E} \left\| (a_{1t}, c_{1t}, a_{2t}, c_{2t}, e_t)^\top \right\|^s = \mathbb{E}|a_{1t}|^s + \mathbb{E}|c_{1t}|^s + \mathbb{E}|a_{2t}|^s + \mathbb{E}|c_{2t}|^s + \mathbb{E}|e_t|^s < \infty, \quad (54)$$

provided that each $\mathbb{E}|a_{it}|^s, \mathbb{E}|c_{it}|^s, \mathbb{E}|e_t|^s < \infty$. To verify this, we detail the bound for $\mathbb{E}|c_{it}|^s$ and show that it is finite by applying the c_s -inequality:

$$\begin{aligned} \mathbb{E}|c_{it}|^s &= \mathbb{E} \left| \mathbf{S}(\mathbf{W}_{it}^\top \boldsymbol{\theta}, Y_t) - \mathbb{E}[\mathbf{S}(\mathbf{W}_{it}^\top \boldsymbol{\theta}, Y_t)] \right|^s \\ &\leq 2^{s-1} \left(\mathbb{E} \left[|\mathbf{S}(\mathbf{W}_{it}^\top \boldsymbol{\theta}, Y_t)|^s \right] + \left| \mathbb{E} \left[\mathbf{S}(\mathbf{W}_{it}^\top \boldsymbol{\theta}, Y_t) \right] \right|^s \right) < \infty. \end{aligned} \quad (55)$$

Finiteness of the sum in [\(55\)](#) follows from the moment conditions in [Assumptions 3.7\(v\)](#) by again applying the c_s -inequality, i.e.,

$$\mathbb{E} \left| \mathbf{S}(\mathbf{W}_{it}^\top \boldsymbol{\theta}, Y_t) \right|^s \leq 3^{2s-1} \left(\mathbb{E} \left[|\phi(Y_t)|^s \right] + \mathbb{E} \left[\left| \phi(\mathbf{W}_{it}^\top \boldsymbol{\theta}) \right|^s \right] + \mathbb{E} \left[\left| \phi'(\mathbf{W}_{it}^\top \boldsymbol{\theta}) (Y_t - \mathbf{W}_{it}^\top \boldsymbol{\theta}) \right|^s \right] \right) < \infty.$$

The same reasoning applies to $\mathbb{E}|a_{it}|^s$ and $\mathbb{E}|e_t|^s$. Since all norms on a finite-dimensional space are equivalent, there exists a constant $K > 0$ such that, for the vector $(a_{1t}, c_{1t}, a_{2t}, c_{2t}, e_t)$, the Euclidean norm is at most K times the L_s -norm, i.e., we can write $\left\| (a_{1t}, c_{1t}, a_{2t}, c_{2t}, e_t)^\top \right\| \leq K \left\| (a_{1t}, c_{1t}, a_{2t}, c_{2t}, e_t)^\top \right\|_s$. Raising this expression to the s -th power, taking expectations, and using [\(54\)](#), we get that

$$\mathbb{E} \left\| (a_{1t}, c_{1t}, a_{2t}, c_{2t}, e_t)^\top \right\|^s \leq K^s \mathbb{E} \left\| (a_{1t}, c_{1t}, a_{2t}, c_{2t}, e_t)^\top \right\|_s^s \leq K^s \left[\mathbb{E}|a_{1t}|^s + \dots + \mathbb{E}|e_t|^s \right] < \infty,$$

because K^s is a constant. Hence, the moment condition of [White \(2001, Theorem 5.20\)](#) is fulfilled and the univariate convergence result in [\(52\)](#) follows, given [Assumption 3.8](#). Further, by the Cramér–Wold device, the conditions of the univariate central limit theorem for mixing series hold for all linear combinations, leading to the desired result,

$$T^{-1/2} \boldsymbol{\Omega}_T^{-1/2} \sum_{t=1}^T (a_{1t}, c_{1t}, a_{2t}, c_{2t}, e_t)^\top \xrightarrow{d} \mathcal{N}(0, I_5). \quad (56)$$

For the verification of the high-level [Assumption 3.3\(iii\)](#), we notice that by [Assumption 3.7\(i\)](#), $\phi(\mathbf{W}_{it}^\top \boldsymbol{\theta})$ is continuously differentiable in $\boldsymbol{\theta}$, implying that $\mathbf{S}(\mathbf{W}_{it}^\top \boldsymbol{\theta}, Y_t)$ is also continuously

differentiable in $\boldsymbol{\theta}$ with derivative

$$\nabla_{\boldsymbol{\theta}} S(\mathbf{W}_{it}^{\top} \boldsymbol{\theta}, Y_t) = \phi''(\mathbf{W}_{it}^{\top} \boldsymbol{\theta}) \mathbf{W}_{it} (\mathbf{W}_{it}^{\top} \boldsymbol{\theta} - Y_t),$$

which can be bounded by

$$\|\phi''(\mathbf{W}_{it}^{\top} \boldsymbol{\theta}) \mathbf{W}_{it} (\mathbf{W}_{it}^{\top} \boldsymbol{\theta} - Y_t)\| \leq \sup_{\boldsymbol{\theta} \in \Theta} \|\phi''(\mathbf{W}_{it}^{\top} \boldsymbol{\theta}) \mathbf{W}_{it} (\mathbf{W}_{it}^{\top} \boldsymbol{\theta} - Y_t)\|,$$

whose expectation is finite by Assumption 3.7(v). Hence, differentiability carries over to the expectation by the Leibniz integral rule. Moreover, under the same assumptions and reasoning, both the first- and second-order derivatives of the expected score with respect to $\boldsymbol{\theta}$ remain continuously differentiable.

For the verification of high-level Assumption 3.3(iv), we can write

$$\nabla_{\boldsymbol{\theta}} \nu_{iT}(\boldsymbol{\theta}) = \frac{1}{\sqrt{T}} \sum_{t=1}^T \mathbf{S}_{it}, \quad \text{with} \quad \mathbf{S}_{it} := \mathbf{W}_{it} S'(\mathbf{W}_{it}^{\top} \boldsymbol{\theta}, Y_t) - \mathbb{E}[\mathbf{W}_{it} S'(\mathbf{W}_{it}^{\top} \boldsymbol{\theta}, Y_t)],$$

with

$$S'(\mathbf{W}_{it}^{\top} \boldsymbol{\theta}, Y_t) = \phi''(\mathbf{W}_{it}^{\top} \boldsymbol{\theta}) (Y_t - \mathbf{W}_{it}^{\top} \boldsymbol{\theta}),$$

such that \mathbf{S}_{it} is a process centered around zero. Stationarity in Assumption 3.1 implies that

$$\begin{aligned} \mathbb{E} \left\| \frac{1}{\sqrt{T}} \sum_{t=1}^T \mathbf{S}_{it} \right\|^2 &= \frac{1}{T} \mathbb{E} \left\| \sum_{t=1}^T \mathbf{S}_{it} \right\|^2 \\ &= \frac{1}{T} \sum_{t=1}^T \sum_{u=1}^T \mathbb{E} [\mathbf{S}_{it}^{\top} \mathbf{S}_{iu}] \\ &= \frac{1}{T} \sum_{t=1}^T \mathbb{E} [\mathbf{S}_{it}^{\top} \mathbf{S}_{it}] + \frac{2}{T} \sum_{1 \leq t < u \leq T} \mathbb{E} [\mathbf{S}_{it}^{\top} \mathbf{S}_{iu}], \end{aligned} \quad (57)$$

where the second equality follows from the definition $\|\mathbf{S}_{it}\|^2 = \mathbf{S}_{it}^{\top} \mathbf{S}_{it}$ which is then split into a diagonal ($t = u$) and an off-diagonal ($t \neq u$) part in the final step. Concerning the diagonal part, Assumption 3.1 implies $\mathbb{E} [\|\mathbf{S}_{it}\|^2] = \mathbb{E} [\|\mathbf{S}_{1t}\|^2]$, which is finite by the moment bounds given in Assumption 3.7(v). It follows that

$$\sup_{T \in \mathbb{N}} \frac{1}{T} \sum_{t=1}^T \mathbb{E} [\mathbf{S}_{it}^{\top} \mathbf{S}_{it}] = \sup_{T \in \mathbb{N}} \frac{1}{T} \sum_{t=1}^T \mathbb{E} [\|\mathbf{S}_{it}\|^2] = \mathbb{E} [\|\mathbf{S}_{i1}\|^2] < \infty. \quad (58)$$

Concerning the off-diagonal part, observe that the summand depends only on the lag $\ell = u - t$. Using stationarity, as assumed in Assumption 3.1, we can rewrite the expression as

$$\frac{2}{T} \sum_{1 \leq t < u \leq T} \mathbb{E} [\mathbf{S}_{it}^{\top} \mathbf{S}_{iu}] = \frac{2}{T} \sum_{\ell=1}^{T-1} (T - \ell) \mathbb{E} [\mathbf{S}_{i1}^{\top} \mathbf{S}_{i,1+\ell}] \leq 2 \sum_{\ell=1}^{\infty} \left| \mathbb{E} [\mathbf{S}_{i1}^{\top} \mathbf{S}_{i,1+\ell}] \right|,$$

where the inequality follows by taking absolute values and noting the simple fact that $(T - \ell)/T <$

1 for all $\ell = 1, \dots, T - 1$.

We now show that $\sum_{\ell=1}^{\infty} |\mathbb{E}[\mathbf{S}_{i1}^\top \mathbf{S}_{i,1+\ell}]| < \infty$ through the (component-wise) covariance inequality for a α -mixing sequence given in Corollary 14.3 of Davidson (1994). Assumption 3.7(ii) assures \mathbf{S}_{it} to be α -mixing of size $-s/(s-2)$ for some $s > 2$, and Assumption 3.7(v) give $\mathbb{E}[\|\mathbf{S}_{it}\|^s] < \infty$ for the same s . In Davidson's notation, we chose $p = r = s > 2$, which always satisfies the required condition $r \geq p/(p-1)$. We denote $\mathbf{S}_{it}^{(j)}$ to be the j -th, $j = 1, \dots, k$, component of \mathbf{S}_{it} , to get by the aforementioned corollary that, for every lag $\ell \geq 1$,

$$\left| \text{Cov}(\mathbf{S}_{i1}^{(j)}, \mathbf{S}_{i,1+\ell}^{(j)}) \right| \leq 6\alpha(\ell)^{1-2/s} \mathbb{E}[\|\mathbf{S}_{i1}^{(j)}\|_s] \mathbb{E}[\|\mathbf{S}_{i,1+\ell}^{(j)}\|_s] = 6\alpha(\ell)^{1-2/s} \mathbb{E}[\|\mathbf{S}_{i1}^{(j)}\|_s]^2. \quad (59)$$

As \mathbf{S}_{it} has zero mean by construction, it follows that

$$\left| \mathbb{E}[\mathbf{S}_{i1}^\top \mathbf{S}_{i,1+\ell}] \right| = \left| \sum_{j=1}^k \mathbb{E}[\mathbf{S}_{i1}^{(j)} \mathbf{S}_{i,1+\ell}^{(j)}] \right| \leq \sum_{j=1}^k \left| \text{Cov}(\mathbf{S}_{i1}^{(j)}, \mathbf{S}_{i,1+\ell}^{(j)}) \right| \leq 6\alpha(\ell)^{1-2/s} \sum_{j=1}^k \mathbb{E}[\|\mathbf{S}_{i1}^{(j)}\|_s]^2, \quad (60)$$

where we factor out $6\alpha(\ell)^{1-2/s}$ in the last step since the decay of the mixing coefficients applies uniformly to each component $\mathbf{S}_{it}^{(j)}$.

To see that the mixing coefficients are sufficiently fast decaying, recall that per definition (White, 2001, Definition 3.45) there exists some $\epsilon > 0$, such that $\alpha(\ell) = \mathcal{O}\left(\ell^{-\frac{s}{s-2}-\epsilon}\right)$. From this, we get $\alpha(\ell)^{1-2/s} = \mathcal{O}\left(\ell^{-(\frac{s}{s-2}+\epsilon)(1-2/s)}\right) = \mathcal{O}\left(\ell^{-[1+\epsilon(1-2/s)]}\right)$ and given that $s > 2$ by Assumption 3.7(ii), we obtain $1 + \epsilon(1 - 2/s) > 1$. Hence, the sum $\sum_{\ell=1}^{\infty} \ell^{-[1+\epsilon(1-2/s)]}$ converges, which implies that $\sum_{\ell=1}^{\infty} \alpha(\ell)^{1-2/s} < \infty$. Therefore,

$$\sum_{\ell=1}^{\infty} |\mathbb{E}[\mathbf{S}_{i1}^\top \mathbf{S}_{i,1+\ell}]| \leq 6 \sum_{j=1}^k \mathbb{E}[\|\mathbf{S}_{i1}^{(j)}\|_s]^2 \sum_{\ell=1}^{\infty} \alpha(\ell)^{1-2/s} < \infty, \quad (61)$$

which does not involve T and it immediately follows that also $\sup_{T \in \mathbb{N}} \sum_{\ell=1}^{\infty} |\mathbb{E}[\mathbf{S}_{i1}^\top \mathbf{S}_{i,1+\ell}]| < \infty$.

Using (57) together with (58) and (61) gives

$$\sup_{T \in \mathbb{N}} \mathbb{E} \left\| \frac{1}{\sqrt{T}} \sum_{t=1}^T \mathbf{S}_{it} \right\|^2 = \sup_{T \in \mathbb{N}} \mathbb{E} \left[\|\nabla_{\boldsymbol{\theta}} \nu_{iT}(\boldsymbol{\theta})\|^2 \right] < \infty,$$

which, according to Davidson (1994, Theorem 21.10) and the discussion below that theorem, implies that the empirical process $\nu_{iT}(\boldsymbol{\theta}) = T^{-1/2} \sum_{t=1}^T \mathbf{S}(\mathbf{W}_{it}^\top \boldsymbol{\theta}, Y_t) - \mathbb{E}[\mathbf{S}(\mathbf{W}_{it}^\top \boldsymbol{\theta}, Y_t)]$ is stochastically equicontinuous.

Hence, we have shown that Assumption 3.3 holds such that Theorem 3.4 applies under the given conditions. We now continue to verify the high-level conditions in Assumption 3.5.

For the verification of the high-level Assumption 3.5(ii), recall that

$$\begin{aligned}
h_T(\boldsymbol{\theta}) &= \frac{1}{T} \sum_{t=1}^T \left| S'''(\mathbf{W}_{it}^\top \boldsymbol{\theta}, Y_t) \right| \|\mathbf{W}_{it}\|^3 \\
&= \frac{1}{T} \sum_{t=1}^T \left| -\phi'''(\mathbf{W}_{it}^\top \boldsymbol{\theta}) + \phi''''(\mathbf{W}_{it}^\top \boldsymbol{\theta})(\mathbf{W}_{it}^\top \boldsymbol{\theta} - Y_t) \right| \cdot \|\mathbf{W}_{it}\|^3 \\
&=: \frac{1}{T} \sum_{t=1}^T g_t(\boldsymbol{\theta}),
\end{aligned} \tag{62}$$

and note that

$$\begin{aligned}
h'_T(\boldsymbol{\theta}) &= \frac{1}{T} \sum_{t=1}^T \operatorname{sgn} \left\{ S'''(\mathbf{W}_{it}^\top \boldsymbol{\theta}, Y_t) \right\} \cdot \left(\phi''''(\mathbf{W}_{it}^\top \boldsymbol{\theta})(\mathbf{W}_{it}^\top \boldsymbol{\theta} - Y_t) \right) \cdot \mathbf{W}_{it} \cdot \|\mathbf{W}_{it}\|^3 \\
&=: \frac{1}{T} \sum_{t=1}^T g'_t(\boldsymbol{\theta}).
\end{aligned} \tag{63}$$

Concerning the first part of the high level Assumption 3.5(ii), we use that $h_T(\boldsymbol{\theta})$ is Lipschitz-continuous with (random) Lipschitz constant $L = \sup_{\boldsymbol{\theta} \in \Theta} \|h'_T(\boldsymbol{\theta})\|$ as ϕ is assumed to be five times differentiable with bounded derivatives; see Assumption 3.7(v). Therefore, we get that

$$T^{-1/2} \sup_{\|\boldsymbol{\theta} - \bar{\boldsymbol{\theta}}_i\| \leq \delta} |h_T(\boldsymbol{\theta}) - h_T(\bar{\boldsymbol{\theta}}_i)| \leq T^{-1/2} \sup_{\|\boldsymbol{\theta} - \bar{\boldsymbol{\theta}}_i\| \leq \delta} L \|\boldsymbol{\theta} - \bar{\boldsymbol{\theta}}_i\| \leq T^{-1/2} L \delta.$$

To establish that $T^{-1/2} L \delta = o_{\mathbb{P}}(1)$, it suffices to verify a uniform law of large numbers for $\|h'_T(\boldsymbol{\theta})\|$. By taking the supremum of $\|g'_t(\boldsymbol{\theta})\|$, we obtain the dominating function

$$d_4(\mathbf{W}_{it}^\top \boldsymbol{\theta}, Y_t) := \sup_{\boldsymbol{\theta} \in \Theta} \left| \phi''''(\mathbf{W}_{it}^\top \boldsymbol{\theta}) \cdot (\mathbf{W}_{it}^\top \boldsymbol{\theta} - Y_t) \right| \cdot \|\mathbf{W}_{it}\|^4,$$

which is bounded in expectation, i.e., $\mathbb{E}[d_4(\mathbf{W}_{it}^\top \boldsymbol{\theta}, Y_t)] < \infty$, given Assumptions 3.7(v). By Assumption 3.1 the data is stationary and the parameter space Θ is compact. As the function $\|g'_t(\boldsymbol{\theta})\|$ is continuous for all $\boldsymbol{\theta} \in \Theta$ by Assumption 3.7(i), we can apply the uniform law of large numbers in Newey and McFadden (1994, Lemma 2.4) to get that

$$\sup_{\boldsymbol{\theta} \in \Theta} \left\| \frac{1}{T} \sum_{t=1}^T \|g'_t(\boldsymbol{\theta})\| - \mathbb{E}[\|g'_t(\boldsymbol{\theta})\|] \right\| \xrightarrow{\mathbb{P}} 0. \tag{64}$$

Hence, the desired stochastic Lipschitz bound follows.

Concerning the second part of the high level Assumption 3.5(ii), we show that $T^{-1/2} h_T(\bar{\boldsymbol{\theta}}_i) = o_{\mathbb{P}}(1)$ by establishing that $h_T(\bar{\boldsymbol{\theta}}_i)$ satisfies the pointwise law of large numbers. Under Assumptions 3.1 and 3.7(v), White (2001, Theorem 3.49) implies that $g_t(\bar{\boldsymbol{\theta}}_i)$ is stationary and α -mixing of size $-s/(s-2)$, $s > 2$. Moreover, ergodicity of $g_t(\bar{\boldsymbol{\theta}}_i)$ follows since the function itself is a measurable transformation of $(\mathbf{W}_{it}^\top, Y_t)$ (White, 2001, Proposition 3.44). We apply the triangle

inequality to $|g_t(\bar{\boldsymbol{\theta}}_i)|$ which, together with Assumption 3.7(v) results in

$$\mathbb{E}[g_t(\boldsymbol{\theta})] \leq \mathbb{E}\left[|\phi'''(\mathbf{W}_{it}\bar{\boldsymbol{\theta}}_i)|\|\mathbf{W}_{it}\|^3\right] + \mathbb{E}\left[|\phi''''(\mathbf{W}_{it}\bar{\boldsymbol{\theta}}_i)|\cdot|\mathbf{W}_{it}\bar{\boldsymbol{\theta}}_i - Y_t|\cdot\|\mathbf{W}_{it}\|^3\right] < \infty. \quad (65)$$

Given (65), Theorem 3.34 in White (2001) implies the point-wise law of large numbers and we have that $h_T(\bar{\boldsymbol{\theta}}_i) = \mathbb{E}[g_t(\bar{\boldsymbol{\theta}}_i)] + o_{\mathbb{P}}(1)$. Hence, $T^{-1/2}h_T(\bar{\boldsymbol{\theta}}_i) = o_{\mathbb{P}}(1)$, as $T \rightarrow \infty$.

For the verification of the high-level Assumption 3.5(i), we note that the true parameter $\bar{\boldsymbol{\theta}}_i$ lies in $\text{int}(\Theta)$ such that consistency ensures that $\hat{\boldsymbol{\theta}}_{iT}$ is in the interior of the parameter space with probability approaching one as $T \rightarrow \infty$. This implies that the first-order condition $\mathbf{0} = \nabla_{\boldsymbol{\theta}}\hat{Q}_{iT}(\hat{\boldsymbol{\theta}}_{iT})$ holds with probability approaching one as $T \rightarrow \infty$.

Based on this, we apply the mean-value theorem to get that

$$\mathbf{0} = \nabla_{\boldsymbol{\theta}}\hat{Q}_{iT}(\bar{\boldsymbol{\theta}}_i) + \nabla_{\boldsymbol{\theta}\boldsymbol{\theta}}\hat{Q}_{iT}(\tilde{\boldsymbol{\theta}}_{iT})\left(\hat{\boldsymbol{\theta}}_{iT} - \bar{\boldsymbol{\theta}}_i\right), \quad (66)$$

where $\tilde{\boldsymbol{\theta}}_{iT}$ is a mean value on the line joining $\hat{\boldsymbol{\theta}}_{iT}$ and $\bar{\boldsymbol{\theta}}_i$. Note, by the mean value theorem, it holds that $\|\tilde{\boldsymbol{\theta}}_{iT} - \bar{\boldsymbol{\theta}}_i\| \leq \|\hat{\boldsymbol{\theta}}_{iT} - \bar{\boldsymbol{\theta}}_i\|$. Thus consistency of the estimator and continuous mapping implies $\left[\nabla_{\boldsymbol{\theta}\boldsymbol{\theta}}\hat{Q}_{iT}(\tilde{\boldsymbol{\theta}}_{iT})\right]^{-1} = \left[\nabla_{\boldsymbol{\theta}\boldsymbol{\theta}}\hat{Q}_{iT}(\bar{\boldsymbol{\theta}}_i)\right]^{-1} + o_{\mathbb{P}}(1)$. Therefore, we get that

$$\begin{aligned} \sqrt{T}\left(\hat{\boldsymbol{\theta}}_{iT} - \bar{\boldsymbol{\theta}}_i\right) &= -\left(\left[\nabla_{\boldsymbol{\theta}\boldsymbol{\theta}}\hat{Q}_{iT}(\bar{\boldsymbol{\theta}}_i)\right]^{-1} + o_{\mathbb{P}}(1)\right)\sqrt{T}\nabla_{\boldsymbol{\theta}}\hat{Q}_{iT}(\bar{\boldsymbol{\theta}}_i) \\ &= -\left[\nabla_{\boldsymbol{\theta}\boldsymbol{\theta}}\hat{Q}_{iT}(\bar{\boldsymbol{\theta}}_i)\right]^{-1}\sqrt{T}\nabla_{\boldsymbol{\theta}}\hat{Q}_{iT}(\bar{\boldsymbol{\theta}}_i) + o_{\mathbb{P}}(1). \end{aligned} \quad (67)$$

Since the central limit theorem applies to $\sqrt{T}\nabla_{\boldsymbol{\theta}}\hat{Q}_{iT}(\bar{\boldsymbol{\theta}}_i)$, as shown in (48), and the law of large numbers for the Hessian (established in (49)) ensures convergence, it follows that

$$\left(\left[\nabla_{\boldsymbol{\theta}\boldsymbol{\theta}}\hat{Q}_{iT}(\bar{\boldsymbol{\theta}}_i)\right]^{-1}\mathbf{V}_T\left[\nabla_{\boldsymbol{\theta}\boldsymbol{\theta}}\hat{Q}_{iT}(\bar{\boldsymbol{\theta}}_i)\right]^{-1}\right)^{-1/2}\sqrt{T}\left(\hat{\boldsymbol{\theta}}_{iT} - \bar{\boldsymbol{\theta}}_i\right) \xrightarrow{d} \mathcal{N}(0, I_k).$$

Recall that Equation (67) establishes the asymptotic behavior of an individual estimator and note that under Assumptions 3.1, 3.7(ii), and 3.7(v), we get that $\frac{1}{T}\sum_{t=1}^T\phi'''(\mathbf{W}_{it}^{\top}\bar{\boldsymbol{\theta}}_i)\mathbf{W}_{it}\mathbf{W}_{it}^{\top}(\mathbf{W}_{it}^{\top}\bar{\boldsymbol{\theta}}_i - Y_t) \xrightarrow{\mathbb{P}} 0$, which allows us to simplify the empirical Hessian at the true parameter, i.e.,

$$\begin{aligned} \nabla_{\boldsymbol{\theta}\boldsymbol{\theta}}\hat{Q}_{iT}(\bar{\boldsymbol{\theta}}_i) &= \frac{1}{T}\sum_{t=1}^T\phi'''(\mathbf{W}_{it}^{\top}\bar{\boldsymbol{\theta}}_i)\mathbf{W}_{it}\mathbf{W}_{it}^{\top}(\mathbf{W}_{it}^{\top}\bar{\boldsymbol{\theta}}_i - Y_t) + \phi''(\mathbf{W}_{it}^{\top}\bar{\boldsymbol{\theta}}_i)\mathbf{W}_{it}\mathbf{W}_{it}^{\top} \\ &= \frac{1}{T}\sum_{t=1}^T\phi''(\mathbf{W}_{it}^{\top}\bar{\boldsymbol{\theta}}_i)\mathbf{W}_{it}\mathbf{W}_{it}^{\top} + o_{\mathbb{P}}(1). \end{aligned}$$

Similarly the asymptotic behavior of the unconditional expectation \bar{r} follows for $\mathbf{W}_{it} = 1$, i.e., $\frac{1}{T}\sum_{t=1}^T\phi'''(\bar{r})(\bar{r} - Y_t) \xrightarrow{\mathbb{P}} 0$. Based on this, we stack the estimators emerging from (67) to get

that

$$\begin{aligned} \sqrt{T} \begin{pmatrix} \widehat{r}_T - \bar{r} \\ \widehat{\boldsymbol{\theta}}_{iT} - \bar{\boldsymbol{\theta}}_i \end{pmatrix} &= - \begin{pmatrix} \left(\frac{1}{T} \sum_{t=1}^T \phi''(\bar{r}) + o_{\mathbb{P}}(1) \right)^{-1} & 0 \\ \left(\frac{1}{T} \sum_{t=1}^T \phi''(\mathbf{W}_{it}^\top \bar{\boldsymbol{\theta}}_i) \mathbf{W}_{it} \mathbf{W}_{it}^\top + o_{\mathbb{P}}(1) \right)^{-1} \end{pmatrix} \times \\ & T^{-1/2} \sum_{t=1}^T \phi''(\mathbf{W}_{it}^\top \bar{\boldsymbol{\theta}}_i) \mathbf{W}_{it} (\mathbf{W}_{it}^\top \bar{\boldsymbol{\theta}}_i - Y_t) + o_{\mathbb{P}}(1). \end{aligned} \quad (68)$$

The law of large numbers established in (49) ensures convergence of the first term in (68) and invertibility follows from Assumption 3.7(iii) for T large enough. Asymptotic normality of the second term in (68) follows from the central limit theorem in (48). This verifies Assumption 3.5(i) and hence concludes this proof. \square

Proof of Proposition 3.11. We check the conditions of Assumption 3.3, for which we use

$$\begin{aligned} \widehat{Q}_{iT}(\boldsymbol{\theta}) &:= \frac{1}{T} \sum_{t=1}^T \mathbf{S}(\mathbf{W}_{it}^\top \boldsymbol{\theta}, Y_t) \quad \text{and} \\ \bar{Q}_{iT}(\boldsymbol{\theta}) &:= \mathbb{E} \left[\widehat{Q}_{iT}(\boldsymbol{\theta}) \right] = \mathbb{E} \left[\frac{1}{T} \sum_{t=1}^T \mathbf{S}(\mathbf{W}_{it}^\top \boldsymbol{\theta}, Y_t) \right] = \mathbb{E} \left[\mathbf{S}(\mathbf{W}_{it}^\top \boldsymbol{\theta}, Y_t) \right], \end{aligned}$$

with

$$\mathbf{S}(\mathbf{W}_{it}^\top \boldsymbol{\theta}, Y_t) = (\mathbf{1}\{\mathbf{W}_{it}^\top \boldsymbol{\theta} \geq Y_t\} - \alpha)(g(\mathbf{W}_{it}^\top \boldsymbol{\theta}) - g(Y_t)).$$

While the scoring function \mathbf{S} itself is non-smooth (at $Y_t = \mathbf{W}_{it}^\top \boldsymbol{\theta}$), we show that its expectation is twice (as required below) continuously differentiable everywhere, which implies condition (iii) of Assumption 3.3. For this, we use the law of iterated expectations and write

$$\begin{aligned} \bar{Q}_{iT}(\boldsymbol{\theta}) &= \mathbb{E} \left[\mathbb{E} \left[(\mathbf{1}\{Y_t \leq \mathbf{W}_{it}^\top \boldsymbol{\theta}\} - \alpha)(g(\mathbf{W}_{it}^\top \boldsymbol{\theta}) - g(Y_t)) \mid \mathcal{W}_{it} \right] \right] \\ &= \mathbb{E} \left[(F_{it}(\mathbf{W}_{it}^\top \boldsymbol{\theta}) - \alpha)g(\mathbf{W}_{it}^\top \boldsymbol{\theta}) \right] - \mathbb{E} \left[\int_{-\infty}^{\mathbf{W}_{it}^\top \boldsymbol{\theta}} g(y) f_{it}(y) dy \right] + \alpha \mathbb{E}[g(Y_t)]. \end{aligned} \quad (69)$$

We interchange expectation and differentiation by the dominated convergence theorem as there exist functions G and G' such that $\|\mathbf{W}_{it}g(\mathbf{W}_{it}^\top \boldsymbol{\theta})\| \leq G(\mathbf{W}_{it})$ with $\mathbb{E}|G(\mathbf{W}_{it})| < \infty$ (as $0 < f_{it}(\cdot) \leq K < \infty$ on its support) and $\|\mathbf{W}_{it}g'(\mathbf{W}_{it}^\top \boldsymbol{\theta})\| \leq G'(\mathbf{W}_{it})$ with $\mathbb{E}|G'(\mathbf{W}_{it})| < \infty$. The first term in (69) is continuously differentiable as F_{it} and g are continuously differentiable, and has derivative $\mathbb{E}[\mathbf{W}_{it}f_{it}(\mathbf{W}_{it}^\top \boldsymbol{\theta})g(\mathbf{W}_{it}^\top \boldsymbol{\theta}) + \mathbf{W}_{it}(F_{it}(\mathbf{W}_{it}^\top \boldsymbol{\theta}) - \alpha)g'(\mathbf{W}_{it}^\top \boldsymbol{\theta})]$, and the third term does not depend on $\boldsymbol{\theta}$. For the middle term, as g and f_{it} are continuous, the fundamental theorem of calculus implies $\nabla_{\boldsymbol{\theta}} \mathbb{E} \left[\int_{-\infty}^{\mathbf{W}_{it}^\top \boldsymbol{\theta}} g(y) f_{it}(y) dy \right] = \mathbb{E} [\mathbf{W}_{it}g(\mathbf{W}_{it}^\top \boldsymbol{\theta})f_{it}(\mathbf{W}_{it}^\top \boldsymbol{\theta})]$. Hence, we obtain differentiability such that condition (iii) of Assumption 3.3 is satisfied and get that

$$\nabla_{\boldsymbol{\theta}} \bar{Q}_{iT}(\boldsymbol{\theta}) = \mathbb{E} \left[\mathbf{W}_{it}g'(\mathbf{W}_{it}^\top \boldsymbol{\theta})(F_{it}(\mathbf{W}_{it}^\top \boldsymbol{\theta}) - \alpha) \right]. \quad (70)$$

For the second derivative, which will be used below, we similarly get that

$$\nabla_{\theta\theta}\bar{Q}_{iT}(\theta) = \mathbb{E}\left[(\mathbf{W}_{it}\mathbf{W}_{it}^\top) \left\{g''(\mathbf{W}_{it}^\top\theta)(F_{it}(\mathbf{W}_{it}^\top\theta) - \alpha) + g'(\mathbf{W}_{it}^\top\theta)f_{it}(\mathbf{W}_{it}^\top\theta)\right\}\right],$$

and as $F_{it}(\mathbf{W}_{it}^\top\bar{\theta}_i) = \alpha$, we have

$$\nabla_{\theta\theta}\bar{Q}_{iT}(\bar{\theta}_i) = \mathbb{E}\left[(\mathbf{W}_{it}\mathbf{W}_{it}^\top)g'(\mathbf{W}_{it}^\top\bar{\theta}_i)f_{it}(\mathbf{W}_{it}^\top\bar{\theta}_i)\right]. \quad (71)$$

We next show condition (iv) of Assumption 3.3, i.e., stochastic equicontinuity of the empirical process $\nu_{iT}(\theta)$ from (15). For this, we first show the following lemma:

Lemma A.1. *Given that the function g is Lipschitz with constant L_g , the GPL loss (7) is Lipschitz with constant $L_g \max(\alpha, 1 - \alpha)$.*

Proof of Lemma A.1. We start to write the function S from (7) as $S(x, y) = \rho(g(x), g(y))$ with

$$\rho(u, v) = \begin{cases} \alpha(v - u), & u \leq v, \\ (1 - \alpha)(u - v), & u > v, \end{cases} \quad (72)$$

which is a piecewise linear function with slopes α and $1 - \alpha$, respectively. Hence, we get that for all $u_1, u_2, v \in \mathbb{R}$ that $|\rho(u_1, v) - \rho(u_2, v)| \leq \max(\alpha, 1 - \alpha)|u_1 - u_2|$ and as a direct consequence,

$$\begin{aligned} |S(x_1, y) - S(x_2, y)| &= |\rho(g(x_1), g(y)) - \rho(g(x_2), g(y))| \\ &\leq \max(\alpha, 1 - \alpha)|g(x_1) - g(x_2)| \\ &\leq L_g \max(\alpha, 1 - \alpha)|x_1 - x_2| \end{aligned}$$

holds for all $x_1, x_2, y \in \mathbb{R}$, which concludes the proof of the lemma. \square

The following lemma shows equicontinuity of $\nu_{iT}(\theta)$ from (15).

Lemma A.2. *Assume that the function g from (7) is Lipschitz continuous, $(Y_t, \mathbf{W}_{it}^\top)$ is α -mixing of size $-s/(s - 2)$ for some $s > k + \delta$ for some $\delta > 0$, for which $\mathbb{E}\|\mathbf{W}_{it}\|^s < \infty$ and $\mathbb{E}|g(\mathbf{W}_{it}^\top\theta) - g(Y_t)|^s < \infty$. Then, the empirical process $\nu_{iT}(\theta)$ from (15) based on the GPL loss S from (7) is stochastically equicontinuous; see (16).*

Proof of Lemma A.2. Using Lemma A.1, we get for all $\theta, \tau \in \Theta$ that

$$\begin{aligned} \left|S(\mathbf{W}_{it}^\top\theta, Y_t) - S(\mathbf{W}_{it}^\top\tau, Y_t)\right| &\leq \|\mathbf{W}_{it}^\top\theta - \mathbf{W}_{it}^\top\tau\| L_g \max(\alpha, 1 - \alpha) \\ &\leq L_g \max(\alpha, 1 - \alpha) \|\mathbf{W}_{it}\| \|\theta - \tau\| \end{aligned}$$

is Lipschitz continuous. Hence, we employ Hansen (1996, Theorem 3) for mixing arrays, for which we verify his Assumption 4. For this, we choose $s > q = \tilde{k} = k + \delta$ for some small $\delta > 0$, where k is the dimensionality of Θ , and the function space $F := \{S(\mathbf{W}_{it}^\top\theta, Y_t) : \theta \in \Theta\}$.

First, by the mixing condition from Assumption 3.10 with mixing coefficients α_m , we have that $\sum_{m=1}^{\infty} \alpha_m^{(s-2)/s} < \infty$. As $\frac{s-\tilde{k}}{\tilde{k}s} < \frac{s-2}{s}$ for any $s > 2$ and $\tilde{k} > 2$, we also have that $\sum_{m=1}^{\infty} \alpha_m^{(s-\tilde{k})/(\tilde{k}s)} < \infty$, such that the first condition Hansen (1996, Assumption 4) holds.

The second condition of Hansen (1996, Assumption 4) holds as we impose stationarity and $\mathbb{E}|g(\mathbf{W}_{it}^\top \boldsymbol{\theta}) - g(Y_t)|^s < \infty$ such that for any $\mathbf{S}(\mathbf{W}_{it}^\top \boldsymbol{\theta}, Y_t) \in F$,

$$\limsup_{n \rightarrow \infty} \left\{ \frac{1}{T} \sum_{t=1}^T \left(\mathbb{E} \left| \mathbf{S}(\mathbf{W}_{it}^\top \boldsymbol{\theta}, Y_t) \right|^s \right)^{2/s} \right\}^{1/2} = \left(\mathbb{E} \left| \mathbf{S}(\mathbf{W}_{it}^\top \boldsymbol{\theta}, Y_t) \right|^s \right)^{1/s} < \infty.$$

Third, a similar condition holds for the Lipschitz constant

$$\limsup_{n \rightarrow \infty} \left\{ \frac{1}{T} \sum_{t=1}^T \left(\mathbb{E} \left| L_g \max(\alpha, 1 - \alpha) \|\mathbf{W}_{it}\|^s \right| \right)^{2/s} \right\}^{1/2} < \infty,$$

as $\mathbb{E}\|\mathbf{W}_{it}\|^s < \infty$ by assumption.

Hence, we can employ Hansen (1996, Theorem 3) to conclude that their Condition 1 holds with the L_q -norm $\rho_q(\cdot) = (\mathbb{E}|\cdot|^q)^{1/q}$. To see that the formulation of stochastic equicontinuity in Hansen (1996, Condition 1) implies (16), notice that

$$\begin{aligned} \left\{ f_1, f_2 \in F : \rho_q(f_1 - f_2) < \delta \right\} &= \left\{ \boldsymbol{\theta}, \boldsymbol{\tau} \in \Theta : \rho_q(\mathbf{S}(\mathbf{W}_{it}^\top \boldsymbol{\theta}, Y_t) - \mathbf{S}(\mathbf{W}_{it}^\top \boldsymbol{\tau}, Y_t)) < \delta \right\} \\ &= \left\{ \boldsymbol{\theta}, \boldsymbol{\tau} \in \Theta : \mathbb{E} \left| \mathbf{S}(\mathbf{W}_{it}^\top \boldsymbol{\theta}, Y_t) - \mathbf{S}(\mathbf{W}_{it}^\top \boldsymbol{\tau}, Y_t) \right|^q < \delta^q \right\} \\ &\supseteq \left\{ \boldsymbol{\theta}, \boldsymbol{\tau} \in \Theta : \|\boldsymbol{\theta} - \boldsymbol{\tau}\|^q < \frac{\delta^q}{L_g^q \max(\alpha, 1 - \alpha)^q \mathbb{E}\|\mathbf{W}_{it}\|^q} \right\}, \end{aligned}$$

such that the supremum over the the left-hand side (in Hansen (1996)) is larger or equal than the supremum over the right-hand side (in (16)). Furthermore, Markov's inequality can be used to transfer the L_q -statement in Hansen (1996) to the probability statement in (16), which concludes this proof. \square

We continue to show consistency of $\widehat{\boldsymbol{\theta}}_{iT}$ through Newey and McFadden (1994, Theorem 2.1), which is required for the verification of Assumption 3.3 (i). Notice that Θ is compact by assumption and that the population objective $\overline{Q}_{iT}(\boldsymbol{\theta})$ is continuous on Θ as shown above. As the GPL scoring function \mathbf{S} from (7) is strictly consistent for the α -quantile, we employ Holzmann and Eulert (2014, Theorem 1) to conclude that

$$\mathbb{E} \left[\mathbf{S}(\mathbf{W}_{it}^\top \bar{\boldsymbol{\theta}}_i, Y_t) \right] \leq \mathbb{E} \left[\mathbf{S}(\mathbf{W}_{it}^\top \boldsymbol{\theta}, Y_t) \right], \quad (73)$$

with equality if and only if $\mathbf{W}_{it}^\top \boldsymbol{\theta} = \mathbf{W}_{it}^\top \bar{\boldsymbol{\theta}}_i$, which is equivalent to $\boldsymbol{\theta} = \bar{\boldsymbol{\theta}}_i$ as shown around (40). Thus, the objective function $\boldsymbol{\theta} \mapsto \overline{Q}_{iT}(\boldsymbol{\theta}) = \mathbb{E} \left[\mathbf{S}(\mathbf{W}_{it}^\top \boldsymbol{\theta}, Y_t) \right]$ is *uniquely* minimized by $\bar{\boldsymbol{\theta}}_i$.

It remains to show the ULLN, $\sup_{\boldsymbol{\theta} \in \Theta} \left| \widehat{Q}_{iT}(\boldsymbol{\theta}) - \overline{Q}_{iT}(\boldsymbol{\theta}) \right| = o_{\mathbb{P}}(1)$ through Davidson (1994, Theorem 21.9). For this, the pointwise LLN, $\widehat{Q}_{iT}(\boldsymbol{\theta}) - \overline{Q}_{iT}(\boldsymbol{\theta}) = o_{\mathbb{P}}(1)$ for all $\boldsymbol{\theta} \in \Theta$, follows by White (2001, Theorem 3.34) as $\mathbf{S}(\mathbf{W}_{it}^\top \boldsymbol{\theta}, Y_t)$ is ergodic by White (2001, Proposition 3.44) and as $\mathbb{E} \left| \mathbf{S}(\mathbf{W}_{it}^\top \boldsymbol{\theta}, Y_t) \right| \leq \mathbb{E} |g(\mathbf{W}_{it}^\top \boldsymbol{\theta})| + \mathbb{E} |g(Y_t)| < \infty$ by assumption. Furthermore, the second condition of Davidson (1994, Theorem 21.9), that $\left\{ \widehat{Q}_{iT}(\boldsymbol{\theta}) - \overline{Q}_{iT}(\boldsymbol{\theta}) \right\}$ is stochastically equicontinuous,

follows immediately as

$$\nu_{iT}(\boldsymbol{\theta}) = T^{-1/2} \sum_{t=1}^T \mathbf{S}(\mathbf{W}_{it}^\top \boldsymbol{\theta}, Y_t) - \mathbb{E}[\mathbf{S}(\mathbf{W}_{it}^\top \boldsymbol{\theta}, Y_t)] = T^{1/2} \left(\widehat{Q}_{iT}(\boldsymbol{\theta}) - \overline{Q}_{iT}(\boldsymbol{\theta}) \right)$$

is shown to be stochastically equicontinuous in Lemma A.2 above.

Thus, consistency holds and we continue to show asymptotic normality through [Newey and McFadden \(1994, Theorem 7.1\)](#). The conditions $\widehat{Q}_{iT}(\widehat{\boldsymbol{\theta}}_{iT}) \leq \inf_{\boldsymbol{\theta} \in \Theta} \widehat{Q}_{iT}(\boldsymbol{\theta}) - o_P(T^{-1})$ is satisfied as $\widehat{\boldsymbol{\theta}}_{iT}$ is defined as the minimizer of $\widehat{Q}_{iT}(\boldsymbol{\theta})$ over Θ .

Item (i) of [Newey and McFadden \(1994, Theorem 7.1\)](#) holds as $\overline{Q}_{iT}(\boldsymbol{\theta})$ is minimized on Θ at $\bar{\boldsymbol{\theta}}_i$; see the arguments around (73). Item (ii) of [Newey and McFadden \(1994, Theorem 7.1\)](#), $\bar{\boldsymbol{\theta}}_i \in \text{int}(\Theta)$ holds by assumption, and item (iii), twice continuous differentiability of $\overline{Q}_{iT}(\boldsymbol{\theta})$ with second derivative $\nabla_{\boldsymbol{\theta}\boldsymbol{\theta}} \overline{Q}_{iT}(\bar{\boldsymbol{\theta}}_i)$ (at $\bar{\boldsymbol{\theta}}_i$), is shown above around (71). The matrix $\nabla_{\boldsymbol{\theta}\boldsymbol{\theta}} \overline{Q}_{iT}(\bar{\boldsymbol{\theta}}_i)$ is non-singular by [Dimitriadis and Bayer \(2019, Lemma B.2\)](#) as $\mathbb{E}[\mathbf{W}_{it} \mathbf{W}_{it}^\top]$ is non-singular by assumption, and $g'(\mathbf{W}_{it}^\top \bar{\boldsymbol{\theta}}_i) f_{it}(\mathbf{W}_{it}^\top \bar{\boldsymbol{\theta}}_i) > 0$.

We continue to show item (iv), i.e., that a multivariate CLT holds for

$$\sqrt{T} \widehat{D}_{iT}(\bar{\boldsymbol{\theta}}_i) = T^{-1/2} \sum_{t=1}^T \mathbf{W}_{it} g'(\mathbf{W}_{it}^\top \bar{\boldsymbol{\theta}}_i) (\mathbb{1}\{Y_t \leq \mathbf{W}_{it}^\top \bar{\boldsymbol{\theta}}_i\} - \alpha), \quad (74)$$

which is the derivative of $\widehat{Q}_{iT}(\bar{\boldsymbol{\theta}}_i)$ almost surely (except when $Y_t = \mathbf{W}_{it}^\top \bar{\boldsymbol{\theta}}_i$). We use the time-series CLT in [White \(2001, Theorem 5.20\)](#) and note that $\nabla_{\boldsymbol{\theta}} \overline{Q}_{iT}(\bar{\boldsymbol{\theta}}_i) = \mathbb{E}[\widehat{D}_{iT}(\bar{\boldsymbol{\theta}}_i)] = 0$; see (70). For this, let $\boldsymbol{\lambda} \in \mathbb{R}^k$ with $\boldsymbol{\lambda}^\top \boldsymbol{\lambda} = 1$ and consider $\boldsymbol{\lambda}^\top \sqrt{T} \widehat{D}_{iT}(\bar{\boldsymbol{\theta}}_i)$ through the Cramér-Wold device.

[White \(2001, Theorem 3.49\)](#) implies that the sequences $\boldsymbol{\lambda}^\top \mathbf{W}_{it} g'(\mathbf{W}_{it}^\top \bar{\boldsymbol{\theta}}_i) (\mathbb{1}\{Y_t \leq \mathbf{W}_{it}^\top \bar{\boldsymbol{\theta}}_i\} - \alpha)$ are mixing of the same size as the underlying random variables. Furthermore, for $s > 2$, we have

$$\mathbb{E} \left[\left| g'(\mathbf{W}_{it}^\top \bar{\boldsymbol{\theta}}_i) \boldsymbol{\lambda}^\top \mathbf{W}_{it} (\mathbb{1}\{Y_t \leq \mathbf{W}_{it}^\top \bar{\boldsymbol{\theta}}_i\} - \alpha) \right|^s \right] \leq \mathbb{E} \left[\left| g'(\mathbf{W}_{it}^\top \bar{\boldsymbol{\theta}}_i) \boldsymbol{\lambda}^\top \mathbf{W}_{it} \right|^s \right] \leq \mathbb{E} \left[\|g'(\mathbf{W}_{it}^\top \bar{\boldsymbol{\theta}}_i) \mathbf{W}_{it}\|^s \right],$$

which is finite by assumption. Using that

$$\boldsymbol{\lambda}^\top \mathbf{V}_T \boldsymbol{\lambda} = \text{Var} \left(T^{-1/2} \sum_{t=1}^T g'(\mathbf{W}_{it}^\top \bar{\boldsymbol{\theta}}_i) (\mathbb{1}\{Y_t \leq \mathbf{W}_{it}^\top \bar{\boldsymbol{\theta}}_i\} - \alpha) \boldsymbol{\lambda}^\top \mathbf{W}_{it} \right)$$

is uniformly bounded away from zero by assumption, [White \(2001, Theorem 5.20\)](#) together with the Cramér-Wold device yields that

$$\sqrt{T} \mathbf{V}_{iT}^{-1/2} \widehat{D}_{iT}(\bar{\boldsymbol{\theta}}_i) \xrightarrow{d} \mathcal{N}(0, I_k). \quad (75)$$

Finally, item (v) of [Newey and McFadden \(1994, Theorem 7.1\)](#) is implied by stochastic equicontinuity of the process ν_{iT} shown in Lemma A.2; see the discussion on page 2187 of [Newey and McFadden \(1994\)](#).

Hence, we can conclude that

$$\sqrt{T} \left((\nabla_{\boldsymbol{\theta}\boldsymbol{\theta}} \overline{Q}_{iT}(\bar{\boldsymbol{\theta}}_i))^{-1} \mathbf{V}_{iT} (\nabla_{\boldsymbol{\theta}\boldsymbol{\theta}} \overline{Q}_{iT}(\bar{\boldsymbol{\theta}}_i))^{-1} \right)^{-1/2} \left(\widehat{\boldsymbol{\theta}}_{iT} - \bar{\boldsymbol{\theta}}_i \right) \xrightarrow{d} \mathcal{N}(0, I_k),$$

which particularly implies $\sqrt{T}(\widehat{\boldsymbol{\theta}}_{iT} - \bar{\boldsymbol{\theta}}_i) = \mathcal{O}_{\mathbb{P}}(1)$. Invoking $\mathbf{W}_{it} = 1$, this also implies $\sqrt{T}(\widehat{r}_T - \bar{r}) = \mathcal{O}_{\mathbb{P}}(1)$ such that condition (i) of Assumption 3.3 holds.

The high-level Assumption 3.3(ii) holds by the same arguments following (52), applied to the GPL loss function and using the respective moment conditions from Assumption 3.10. \square

Proof of Proposition 4.1. Consider the squared error scoring function and notice that

$$\begin{aligned} \overline{\text{MCB}}_i &= \mathbb{E} \left[\text{S}(X_{it}, Y_t) - \text{S}(\mathbb{E}[Y_t | \mathbf{W}_{it}], Y_t) \right] \\ &= \mathbb{E} \left[(X_{it} - Y_t)^2 - (\mathbb{E}[Y_t | \mathbf{W}_{it}] - Y_t)^2 \right] \\ &= \mathbb{E}[X_{it}^2] - \mathbb{E}[\mathbb{E}[Y_t | \mathbf{W}_{it}]^2] - 2\mathbb{E}[X_{it}Y_t] + 2\mathbb{E}[Y_t\mathbb{E}[Y_t | \mathbf{W}_{it}]] \\ &= \mathbb{E}[X_{it}^2] + \mathbb{E}[\mathbb{E}[Y_t | \mathbf{W}_{it}]^2] - 2\mathbb{E}[X_{it}Y_t], \end{aligned} \tag{76}$$

and

$$\begin{aligned} \overline{\text{DSC}}_i &= \mathbb{E} \left[\text{S}(\mathbb{E}[Y_t], Y_t) \right] - \mathbb{E} \left[\text{S}(\mathbb{E}[Y_t | \mathbf{W}_{it}], Y_t) \right] \\ &= \mathbb{E} \left[(\mathbb{E}[Y_t] - Y_t)^2 - (\mathbb{E}[Y_t | \mathbf{W}_{it}] - Y_t)^2 \right] \\ &= -\mathbb{E} \left[\mathbb{E}[Y_t | \mathbf{W}_{it}]^2 \right] + 2\mathbb{E} \left[Y_t \mathbb{E}[Y_t | \mathbf{W}_{it}] \right] \\ &= \mathbb{E} \left[\mathbb{E}[Y_t | \mathbf{W}_{it}]^2 \right], \end{aligned} \tag{77}$$

where the final equality follows from the law of iterated expectations.

Recall that $\varsigma = \text{Var}(M_t) = \text{Var}(K_t) = \text{Var}(L_t) = \text{Var}(N_t) = \frac{1}{1 - \beta^2}$. As the processes M_t, K_t, L_t, N_t are independent, it also follows that $\mathbb{E}[M_t K_t] = \mathbb{E}[M_t L_t] = \mathbb{E}[M_t N_t] = \mathbb{E}[K_t L_t] = \mathbb{E}[K_t N_t] = \mathbb{E}[L_t N_t] = 0$. Hence, for forecaster $i = 1$, we have $\mathbb{E}[X_{1t}] = \delta_0$ and

$$\mathbb{E}[X_{1t}^2] = \delta_0^2 + (\delta_M^2 + \delta_K^2 + \delta_N^2)\varsigma = \delta_0^2 + \varsigma \cdot \boldsymbol{\delta}^\top \boldsymbol{\delta}, \quad \text{and} \tag{78}$$

$$\mathbb{E}[X_{1t}Y_t] = (\delta_K\gamma_K + \gamma_M\delta_M + \gamma_N\delta_N)\varsigma = \varsigma \cdot \boldsymbol{\delta}^\top \boldsymbol{\gamma}. \tag{79}$$

For forecaster $i = 2$, we accordingly have $\mathbb{E}[X_{2t}] = \xi_0$ and

$$\mathbb{E}[X_{2t}^2] = \xi_0^2 + (\xi_M^2 + \xi_L^2 + \xi_N^2)\varsigma = \xi_0^2 + \varsigma \cdot \boldsymbol{\xi}^\top \boldsymbol{\xi}, \quad \text{and} \tag{80}$$

$$\mathbb{E}[X_{2t}Y_t] = (\xi_M\gamma_M + \gamma_L\xi_L + \xi_N\gamma_N)\varsigma = \varsigma \cdot \boldsymbol{\xi}^\top \boldsymbol{\gamma}. \tag{81}$$

For the term $\mathbb{E}[\mathbb{E}[Y_t | \mathbf{W}_{it}]^2]$, with $\mathbf{W}_{it} = (1, X_{it})^\top$, we use $\mathbb{E}[Y_t | \mathbf{W}_{it}] = \mathbb{E}[Y_t | X_{it}]$. Given the linearity of our DGP in (22) and as $\mathbb{E}[Y_t] = 0$, we get that

$$\mathbb{E}[Y_t | \mathbf{W}_{it}] = \mathbf{W}_{it}^\top \bar{\boldsymbol{\theta}}_i = \bar{k}_i + \bar{\vartheta}_i X_{it},$$

with

$$\bar{\vartheta}_i = \text{Cov}(X_{it}, Y_t) / \text{Var}(X_{it}) \quad \text{and} \quad \bar{k}_i = -\bar{\vartheta}_i \cdot \mathbb{E}[X_{it}].$$

Using the expressions (78)–(81), we get

$$\mathbb{E}[\mathbb{E}[Y_t | \mathbf{W}_{1t}]^2] = \mathbb{E}\left[\left(\frac{\boldsymbol{\delta}^\top \boldsymbol{\gamma}}{\boldsymbol{\delta}^\top \boldsymbol{\delta}}\right)^2 X_{1t}^2\right] = \varsigma \cdot \frac{(\boldsymbol{\delta}^\top \boldsymbol{\gamma})^2}{\boldsymbol{\delta}^\top \boldsymbol{\delta}}, \quad (82)$$

$$\mathbb{E}[\mathbb{E}[Y_t | \mathbf{W}_{2t}]^2] = \mathbb{E}\left[\left(\frac{\boldsymbol{\xi}^\top \boldsymbol{\gamma}}{\boldsymbol{\xi}^\top \boldsymbol{\xi}}\right)^2 X_{2t}^2\right] = \varsigma \cdot \frac{(\boldsymbol{\xi}^\top \boldsymbol{\gamma})^2}{\boldsymbol{\xi}^\top \boldsymbol{\xi}}. \quad (83)$$

Hence, the expression for $\overline{\text{MCB}}_1$ from (25) follows by substituting (78), (79) and (82) into (76) and by using the identity $a + b^2/a - 2b = (a - b)^2/a$ with $a = \boldsymbol{\delta}^\top \boldsymbol{\delta}$ and $b = \boldsymbol{\delta}^\top \boldsymbol{\gamma}$. The formula for forecaster X_{2t} follows analogously.

For the uncertainty component under squared error loss $\overline{\text{UNC}} = \mathbb{E}[(\mathbb{E}[Y_t] - Y_t)^2] = \mathbb{E}[Y_t^2]$ since $\mathbb{E}[Y_t] = 0$. Since $\varepsilon_{Y,t} \sim \mathcal{N}(0, 1)$ and $\text{Var}(\varepsilon_{Y,t}) = \mathbb{E}[\varepsilon_{Y,t}^2] = 1$, the uncertainty component is given by

$$\begin{aligned} \overline{\text{UNC}} &= \mathbb{E}[Y_t^2] \\ &= \gamma_K^2 \mathbb{E}[K_t^2] + \gamma_L^2 \mathbb{E}[L_t^2] + \gamma_M^2 \mathbb{E}[M_t^2] + \gamma_N^2 \mathbb{E}[N_t^2] + \mathbb{E}[\varepsilon_{Y,t}^2] \\ &= (\gamma_K^2 + \gamma_L^2 + \gamma_M^2 + \gamma_N^2)\varsigma + 1 \\ &= \varsigma \cdot \boldsymbol{\gamma}^\top \boldsymbol{\gamma} + 1, \end{aligned}$$

which concludes the proof. □

B Relation to other decompositions

Several early contributions to the forecast evaluation literature propose score decompositions that are structurally similar to the one employed in this paper.

First, the population decomposition of the squared error score in [Murphy \(1973\)](#) coincides with the population score decomposition in (11). For the squared error score, (11) simplifies to $\bar{S}_i = \mathbb{E}[\mathbf{S}(X_{it}, X_{it}^C)] - \mathbb{E}[\mathbf{S}(X_{it}^C, \bar{r})] + \overline{\text{UNC}}$. [Murphy \(1973\)](#) labels these components calibration, resolution, and uncertainty. This representation is prevalent in the literature and it is often applied to the [Brier \(1950\)](#) score, which describes the squared error in the context of probability forecasts for binary outcomes; see e.g., [Elliott and Timmermann \(2016\)](#) and [Pohle \(2020\)](#). As such, our paper augments the original [Murphy \(1973\)](#) decomposition with inference under linear recalibration.

Second, the squared error score decomposition of [Mincer and Zarnowitz \(1969, Equation 5a\)](#) reads as

$$\text{Average Score} = \text{Mean Component} + \text{Slope Component} + \text{Residual Component}. \quad (84)$$

In terms of our notation, and the refinement of unconditional and conditional miscalibration terms of [Gneiting and Resin \(2023\)](#), the components in (84) are $\bar{S}_i = \overline{\text{uMCB}}_i + \overline{\text{cMCB}}_i + (\overline{\text{UNC}} + \overline{\text{DSC}}_i)$, where $\overline{\text{uMCB}}_i$ and $\overline{\text{cMCB}}_i$ are denoted as unconditional and conditional miscalibration components, which are non-negative and satisfy $\overline{\text{MCB}}_i = \overline{\text{uMCB}}_i + \overline{\text{cMCB}}_i$ given that

they are obtained from

$$\overline{\text{uMCB}}_i = \bar{S}_i - \mathbb{E}[\mathcal{S}(X_{it} + c, Y_t)] \quad \text{and} \quad \overline{\text{cMCB}}_i = \mathbb{E}[\mathcal{S}(X_{it} + c, Y_t)] - \bar{S}_i^c,$$

with constant c chosen such that $X_{it} + c$ is unconditionally calibrated, i.e., $\mathbb{E}[X_{it} + c] = \mathbb{E}[Y_t]$.

In this sense, the score decomposition in [Mincer and Zarnowitz \(1969\)](#) closely mirrors the structure considered here. Although the residual component in (84) conflates uncertainty and discrimination, this is unproblematic for comparative evaluation, as the uncertainty term is forecast-invariant and cancels out in pairwise comparisons. Accordingly, the residual component can be viewed as a re-normalized version of discrimination. [Mincer and Zarnowitz \(1969\)](#) however place little emphasis on this residual component, referring to it merely as a residual term without further interpretation or diagnostic use.

In summary, the aforementioned decompositions can be viewed as special cases of the general score decomposition in (11). The asymptotic theory developed in this paper is sufficiently general to be readily applicable to these alternative representations. For example, in the case of the [Mincer and Zarnowitz \(1969\)](#) decomposition, inference for the combined term $(\overline{\text{UNC}} + \overline{\text{DSC}}_i)$ follows directly from our results, and inference for $\overline{\text{uMCB}}_i$ and $\overline{\text{cMCB}}_i$ only requires one additional unconditional estimation step for the constant c .

C Details on the simulation setup for quantile forecasts

Here, we provide detailed calculations for the population $\overline{\text{MCB}}_i$ and $\overline{\text{DSC}}_i$ components on the check loss decomposition for quantile forecasts for the simulations from Section 4.

Proposition C.1. *Consider the DGP in (22) and (26). For $\alpha \in (0, 1)$, define $z_\alpha = \Phi^{-1}(\alpha)$. Using $\mathcal{W}_{it} = \sigma\{\mathbf{W}_{it}\}$ with $\mathbf{W}_{it} = (1, X_{it}^\alpha)^\top$ and the check loss $\mathcal{S}_\alpha(x, y) = (\mathbb{1}\{x \geq y\} - \alpha)(x - y)$, we get*

$$\overline{\text{MCB}}_1 = m_1 \left(\Phi(\kappa_1) + \alpha - 1 \right) + s_1 \phi(\kappa_1) - \sigma_{1|X} \phi(z_\alpha), \quad (85)$$

$$\overline{\text{DSC}}_1 = \phi(z_\alpha) (\sigma_Y - \sigma_{1|X}), \quad (86)$$

and $\overline{\text{UNC}} = \sigma_Y \phi(z_\alpha)$. In the above, $\sigma_Y^2 = \text{Var}(Y_t^2) = \varsigma \boldsymbol{\gamma}^\top \boldsymbol{\gamma} + 1$ with $\varsigma = \frac{1}{1-\beta^2}$, and

$$\begin{aligned} \sigma_{1|X}^2 &:= \text{Var}(Y_t | X_{1t}^\alpha) = \sigma_Y^2 - \varsigma \frac{(\boldsymbol{\delta}^\top \boldsymbol{\gamma})^2}{\boldsymbol{\delta}^\top \boldsymbol{\delta}} \\ m_1 &:= \mathbb{E}[Y_t - X_{1t}^\alpha] = -(\delta_0 + z_\alpha), \\ s_1^2 &:= \text{Var}(Y_t - X_{1t}^\alpha) = 1 + \varsigma (\boldsymbol{\gamma}^\top \boldsymbol{\gamma} + \boldsymbol{\delta}^\top \boldsymbol{\delta} - 2\boldsymbol{\delta}^\top \boldsymbol{\gamma}), \\ \kappa_1 &:= \frac{m_1}{s_1}. \end{aligned}$$

It further holds that $\overline{\text{DSC}}_1$ is increasing with $\frac{(\boldsymbol{\delta}^\top \boldsymbol{\gamma})^2}{\boldsymbol{\delta}^\top \boldsymbol{\delta}}$ and $\overline{\text{MCB}}_1$ is increasing in s_1 and in $\frac{(\boldsymbol{\delta}^\top \boldsymbol{\gamma})^2}{\boldsymbol{\delta}^\top \boldsymbol{\delta}}$. For the second forecaster X_{2t}^α , equivalent statements hold with $(\delta_0, \boldsymbol{\delta})$ replaced by $(\xi_0, \boldsymbol{\xi})$.

For the four parameterizations given in Table 4, we continue to simplify the closed-form expressions for $\overline{\text{MCB}}_i$ and $\overline{\text{DSC}}_i$ from Proposition C.1 as functions of k , α , and ς such that

the $\overline{\text{MCB}}$ and $\overline{\text{DSC}}$ relations from Table 4 can be verified. Notice that in the following, the expressions for $\kappa(k)$ vary for the different DGPs denoted 1), 2), 4) and 5).

First, for the check loss decomposition for DGP 1) in Table 4, we have

$$\begin{aligned}\overline{\text{MCB}}_1(k) &= \overline{\text{MCB}}_2(k) = -z_\alpha \left(\Phi\left(\frac{-z_\alpha}{s(k)}\right) + \alpha - 1 \right) + s(k) \phi\left(\frac{-z_\alpha}{s(k)}\right) - \sqrt{1 + \frac{\varsigma}{16}} \phi(z_\alpha), \\ \overline{\text{DSC}}_1 &= \overline{\text{DSC}}_2 = \phi(z_\alpha) \left(\sqrt{1 + \frac{3\varsigma}{16}} - \sqrt{1 + \frac{\varsigma}{16}} \right), \\ s(k) &= \text{Var}(Y_t - X_{it}^\alpha) = \sqrt{1 + \varsigma \left(\frac{k^2}{2} + \frac{1}{16} \right)}.\end{aligned}\tag{87}$$

Here, $s(k)$ is increasing in k , such that $\overline{\text{MCB}}_1(k) = \overline{\text{MCB}}_2(k)$ are increasing in k . $\overline{\text{MCB}}_1(0) = \overline{\text{MCB}}_2(0)$ can be obtained by simplifying the above formula for $k = 0$. Furthermore, $\overline{\text{DSC}}_1 = \overline{\text{DSC}}_2 > 0$ does not depend on k .

Second, for the check loss decomposition for DGP 2) in Table 4, we have

$$\begin{aligned}\overline{\text{MCB}}_1 &= 0, \\ \overline{\text{MCB}}_2(k) &= -z_\alpha \left(\Phi\left(\frac{-z_\alpha}{s_2(k)}\right) + \alpha - 1 \right) + s_2(k) \phi\left(\frac{-z_\alpha}{s_2(k)}\right) - \sqrt{1 + \frac{\varsigma}{16}} \phi(z_\alpha), \\ \overline{\text{DSC}}_1 &= \overline{\text{DSC}}_2 = \phi(z_\alpha) \left(\sqrt{1 + \frac{3\varsigma}{16}} - \sqrt{1 + \frac{\varsigma}{16}} \right), \\ s_2(k) &= \text{Var}(Y_t - X_{2t}^\alpha) = \sqrt{1 + \frac{\varsigma}{16} + \frac{\varsigma k^2}{2}}.\end{aligned}\tag{88}$$

As before, $s_2(k)$ is increasing in k , such that $\overline{\text{MCB}}_2(k)$ is increasing in k , and $\overline{\text{DSC}}_1 = \overline{\text{DSC}}_2 > 0$ are independent of k . $\overline{\text{MCB}}_2(0)$ can again be obtained by simplifying the above formula for $k = 0$.

Third, for the check loss decomposition for DGP 4) in Table 4, we have

$$\begin{aligned}\overline{\text{MCB}}_1(k) &= \overline{\text{MCB}}_2(k) = -z_\alpha \left(\Phi\left(\frac{-z_\alpha}{s(k)}\right) + \alpha - 1 \right) + s(k) \phi\left(\frac{-z_\alpha}{s(k)}\right) - \sqrt{\frac{\varsigma k^2}{2} + 1} \phi(z_\alpha), \\ \overline{\text{DSC}}_1(k) &= \overline{\text{DSC}}_2(k) = \phi(z_\alpha) \left(\sqrt{\varsigma k^2 + 1} - \sqrt{\frac{\varsigma k^2}{2} + 1} \right), \\ s(k) &= \text{Var}(Y_t - X_{it}^\alpha) = \sqrt{1 + \frac{\varsigma k^2}{2} + \frac{\varsigma}{8}}.\end{aligned}\tag{89}$$

Here, $\overline{\text{DSC}}_1(k) = \overline{\text{DSC}}_2(k)$ are increasing in k (as k^2 grows faster than $k^2/2$) and we have $\overline{\text{DSC}}_1(0) = \overline{\text{DSC}}_2(0) = 0$. Furthermore, $\overline{\text{MCB}}_1(k) = \overline{\text{MCB}}_2(k) > 0$ holds by (89).

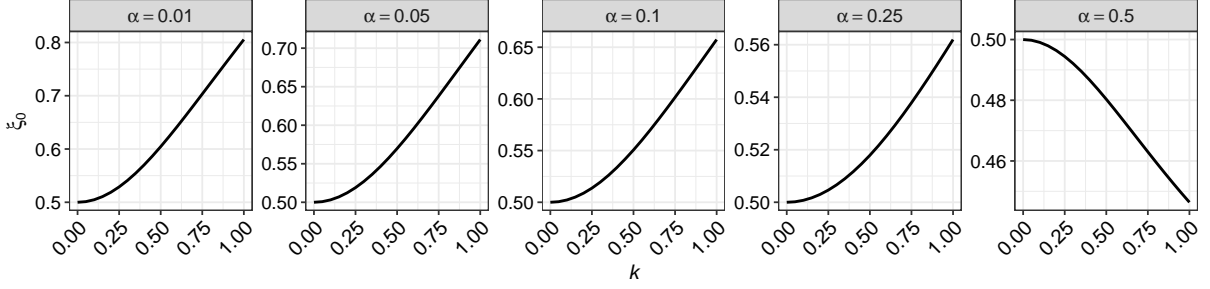


Figure C.1: Values for $\xi_0(k, \alpha)$ used for the quantile DGP 5) in Table 4 for $k \in [0, 1]$ and $\alpha \in \{0.01, 0.05, 0.1, 0.25, 0.5\}$, such that $\overline{\text{MCB}}_1(k) = \overline{\text{MCB}}_2(k)$ holds as accurately as possible for all k and α for the quantities from (90).

Fourth, for the check loss decomposition for DGP 5) in Table 4 with $\xi_0 = \xi_0(k, \alpha)$, we have

$$\begin{aligned}
\overline{\text{DSC}}_1 &= 0, \\
\overline{\text{DSC}}_2(k) &= \phi(z_\alpha) \left(\sqrt{\varsigma k^2 + 1} - \sqrt{\frac{\varsigma k^2}{2} + 1} \right), \\
\overline{\text{MCB}}_1(k) &= -(\delta_0 + z_\alpha) \left(\Phi\left(\frac{-(\delta_0 + z_\alpha)}{s_1(k)}\right) + \alpha - 1 \right) + s_1(k) \phi\left(\frac{-(\delta_0 + z_\alpha)}{s_1(k)}\right) - \sqrt{\varsigma k^2 + 1} \phi(z_\alpha), \\
\overline{\text{MCB}}_2(k) &= -(\xi_0 + z_\alpha) \left(\Phi\left(\frac{-(\xi_0 + z_\alpha)}{s_2(k)}\right) + \alpha - 1 \right) + s_2(k) \phi\left(\frac{-(\xi_0 + z_\alpha)}{s_2(k)}\right) - \sqrt{\frac{\varsigma k^2}{2} + 1} \phi(z_\alpha), \\
s_1(k) &:= \text{Var}(Y_t - X_{1t}^\alpha) = \sqrt{1 + \varsigma k^2 + \frac{\varsigma}{8}}, \\
s_2(k) &:= \text{Var}(Y_t - X_{2t}^\alpha) = \sqrt{1 + \frac{\varsigma k^2}{2} + \frac{\varsigma}{8}}.
\end{aligned} \tag{90}$$

As before, $\overline{\text{DSC}}_2(k)$ is increasing in k (as k^2 grows faster than $k^2/2$) and we have $\overline{\text{DSC}}_2(0) = 0$. Notice for this that the choice of ξ_0 does not affect the discrimination of the second forecast at all.

Equality of the $\overline{\text{MCB}}_i$, $i = 1, 2$ terms in (90) is difficult to obtain analytically. Hence, we choose $\xi_0 = \xi_0(k, \alpha)$ depending on $\alpha \in \{0.01, 0.05, 0.1, 0.25, 0.5\}$ and a sequence of values of $k \in [0, 1]$ numerically such that $\overline{\text{MCB}}_1(k, \alpha) = \overline{\text{MCB}}_2(k, \alpha)$ holds as accurately as possible. Figure C.1 displays these numeric solutions for $\xi_0 = \xi_0(k, \alpha)$ as functions of k and α .

Figure C.2 displays the expressions of $\overline{\text{MCB}}_i$ and $\overline{\text{DSC}}_i$, $i = 1, 2$ from (87)–(90) for the considered values of k and α , which confirms the properties of our simulation setup discussed above. In particular, Figure C.2 confirms that the numeric choices of $\xi_0(k, \alpha)$ yield the desired results.

Proof of Proposition C.1. We prove the claims for $i = 1$; the case $i = 2$ follows by replacing $(\delta_0, \boldsymbol{\delta})$ with $(\xi_0, \boldsymbol{\xi})$.

First, under (22), the vector \mathbf{V}_t has mean zero and covariance matrix ςI_4 , hence $\boldsymbol{\gamma}^\top \mathbf{V}_t \sim \mathcal{N}(0, \varsigma \boldsymbol{\gamma}^\top \boldsymbol{\gamma})$ and

$$Y_t = \boldsymbol{\gamma}^\top \mathbf{V}_t + \varepsilon_{Y,t} \sim \mathcal{N}(0, \sigma_Y^2), \quad \sigma_Y^2 = \varsigma \boldsymbol{\gamma}^\top \boldsymbol{\gamma} + 1.$$

Moreover, with $X_{1t}^\alpha = \mathbf{V}_t^\top \boldsymbol{\delta} + \delta_0 + z_\alpha$ we have

$$\text{Var}(X_{1t}^\alpha) = \varsigma \boldsymbol{\delta}^\top \boldsymbol{\delta}, \quad \text{and} \quad \text{Cov}(Y_t, X_{1t}^\alpha) = \varsigma \boldsymbol{\delta}^\top \boldsymbol{\gamma}.$$

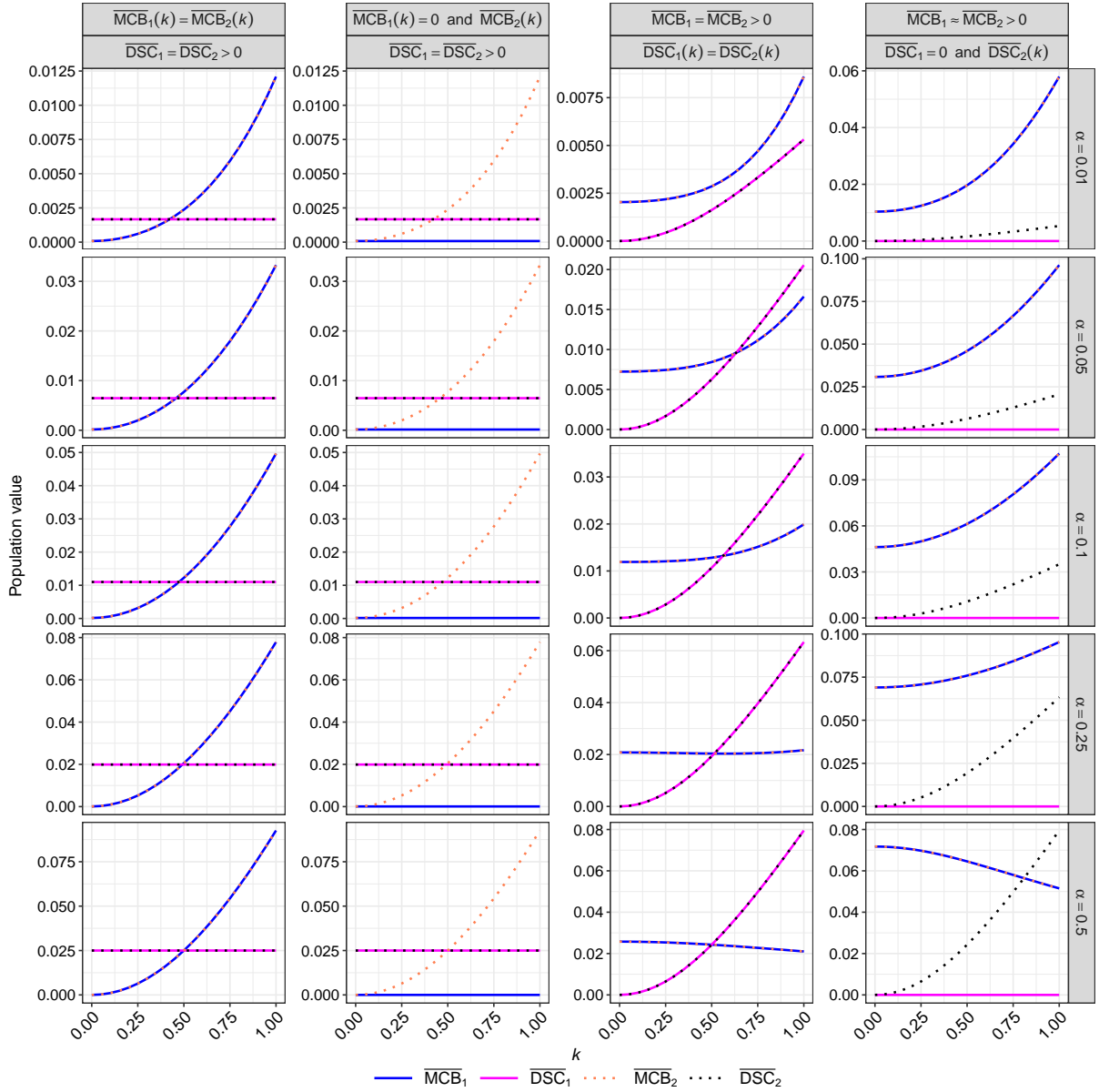


Figure C.2: Population values of \overline{MCB}_i and \overline{DSC}_i , $i = 1, 2$ from (87)–(90) for a range of values for k , our five choices of α , and the parameter values $\xi_0(k, \alpha)$ displayed in Figure C.1.

Since (Y_t, X_{1t}^α) is jointly Gaussian, $Y_t | X_{1t}^\alpha$ is Gaussian with constant conditional variance

$$\sigma_{1|X}^2 = \text{Var}(Y_t) - \frac{\text{Cov}(Y_t, X_{1t}^\alpha)^2}{\text{Var}(X_{1t}^\alpha)} = \sigma_Y^2 - \varsigma \frac{(\boldsymbol{\delta}^\top \boldsymbol{\gamma})^2}{\boldsymbol{\delta}^\top \boldsymbol{\delta}}. \quad (91)$$

We continue by deriving the formula for $\overline{\text{UNC}}$. Since the α -quantile functional is strictly consistent for the check loss, the expected loss $\mathbb{E}[\mathbf{S}_\alpha(x, Y_t)]$ is uniquely minimized at the true conditional quantile $Q_\alpha(Y_t) = \sigma_Y z_\alpha = \sigma_Y \Phi^{-1}(\alpha)$.

To obtain an explicit formula for the check loss at the true quantile, let $Y_t = \sigma_Y Z_t$ with $Z_t \sim \mathcal{N}(0, 1)$. Then,

$$\begin{aligned} \mathbb{E}[\mathbf{S}_\alpha(\sigma_Y z_\alpha, Y_t)] &= \mathbb{E}[(\alpha - \mathbf{1}\{Z_t \leq z_\alpha\})(\sigma_Y Z_t - \sigma_Y z_\alpha)] \\ &= \sigma_Y \mathbb{E}[(\alpha - \mathbf{1}\{Z_t \leq z_\alpha\})(Z_t - z_\alpha)] \\ &= \sigma_Y (\alpha \mathbb{E}[Z_t - z_\alpha] - \mathbb{E}[(Z_t - z_\alpha)\mathbf{1}\{Z_t \leq z_\alpha\}]). \end{aligned}$$

Since $\mathbb{E}[Z_t] = 0$, the first term becomes $-\alpha z_\alpha$. For the second term,

$$\mathbb{E}[(Z_t - z_\alpha)\mathbf{1}\{Z_t \leq z_\alpha\}] = \int_{-\infty}^{z_\alpha} (z - z_\alpha)\phi(z) dz = -\phi(z_\alpha) - z_\alpha \alpha,$$

which yields

$$\mathbb{E}[\mathbf{S}_\alpha(\sigma_Y z_\alpha, Y_t)] = \sigma_Y [-\alpha z_\alpha + \phi(z_\alpha) + z_\alpha \alpha] = \sigma_Y \phi(z_\alpha). \quad (92)$$

We continue to derive the close-form expression for the discrimination component. Because (Y_t, X_{1t}^α) is jointly Gaussian, the conditional distribution $Y_t | X_{1t}^\alpha$ is normal with conditional variance $\sigma_{1|X}^2 = \text{Var}(Y_t | X_{1t}^\alpha)$ from (91) that does not depend on X_{1t}^α . Hence,

$$Y_t | X_{1t}^\alpha \sim \mathcal{N}(\mathbb{E}[Y_t | X_{1t}^\alpha], \sigma_{1|X}^2) \quad \text{and} \quad Q_\alpha(Y_t | X_{1t}^\alpha) = \mathbb{E}[Y_t | X_{1t}^\alpha] + \sigma_{1|X} z_\alpha.$$

By the check loss identity for Gaussian distribution from (92), we obtain

$$\mathbb{E}[\mathbf{S}_\alpha(Q_\alpha(Y_t | X_{1t}^\alpha), Y_t) | X_{1t}^\alpha] = \sigma_{1|X} \phi(z_\alpha) \quad \text{a.s.},$$

and therefore also

$$\mathbb{E}[\mathbf{S}_\alpha(Q_\alpha(Y_t | X_{1t}^\alpha), Y_t)] = \sigma_{1|X} \phi(z_\alpha).$$

Consequently,

$$\overline{\text{DSC}}_1 = \overline{\text{UNC}} - \mathbb{E}[\mathbf{S}_\alpha(Q_\alpha(Y_t | X_{1t}^\alpha), Y_t)] = \sigma_Y \phi(z_\alpha) - \sigma_{1|X} \phi(z_\alpha),$$

which is (86), and

$$\overline{\text{MCB}}_1 = \mathbb{E}[\mathbf{S}_\alpha(X_{1t}^\alpha, Y_t)] - \mathbb{E}[\mathbf{S}_\alpha(Q_\alpha(Y_t | X_{1t}^\alpha), Y_t)] = \mathbb{E}[\mathbf{S}_\alpha(X_{1t}^\alpha, Y_t)] - \sigma_{1|X} \phi(z_\alpha),$$

for which we derive a closed form for $\mathbb{E}[\mathbf{S}_\alpha(X_{1t}^\alpha, Y_t)]$ in the following.

For this, define the forecast error $E_{1t} := Y_t - X_{1t}^\alpha$. Then E_{1t} is Gaussian with mean

$$m_1 = \mathbb{E}[E_{1t}] = \mathbb{E}[Y_t] - \mathbb{E}[X_{1t}^\alpha] = -(\delta_0 + z_\alpha),$$

and variance

$$\begin{aligned} s_1^2 &= \text{Var}(Y_t - X_{1t}^\alpha) = \text{Var}(Y_t) + \text{Var}(X_{1t}^\alpha) - 2 \text{Cov}(Y_t, X_{1t}^\alpha) \\ &= 1 + \varsigma(\boldsymbol{\gamma}^\top \boldsymbol{\gamma} + \boldsymbol{\delta}^\top \boldsymbol{\delta} - 2\boldsymbol{\delta}^\top \boldsymbol{\gamma}), \end{aligned}$$

To compute $\mathbb{E}[\mathbb{S}_\alpha(X_{1t}^\alpha, Y_t)]$, note that for $U = x + E$,

$$\mathbb{S}_\alpha(x, U) = (\mathbf{1}\{U < x\} - \alpha)(x - U) = (\alpha - \mathbf{1}\{E < 0\})E.$$

Hence,

$$\mathbb{E}[\mathbb{S}_\alpha(x, U)] = \alpha \mathbb{E}[E] - \mathbb{E}[E \mathbf{1}\{E < 0\}].$$

For $E \sim \mathcal{N}(m, s^2)$, a direct calculation yields

$$\mathbb{E}[E \mathbf{1}\{E < 0\}] = m \Phi(-m/s) - s \phi(m/s),$$

and therefore

$$\mathbb{E}[\mathbb{S}_\alpha(x, U)] = m(\Phi(m/s) + \alpha - 1) + s \phi(m/s).$$

Applying this with $x = X_{1t}^\alpha$ and $U = Y_t$ and using $\kappa_1 = m_1/s_1$ gives

$$\mathbb{E}[\mathbb{S}_\alpha(X_{1t}^\alpha, Y_t)] = m_1(\Phi(\kappa_1) + \alpha - 1) + s_1 \phi(\kappa_1).$$

We continue to establish monotonicity of $\overline{\text{MCB}}_1$ and $\overline{\text{DSC}}_1$ with respect to κ_1 and $R_1 = \frac{(\boldsymbol{\delta}^\top \boldsymbol{\gamma})^2}{\boldsymbol{\delta}^\top \boldsymbol{\delta}}$. For $\overline{\text{DSC}}_1$, it is immediate that $\sigma_{1|X}$ is decreasing in R_1 , such that $\overline{\text{DSC}}_1$ is increasing in R_1 . The same argument applies to $\overline{\text{MCB}}_1$ being increasing in R_1 as only the latter part in (85) depends on $\sigma_{1|X}$.

From (85), only the first two terms of $\overline{\text{MCB}}_1$ depend on s_1 . Define

$$g(s_1) := m_1(\Phi(\kappa_1) + \alpha - 1) + s_1 \phi(\kappa_1), \quad \kappa_1 = \frac{m_1}{s_1}.$$

Differentiating with respect to s_1 and using $\frac{d\kappa_1}{ds_1} = -\kappa_1/s_1$, we obtain

$$\begin{aligned} \frac{dg(s_1)}{ds_1} &= m_1 \phi(\kappa_1) \frac{d\kappa_1}{ds_1} + \phi(\kappa_1) + s_1 \phi'(\kappa_1) \frac{d\kappa_1}{ds_1} \\ &= -\frac{m_1 \kappa_1}{s_1} \phi(\kappa_1) + \phi(\kappa_1) + \kappa_1^2 \phi(\kappa_1) \\ &= \phi(\kappa_1) > 0, \end{aligned}$$

where we used $\phi'(x) = -x\phi(x)$ and $\kappa_1 = m_1/s_1$. Since the remaining term $-\sigma_{1|X}\phi(z_\alpha)$ does not depend on s_1 , $\overline{\text{MCB}}_1$ is strictly increasing in s_1 . \square

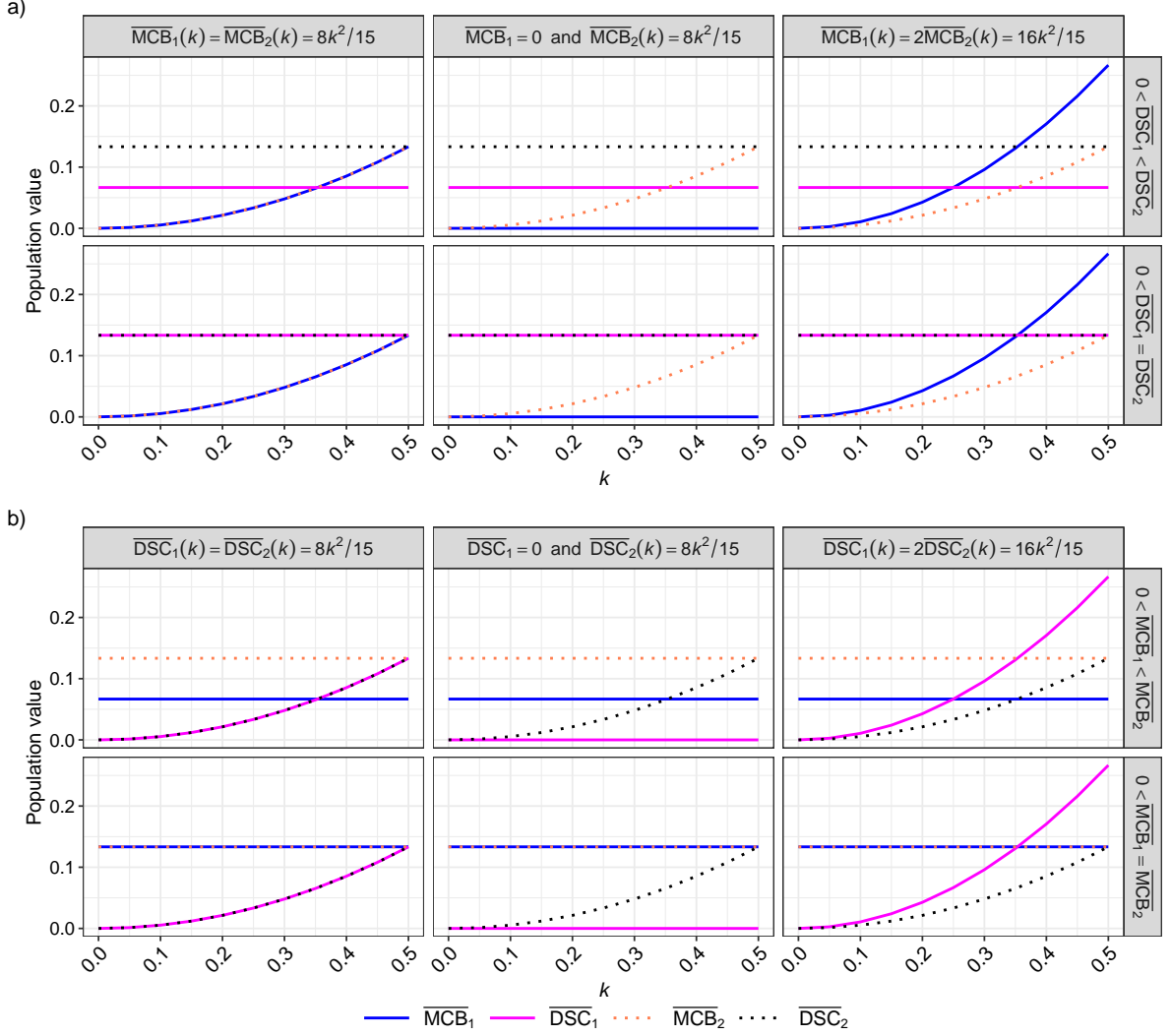


Figure D.1: Population values of $\overline{\text{MCB}}_i$ and $\overline{\text{DSC}}_i$, $i = 1, 2$ for the mean forecasts from the DGP in (22)–(24) for the twelve parametrizations from Table 3, following the close-form expressions of Proposition 4.1.

D Additional Figures

Figure D.1 plots the population values for $\overline{\text{MCB}}_i$ and $\overline{\text{DSC}}_i$, $i = 1, 2$ for the mean forecasts for the twelve DGPs from Table 3.

Figure D.2 plots the time series of the variance and VaR forecasts together with their corresponding evaluation targets for the application of Section 5.2.

Figures D.3–D.5 show model diagnostics for the linear recalibration regressions that are used for the score decompositions for the forecasts of the applications of Sections 5.1–5.2. For the mean forecasts in Figures D.3–D.4, we plot the model residuals $Y_t - \mathbf{W}_{it}^\top \hat{\boldsymbol{\theta}}_{iT}$ on the y -axis against the forecasts X_{it} (as the covariates of the underlying recalibration regressions) on the x -axis. The blue curve and its pointwise 95% confidence band are obtained from a local polynomial mean regression, implemented via the `loess` function in the statistical software R, with automatically selected tuning parameters. The black-dashed zero-line being inside these confidence bands for the majority of forecast values indicates no evidence against correct specification of the linear recalibration regressions.

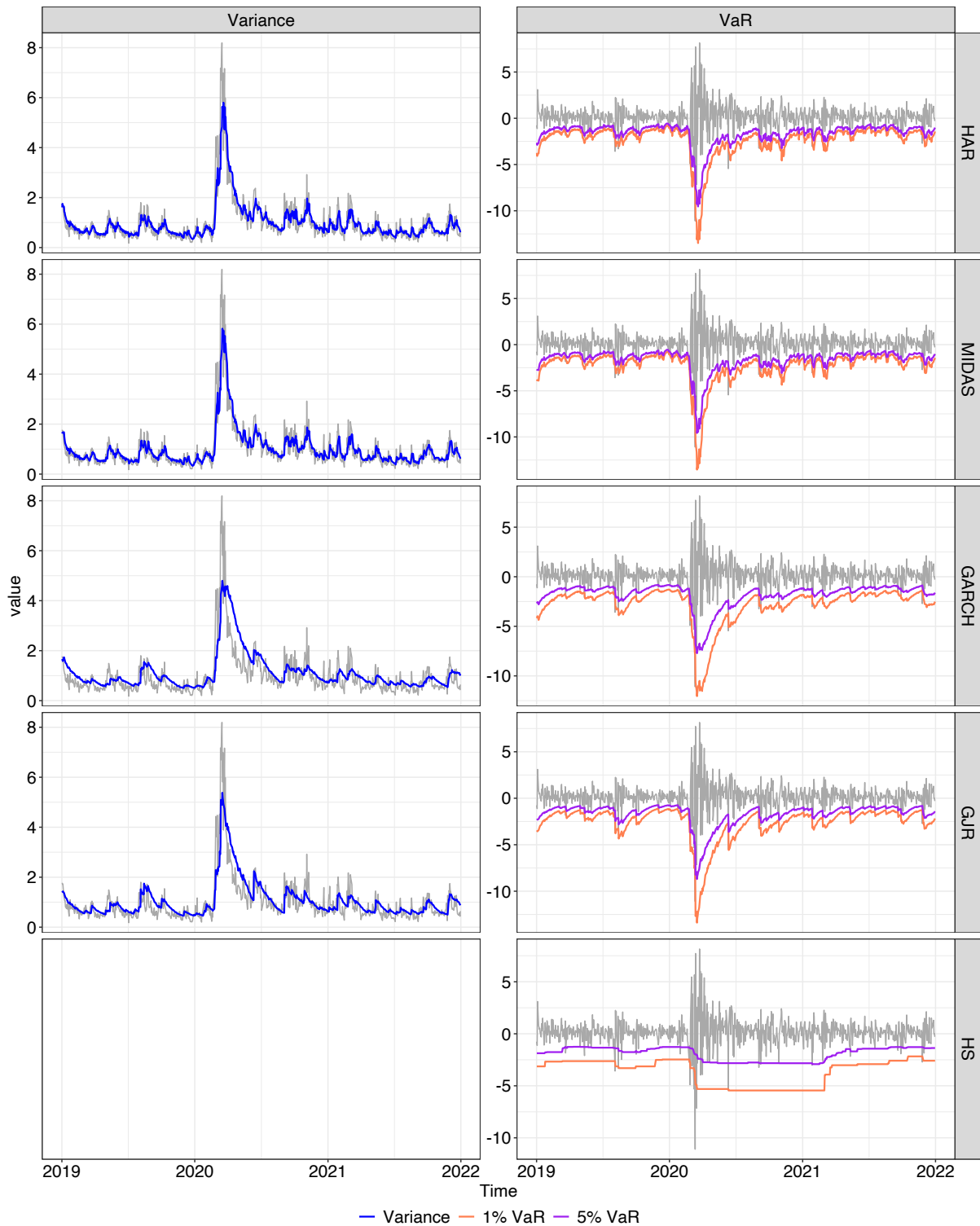


Figure D.2: Daily E-mini returns (right) and Realized Variances (left) in gray, together with the corresponding variance forecasts in blue (left) and VaR forecast at levels 1% in orange and 5% in purple (right) for the forecasting models considered in Section 5.2 and the time period after the year 2019.

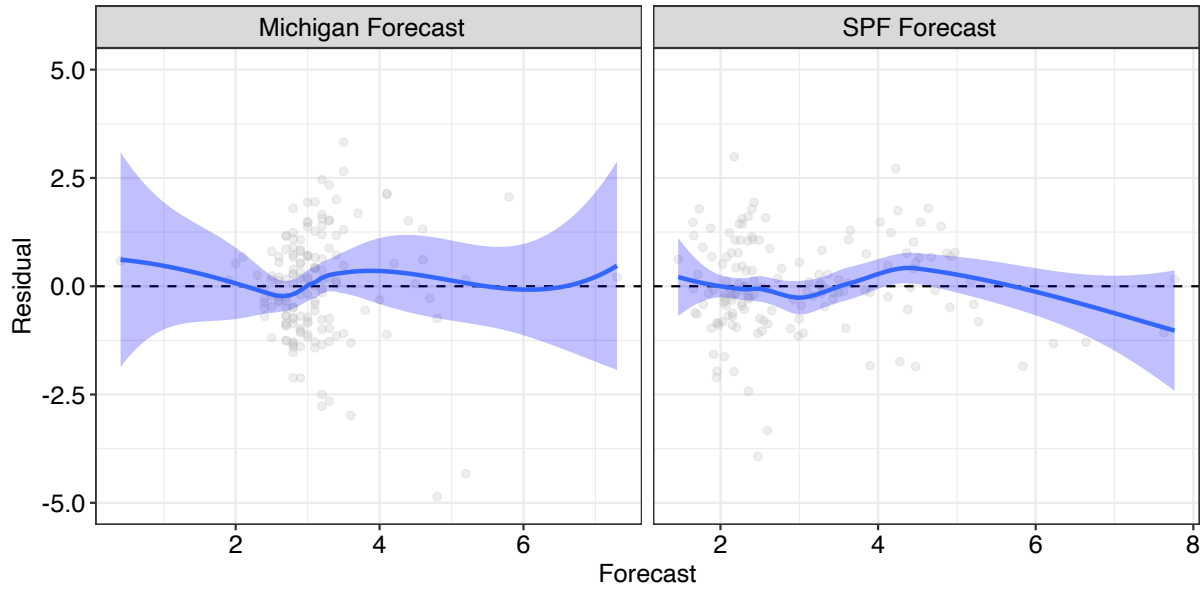
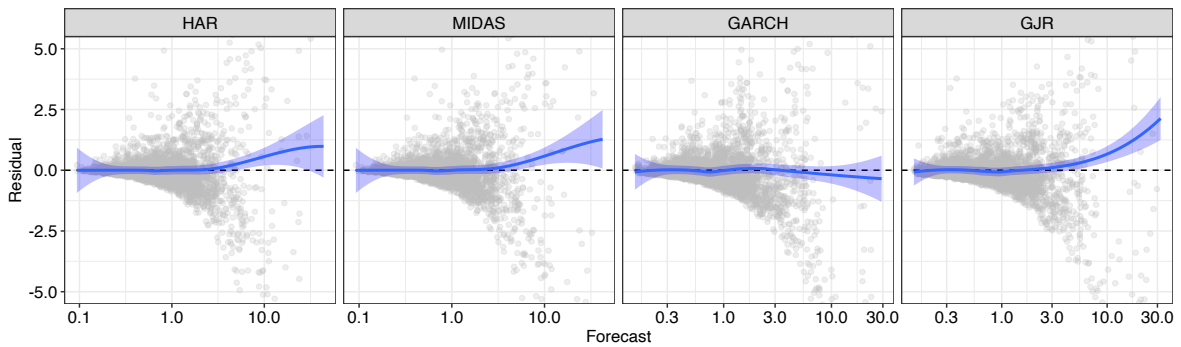


Figure D.3: Model diagnostics for the linear recalibration regression for the inflation rate forecasts in Section 5.1. We plot the model residuals against the forecasts (as the covariates of the underlying recalibration regression) together with a nonparametric polynomial regression and its 95% confidence bands. The zero-line being mostly contained in the confidence bands implies no evidence against correct model specification. For further details, see the text of Appendix D.

a) Mincer-Zarnowitz Regression with QLIKE Score



b) Mincer-Zarnowitz Regression with SE Score

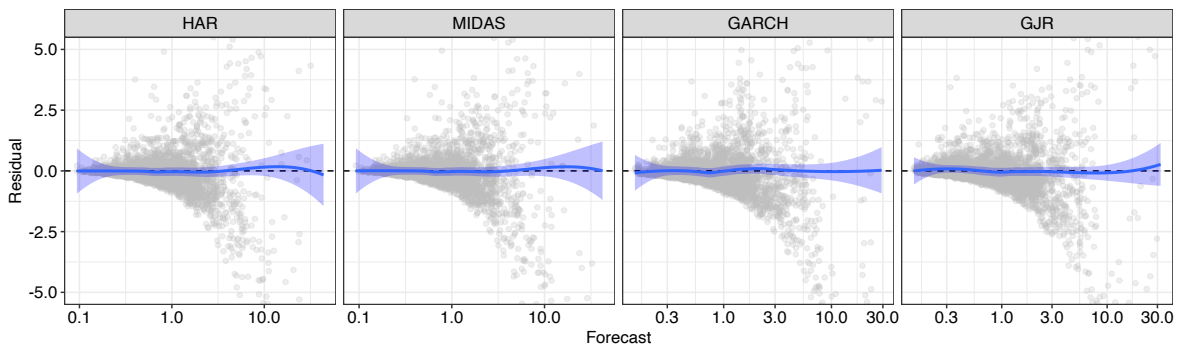


Figure D.4: Model diagnostics for the linear recalibration regression for the variance forecasts in Section 5.2. We plot the model residuals against the forecasts (as the covariates of the underlying recalibration regression) on a log-transformed x -axis together with a nonparametric polynomial regression and its 95% confidence bands. The zero-line being mostly contained in the confidence bands implies no evidence against correct model specification. For further details, see the text of Appendix D.

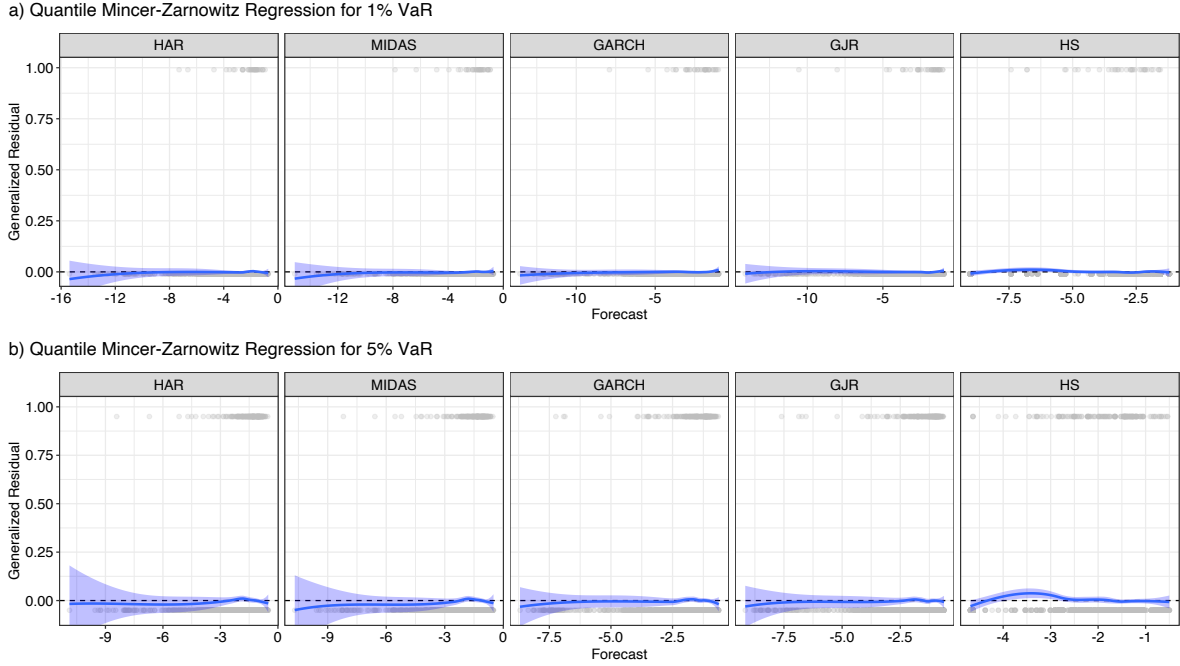


Figure D.5: Model diagnostics for the linear recalibration regression for the VaR forecasts in Section 5.2. We plot the generalized model residuals against the forecasts (as the covariates of the underlying recalibration regression) together with a nonparametric polynomial regression and its 95% confidence bands. The zero-line being mostly contained in the confidence bands implies no evidence against correct model specification. For further details, see the text of Appendix D.

In Figure D.5, we follow Pohle et al. (2024) and Dimitriadis and Hoga (2026, Figures 4 and 6) and plot the generalized quantile residuals, i.e., the identification functions, $V(\mathbf{W}_{it}^\top \hat{\boldsymbol{\theta}}_{iT}, Y_t) = \mathbb{1}\{Y_t \leq \mathbf{W}_{it}^\top \hat{\boldsymbol{\theta}}_{iT}\} - \alpha$, against the quantile forecasts X_{it} together with a corresponding nonparametric mean regression and their pointwise 95% confidence bands. The zero-line being mostly contained in the confidence bands again does not provide evidence against correct specification of the linear recalibration regressions.

References

- Allen, S., Burnello, J., and Ziegel, J. (2025). Assessing the conditional calibration of interval forecasts using decompositions of the interval score. *Preprint*. <https://arxiv.org/abs/2508.18034>.
- Andrews, D. (1994). Empirical process methods in econometrics. In Engle, R. and McFadden, D., editors, *Handbook of Econometrics*, volume 4, chapter 37, pages 2247–2294. Elsevier, Amsterdam.
- Andrews, D. W. K. (1991). Heteroskedasticity and autocorrelation consistent covariance matrix estimation. *Econometrica*, 59(3):817–858.
- Angeletos, G.-M., Huo, Z., and Sastry, K. A. (2021). Imperfect macroeconomic expectations: Evidence and theory. *NBER Macroeconomics Annual*, 35:1–86.
- Arnold, S., Walz, E.-M., Ziegel, J., and Gneiting, T. (2024). Decompositions of the mean continuous ranked probability score. *Electronic Journal of Statistics*, 18(2):4992–5044.
- Basel Committee (1996). Overview of the amendment to the capital accord to incorporate market risks. Technical report, Bank for International Settlements. <http://www.bis.org/publ/bcbs23.pdf>.
- Basel Committee (2019a). CRE: Calculation of RWA for credit risk. Technical report, Bank for International Settlements. https://www.bis.org/basel_framework/chapter/CRE/36.htm?inforce=20191215&published=20191215&export=pdf.

- Basel Committee (2019b). Minimum capital requirements for market risk. Technical report, Bank for International Settlements. <https://www.bis.org/bcbs/publ/d457.pdf>.
- Bayer, S. and Dimitriadis, T. (2022). Regression-based Expected Shortfall backtesting. *Journal of Financial Econometrics*, 20(3):437–471.
- Bentzien, S. and Friederichs, P. (2014). Decomposition and graphical portrayal of the quantile score. *Quarterly Journal of the Royal Meteorological Society*, 140(683):1924–1934.
- Berger, R. L. (1997). Likelihood ratio tests and intersection-union tests. In Panchapakesan, S. and Balakrishnan, N., editors, *Advances in Statistical Decision Theory and Applications*, pages 225–237. Birkhäuser, Boston, MA.
- Berkowitz, J., Christoffersen, P., and Pelletier, D. (2011). Evaluating Value-at-Risk models with desk-level data. *Management Science*, 57(12):2213–2227.
- Bollerslev, T. (1986). Generalized autoregressive conditional heteroskedasticity. *Journal of Econometrics*, 31(3):307–327.
- Bollerslev, T., Hood, B., Huss, J., and Pedersen, L. H. (2018). Risk everywhere: Modeling and managing volatility. *The Review of Financial Studies*, 31(7):2729–2773.
- Bordalo, P., Gennaioli, N., Ma, Y., and Shleifer, A. (2020). Overreaction in macroeconomic expectations. *American Economic Review*, 110(9):2748–82.
- Brehmer, J. R., Kraus, K., Gneiting, T., Herrmann, M., and Marzocchi, W. (2024). Enhancing the statistical evaluation of earthquake forecasts—an application to Italy. *Seismological Research Letters*, 96(3):1966–1988.
- Brier, G. W. (1950). Verification of forecasts expressed in terms of probability. *Monthly Weather Review*, 78(1):1–3.
- Bröcker, J. (2009). Reliability, sufficiency, and the decomposition of proper scores. *Quarterly Journal of the Royal Meteorological Society*, 135(643):1512–1519.
- Broer, T. and Kohlhas, A. N. (2024). Forecaster (mis-)behavior. *Review of Economics and Statistics*, 106(5):1334–1351.
- Campbell, S. D. (2007). A review of backtesting and backtesting procedures. *Journal of Risk*, 9(2):1–17.
- Choe, Y. J. and Ramdas, A. (2024). Comparing sequential forecasters. *Operations Research*, 72(4):1368–1387.
- Christoffersen, P. (1998). Evaluating interval forecasts. *International Economic Review*, 39(4):841–862.
- Clark, T. and McCracken, M. (2013). Advances in forecast evaluation. In Elliott, G. and Timmermann, A., editors, *Handbook of Economic Forecasting*, volume 2 of *Handbook of Economic Forecasting*, chapter 20, pages 1107–1201. Elsevier, Amsterdam.
- Clark, T. E. and McCracken, M. W. (2001). Tests of equal forecast accuracy and encompassing for nested models. *Journal of Econometrics*, 105(1):85–110.
- Coibion, O. and Gorodnichenko, Y. (2015). Information rigidity and the expectations formation process: A simple framework and new facts. *American Economic Review*, 105(8):2644–2678.
- Corsi, F. (2009). A simple approximate long-memory model of Realized Volatility. *Journal of Financial Econometrics*, 7(2):174–196.
- Davidson, J. (1994). *Stochastic Limit Theory: An Introduction for Econometricians*. Advanced Texts in Econometrics. Oxford University Press, Oxford.
- Dawid, A. P. (1986). Probability forecasting. In Kotz, S., Johnson, N. L., and Read, C. B., editors, *Encyclopedia of Statistical Sciences*, volume 7, page 210–218.
- DeGroot, M. H. and Fienberg, S. E. (1981). Assessing probability assessors: Calibration and refinement. Technical report.
- Diebold, F. X. (2015). Comparing predictive accuracy, twenty years later: A personal perspective on the use and abuse of Diebold–Mariano tests. *Journal of Business & Economic Statistics*, 33(1):1–9.
- Diebold, F. X., Gunther, T. A., and Tay, A. S. (1998). Evaluating density forecasts with applications to financial risk management. *International Economic Review*, 39(4):863–883.
- Diebold, F. X. and Mariano, R. S. (1995). Comparing predictive accuracy. *Journal of Business & Economic Statistics*, 20(1):134–144.
- Dimitriadis, T. and Bayer, S. (2019). A joint quantile and Expected Shortfall regression framework.

- Electronic Journal of Statistics*, 13(1):1823–1871.
- Dimitriadis, T., Fissler, T., and Ziegel, J. (2024a). Characterizing M-estimators. *Biometrika*, 111(1):339–346.
- Dimitriadis, T., Gneiting, T., and Jordan, A. I. (2021). Stable reliability diagrams for probabilistic classifiers. *Proceedings of the National Academy of Sciences*, 118(8):1–10.
- Dimitriadis, T., Gneiting, T., Jordan, A. I., and Vogel, P. (2024b). Evaluating probabilistic classifiers: The triptych. *International Journal of Forecasting*, 40(3):1101–1122.
- Dimitriadis, T. and Hoga, Y. (2025). Dynamic CoVaR modeling and estimation. *Journal of Business & Economic Statistics*. <https://doi.org/10.1080/07350015.2025.2590126>.
- Dimitriadis, T. and Hoga, Y. (2026). Regressions under adverse conditions. *Journal of Business & Economic Statistics*, 44(1):227–241.
- Duchesne, P. and Lafaye De Micheaux, P. (2010). Computing the distribution of quadratic forms: Further comparisons between the Liu-Tang-Zhang approximation and exact methods. *Computational Statistics and Data Analysis*, 54:858–862.
- Ehm, W., Gneiting, T., Jordan, A., and Krüger, F. (2016). Of quantiles and expectiles: Consistent scoring functions, choquet representations and forecast rankings. *Journal of the Royal Statistical Society Series B: Statistical Methodology*, 78(3):505–562.
- Elliott, G., Ghanem, D., and Krüger, F. (2016). Forecasting conditional probabilities of binary outcomes under misspecification. *Review of Economics and Statistics*, 98(4):742–755.
- Elliott, G. and Timmermann, A. (2016). *Economic Forecasting*. Princeton University Press.
- Engle, R. F. and Manganelli, S. (2004). CAViaR: Conditional autoregressive value at risk by regression quantiles. *Journal of Business & Economic Statistics*, 22(4):367–381.
- Farmer, L. E., Nakamura, E., and Steinsson, J. (2024). Learning about the long run. *Journal of Political Economy*, 132(10):3334–3377.
- Faust, J. and Wright, J. H. (2013). Forecasting inflation. In Elliott, G. and Timmermann, A., editors, *Handbook of Economic Forecasting*, volume 2, chapter 1, pages 2–56. Elsevier, Amsterdam.
- Fissler, T. and Hoga, Y. (2024). Backtesting systemic risk forecasts using multi-objective elicibility. *Journal of Business & Economic Statistics*, 42(2):485–498.
- Fissler, T., Lorentzen, C., and Mayer, M. (2022). Model comparison and calibration assessment: User guide for consistent scoring functions in machine learning and actuarial practice. *Preprint*. <https://arxiv.org/abs/2202.12780>.
- Fissler, T. and Ziegel, J. F. (2016). Higher order elicibility and Osband’s principle. *The Annals of Statistics*, 44(4):1680 – 1707.
- Fosten, J., Gutknecht, D., and Pohle, M.-O. (2024). Testing quantile forecast optimality. *Journal of Business & Economic Statistics*, 42(4):1367–1378.
- Gaglianone, W. P., Lima, L. R., Linton, O., and Smith, D. R. (2011). Evaluating Value-at-Risk models via quantile regression. *Journal of Business & Economic Statistics*, 29(1):150–160.
- Galvao, A. F. and Yoon, J. (2024). HAC covariance matrix estimation in quantile regression. *Journal of the American Statistical Association*, 119(547):2305–2316.
- Ghysels, E., Kvedaras, V., and Zemlys, V. (2016). Mixed frequency data sampling regression models: The R package midasr. *Journal of Statistical Software*, 72(4):1–35.
- Ghysels, E., Santa-Clara, P., and Valkanov, R. (2006). Predicting volatility: Getting the most out of return data sampled at different frequencies. *Journal of Econometrics*, 131(1):59–95.
- Giacomini, R. and White, H. (2006). Tests of conditional predictive ability. *Econometrica*, 74(6):1545–1578.
- Glosten, L. R., Jagannathan, R., and Runkle, D. E. (1993). On the relation between the expected value and the volatility of the nominal excess return on stocks. *The Journal of Finance*, 48(5):1779–1801.
- Gneiting, T. (2011). Making and evaluating point forecasts. *Journal of the American Statistical Association*, 106(494):746–762.
- Gneiting, T., Balabdaoui, F., and Raftery, A. E. (2007). Probabilistic forecasts, calibration and sharpness. *Journal of the Royal Statistical Society Series B: Statistical Methodology*, 69(2):243–268.
- Gneiting, T. and Resin, J. (2023). Regression diagnostics meets forecast evaluation: Conditional calibra-

- tion, reliability diagrams, and coefficient of determination. *Electronic Journal of Statistics*, 17(2):3226–3286.
- Gneiting, T., Wolfram, D., Resin, J., Kraus, K., Bracher, J., Dimitriadis, T., Hagenmeyer, V., Jordan, A. I., Lerch, S., Phipps, K., and Schienle, M. (2023). Model diagnostics and forecast evaluation for quantiles. *Annual Review of Statistics and Its Application*, 10(1):597–621.
- Guler, K., Ng, P. T., and Xiao, Z. (2017). Mincer-Zarnowitz quantile and expectile regressions for forecast evaluations under asymmetric loss functions. *Journal of Forecasting*, 36(6):651–679.
- Hansen, B. E. (1996). Stochastic equicontinuity for unbounded dependent heterogeneous arrays. *Econometric Theory*, 12(2):347–359.
- Hansen, P. R. (2005). A test for superior predictive ability. *Journal of Business & Economic Statistics*, 23(4):365–380.
- Hansen, P. R., Lunde, A., and Nason, J. M. (2011). The model confidence set. *Econometrica*, 79(2):453–497.
- He, X. D., Kou, S., and Peng, X. (2022). Risk measures: Robustness, elicibility, and backtesting. *Annual Review of Statistics and Its Application*, 9:141–166.
- Henzi, A. and Ziegel, J. F. (2022). Valid sequential inference on probability forecast performance. *Biometrika*, 109(3):647–663.
- Hoga, Y. and Demetrescu, M. (2023). Monitoring Value-at-Risk and Expected Shortfall forecasts. *Management Science*, 69(5):2954–2971.
- Hoga, Y. and Dimitriadis, T. (2023). On testing equal conditional predictive ability under measurement error. *Journal of Business & Economic Statistics*, 41(2):364–376.
- Holzmann, H. and Eulert, M. (2014). The role of the information set for forecasting—with applications to risk management. *The Annals of Applied Statistics*, 8(1):595 – 621.
- Imhof, J. P. (1961). Computing the distribution of quadratic forms in normal variables. *Biometrika*, 48(3/4):419–426.
- Kohlhas, A. N. and Walther, A. (2021). Asymmetric attention. *American Economic Review*, 111(9):2879–2925.
- Kuester, K., Mittnik, S., and Paolella, M. S. (2005). Value-at-Risk prediction: A comparison of alternative strategies. *Journal of Financial Econometrics*, 4(1):53–89.
- Kupiec, P. H. (1995). Techniques for verifying the accuracy of risk measurement models. *The Journal of Derivatives*, 3(2):73–84.
- Li, J., Liao, Z., and Quaedvlieg, R. (2022). Conditional superior predictive ability. *The Review of Economic Studies*, 89(2):843–875.
- Liu, L. Y., Patton, A. J., and Sheppard, K. (2015). Does anything beat 5-minute RV? A comparison of realized measures across multiple asset classes. *Journal of Econometrics*, 187(1):293–311.
- Mincer, J. and Zarnowitz, V. (1969). The evaluation of economic forecasts. In Mincer, J., editor, *Economic Forecasts and Expectations: Analysis of Forecasting Behavior and Performance*, pages 3–46. National Bureau of Economic Research, New York.
- Mitchell, K. (2019). *Score decompositions in forecast verification*. PhD thesis, University of Exeter, Exeter, United Kingdom.
- Mühlemann, A. (2021). *The role of loss functions in regression problems*. PhD thesis, University of Bern, Bern, Switzerland.
- Murphy, A. H. (1973). A new vector partition of the probability score. *Journal of Applied Meteorology and Climatology*, 12(4):595–600.
- Murphy, A. H. and Winkler, R. L. (1987). A general framework for forecast verification. *Monthly Weather Review*, 115(7):1330 – 1338.
- Murphy, A. H. and Winkler, R. L. (1992). Diagnostic verification of probability forecasts. *International Journal of Forecasting*, 7(4):435–455.
- Newey, W. K. (1994). The asymptotic variance of semiparametric estimators. *Econometrica*, pages 1349–1382.
- Newey, W. K. and McFadden, D. (1994). Large sample estimation and hypothesis testing. In Engle, R. and McFadden, D., editors, *Handbook of Econometrics*, volume 4, chapter 36, pages 2111–2245.

- Elsevier, Amsterdam.
- Newey, W. K. and West, K. D. (1987). A simple, positive semi-definite, heteroskedasticity and autocorrelation consistent covariance matrix. *Econometrica*, 55(3):703–708.
- Nieto, M. R. and Ruiz, E. (2016). Frontiers in VaR forecasting and backtesting. *International Journal of Forecasting*, 32(2):475–501.
- Nolde, N. and Ziegel, J. F. (2017). Elicitability and backtesting: Perspectives for banking regulation. *The Annals of Applied Statistics*, 11(4):1833–1874.
- Patton, A. J. (2011). Volatility forecast comparison using imperfect volatility proxies. *Journal of Econometrics*, 160(1):246–256.
- Patton, A. J. (2020). Comparing possibly misspecified forecasts. *Journal of Business & Economic Statistics*, 38(4):796–809.
- Patton, A. J., Ziegel, J. F., and Chen, R. (2019). Dynamic semiparametric models for Expected Shortfall (and Value-at-Risk). *Journal of Econometrics*, 211(2):388–413.
- Pohle, M.-O. (2020). The Murphy decomposition and the calibration-resolution principle: A new perspective on forecast evaluation. *Preprint*. <https://arxiv.org/abs/2005.01835>.
- Pohle, M.-O., Demetrescu, M., Dimitriadis, T., and Wermuth, J.-L. (2024). Generalised residual diagnostics. *Mimeo*.
- R Core Team (2026). *R: A language and environment for statistical computing*. R Foundation for Statistical Computing, Vienna, Austria.
- Ranjan, R. and Gneiting, T. (2010). Combining probability forecasts. *Journal of the Royal Statistical Society Series B: Statistical Methodology*, 72(1):71–91.
- Sanders, F. (1963). On subjective probability forecasting. *Journal of Applied Meteorology and Climatology*, 2(2):191–201.
- Savage, L. J. (1971). Elicitation of personal probabilities and expectations. *Journal of the American Statistical Association*, 66(336):783–801.
- Siegert, S. (2014). Variance estimation for Brier score decomposition. *Quarterly Journal of the Royal Meteorological Society*, 140(682):1771–1777.
- Siegert, S. (2017). Simplifying and generalising Murphy’s Brier score decomposition. *Quarterly Journal of the Royal Meteorological Society*, 143(703):1178–1183.
- Strähl, C. and Ziegel, J. (2017). Cross-calibration of probabilistic forecasts. *Electronic Journal of Statistics*, 11(1):608–639.
- Theil, H. (1966). *Applied economic forecasting*. North-Holland, Amsterdam.
- van der Vaart, A. W. and Wellner, J. A. (1996). *Weak convergence and empirical processes: With applications to statistics*. Springer Science & Business Media.
- Wang, Q., Wang, R., and Ziegel, J. (2025). E-backtesting. *Management Science*. <https://doi.org/10.1287/mnsc.2023.01659>.
- West, K. D. (1996). Asymptotic inference about predictive ability. *Econometrica*, 64(5):1067–1084.
- West, K. D. (2006). Forecast evaluation. *Handbook of Economic Forecasting*, 1:99–134.
- White, H. (2001). *Asymptotic Theory for Econometricians*. Academic Press, San Diego, 2nd edition.
- Wüthrich, M. V., Richman, R., Avanzi, B., Lindholm, M., Maggi, M., Mayer, M., Schelldorfer, J., and Scognamiglio, S. (2025). AI tools for actuaries. *Preprint*. <https://ssrn.com/abstract=5162304>.
- Xu, M. (2022). Semiparametric estimation with plug-in isotonic estimator. *Preprint*. https://drive.google.com/file/d/1jAPyEKur8s3Z1WFLuFBg5gEwYpF3DX_n/view?usp=sharing.
- Zeileis, A. (2004). Econometric computing with HC and HAC covariance matrix estimators. *Journal of Statistical Software*, 11(10):1–17.